REPORT NO. 26960-6001-TU-00

ZERO-G FLIGHT TEST OF A GAUGING SYSTEM

VOLUME I: SUMMARY

CONTRACT NO. NAS 9-14349
JANUARY 1976

PREPARED FOR:
NATIONAL AERONAUTICS AND SPACE ADMINISTRATION
LYNDON B. JOHNSON SPACE CENTER
HOUSTON, TEXAS 77058

TRW
DEFENSE AND SPACE SYSTEMS GROUP

REPORT NO. 26960-6001-TU-00

ZERO-G FLIGHT TEST OF A GAUGING SYSTEM

VOLUME I: SUMMARY

CONTRACT NO. NAS 9-14349
JANUARY 1976

PREPARED FOR:
NATIONAL AERONAUTICS AND SPACE ADMINISTRATION
LYNDON B. JOHNSON SPACE CENTER
HOUSTON, TEXAS 77058

TRW
DEFENSE AND SPACE SYSTEMS GROUP

FOREWORD

This technical report concludes Contract No. NAS 9-14349, "Zero-G Flight Test of a Gauging System," and covers the experimental flight testing of a nucleonic quantity gauging system conducted on-board a KC-135 Zero-G Aircraft. The report was prepared by Frank E. Bupp of TRW Defense and Space Systems Group, One Space Park, Redondo Beach, California. The author is grateful to numerous personnel for assistance in completion of this program, particularly to Mr. M. McFarlin of TRW, who was responsible for the development of the flight system software and data reduction and analysis, and Mr. R. Cardon of TRW for electronic support. The author also expresses his grateful appreciation to Mr. J. Alexander of the NASA/JSC and to Mr. D. Griggs, Chief, Zero-G Project Office, and the members of the flight crew for their contributions and dedicated participation in the conduct of the flight tests.

This report contains no classified information extracted from other classified reports; this report was submitted in January 1976.

ABSTRACT

The capability of a nucleonic gauging system to gauge the content of a reduced-scale storable liquid tank in a zero-g environment as provided by a KC-135 Zero-G Aircraft was demonstrated. Although the propellant-ullage interface never achieved the stable, zero-g equilibrium configuration, the gauging system gauged liquid quantity over all tank loadings to a total system accuracy the order of two percent. During the program, it was also determined that the gauging system presented no undue safety hazard to operating personnel in either ground and/or flight testing.

CONTENTS

ILLUSTRATIONS

ILLUSTRATIONS (Continued)

ILLUSTRATIONS (Continued)

TABLES

SECTION I

INTRODUCTION

Over the past several years many different methods of gauging propellants in a zero-g environment have been identified, among the more common being pressure-temperature-volume (PVT), ultrasonic, radio frequency (RF), capacitance, various nucleonic tracer techniques, and systems which operate on the principle of "X-raying" the interior of the tank. All of these techniques have their advantages and disadvantages, but in the final analysis — particularly where high levels of accuracy and reliability are required — the most attractive system is usually the one based on X-raying the interior of the tank by nucleonic means. The advantages of such a system are:

- It is capable of system accuracies of better than one percent.
- It measures the propellant mass directly (and not the ullage space or propellant volume).
- It is simple and reliable; it has no moving parts and utilizes only solid state circuitry.
- It can be made completely external to the propellant tanks.
- The same basic gauge can be used to measure the quantity of any propellant including slurries, gels, and cryogenic propellants.
- The propellant measurement is completely independent of propellant orientation or any obstruction that may be placed within the tank (such as baffles, zero-g cans, etc.).

Under joint sponsorship of NASA and the USAF, a program was initiated with TRW Systems in November of 1970 to demonstrate the feasibility of a nucleonic gauging system based on the X-ray technique. After extensive analyses, a nucleonic gauge was designed, fabricated in breadboard form, and tested. This feasibility model exhibited a total system error of 0.36 percent (21.6 pounds) when gauging a brine solution ($\rho = 1.14$) in an 8-foot diameter spherical tank over the range of empty to 6000 pounds.

After the successful feasibility demonstration, the basic program was expanded with the ultimate objective of designing and fabricating a flight-type nucleonic gauging system for highly accurate gauging of the OMS propellant tanks on the Space Shuttle Vehicle under zero-g conditions. This flight-type gauging system was subsequently tested under one-g conditions on a mock-up of the OMS tank in November 1973 and, based on some 20,000 data points, exhibited a total system error of 0.27 percent.

During the fabrication and test of the flight-type system, a second generation nucleonic gauging system — the Flight Test Article (FTA) — was designed and fabricated. The FTA consisted basically of a scaled, optically-clear test tank instrumented on the Electronic Subsystem (of the flight-type system) in modified form. The FTA, Electronic Subsystem, and supporting peripherals were delivered to NASA in August 1974 for subsequent zero-g flight testing on a KC-135A zero-g aircraft.

The purpose of this volume then is to describe the flight-test program and to present the gauging results that were obtained.

SECTION II

SUMMARY

2.1 OBJECTIVES

The overall objective of this flight test program was to demonstrate the capability of the nucleonic gauging system to gauge the content of reduced-scale storable liquid tanks in a zero-g environment as provided by a KC-135 zero-g aircraft. Also included within this objective were the following:

1) The gauging system would be compatible with the requirements for zero-g experiments to be conducted on the KC-135 zero-g aircraft and would operate reliably with the varying environmental conditions.

2) The gauging system would present no undue radiation hazard to operating personnel in either ground and/or flight testing.

3) The gauging data would be repeatable.

2.2 TEST ARRANGEMENT

The nucleonic gauging system employed in the flight test program consisted of a Flight Test Article (FTA) and an Electronic Subsystem (ESS); a simplified block diagram of this system is presented in Figure 2-1 whereas Figures 2-2 and 2-3 show physically the FTA and ESS, respectively. As designed and tested under one-g conditions, this nucleonic gauging system has a total system accuracy of better than 0.5 percent with a 1-second response time.

The experimental arrangement that was used in the flight test program is presented in Figure 2-4; the peripherals shown were used primarily for data acquisition, but also provided the capability to perform on-line, in-flight diagnostics. Gauging data were recorded directly on magnetic tape and later reduced in a large-scale scientific computer.

The aircraft employed was the NASA 930, a KC-135 equipped for zero-g flight tests. Although the FTA was designed to be free-floated in the aircraft cabin and have a (liquid) response of approximately 1.5 seconds using water as the propellant simulant, it was decided to hard-attach the FTA to the aircraft cabin floor. In the manner, the length of available gauging time would be at least twice that available in a free-float configuration, but at the penalty associated with small, aircraft-induced g-forces.

2.3 TEST RESULTS

Three flights were flown on three separate days encompassing eight different tank loadings and eleven zero-g parabolas for each loading; gauging was also conducted at these loadings during level flight conditions (one-g).

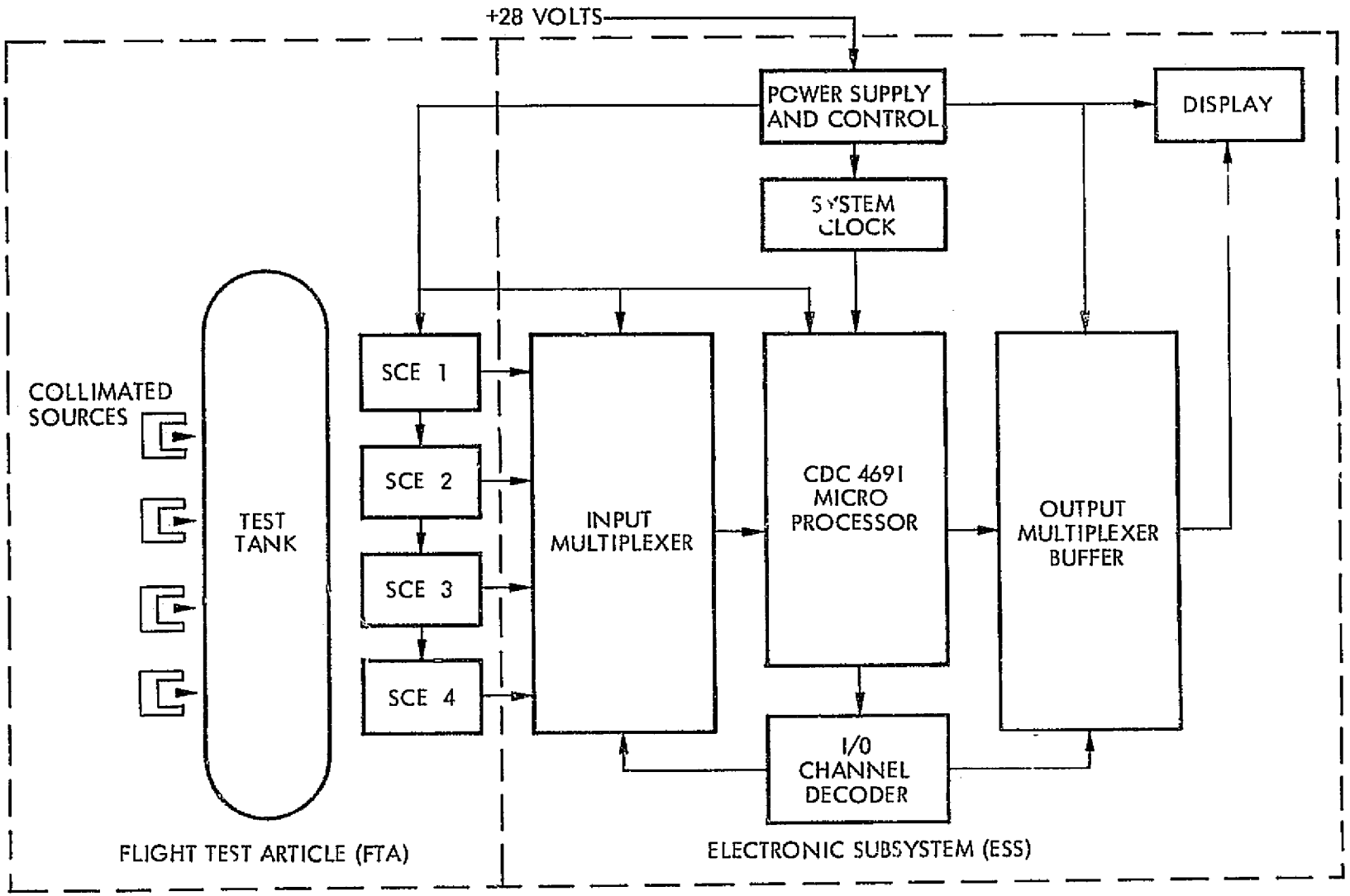

Figure 2-1. Nucleonic Gauging System Block Diagram

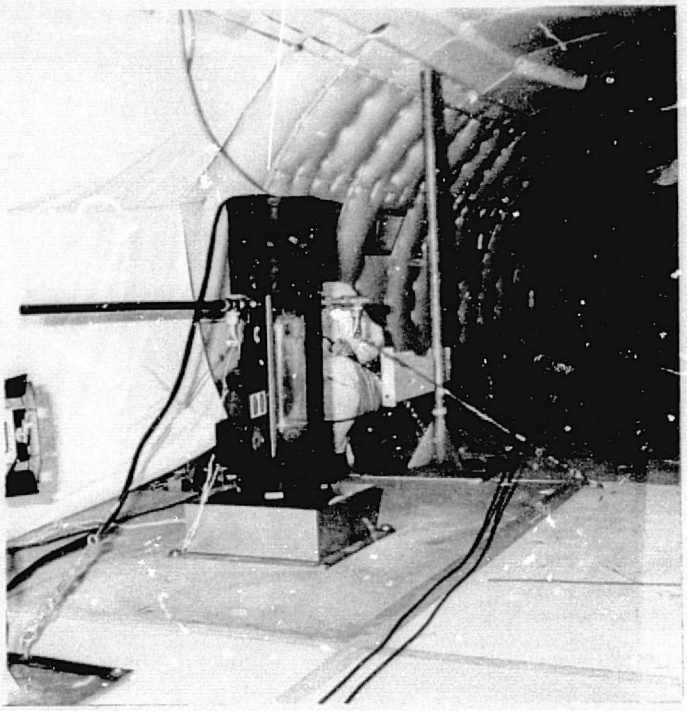

Figure 2-2. The Flight Test Article (FTA)

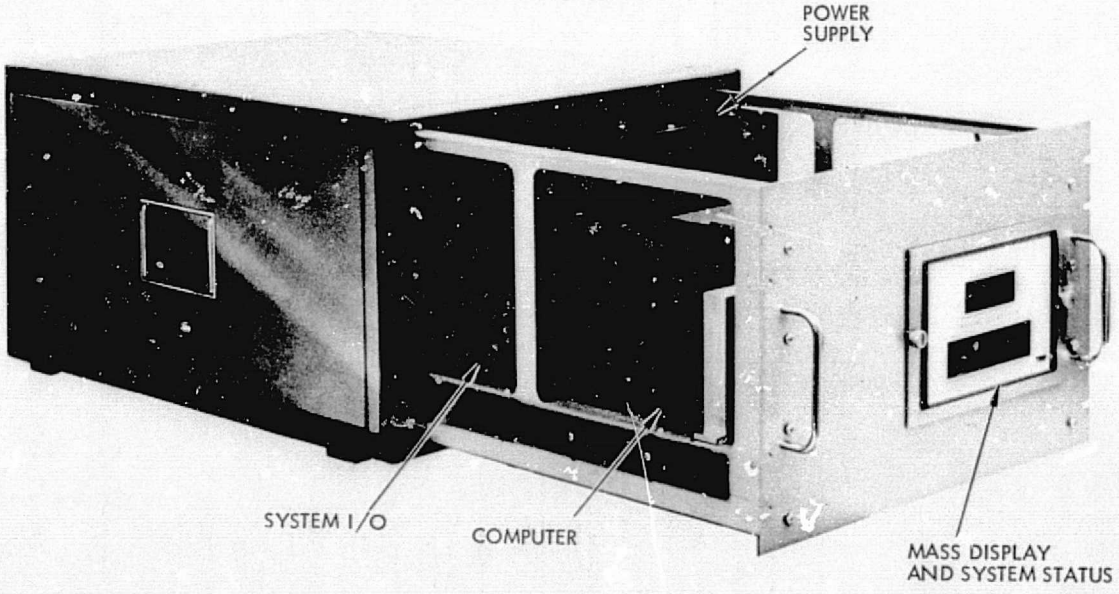

Figure 2-3. The Electronic Subsystem (ESS)

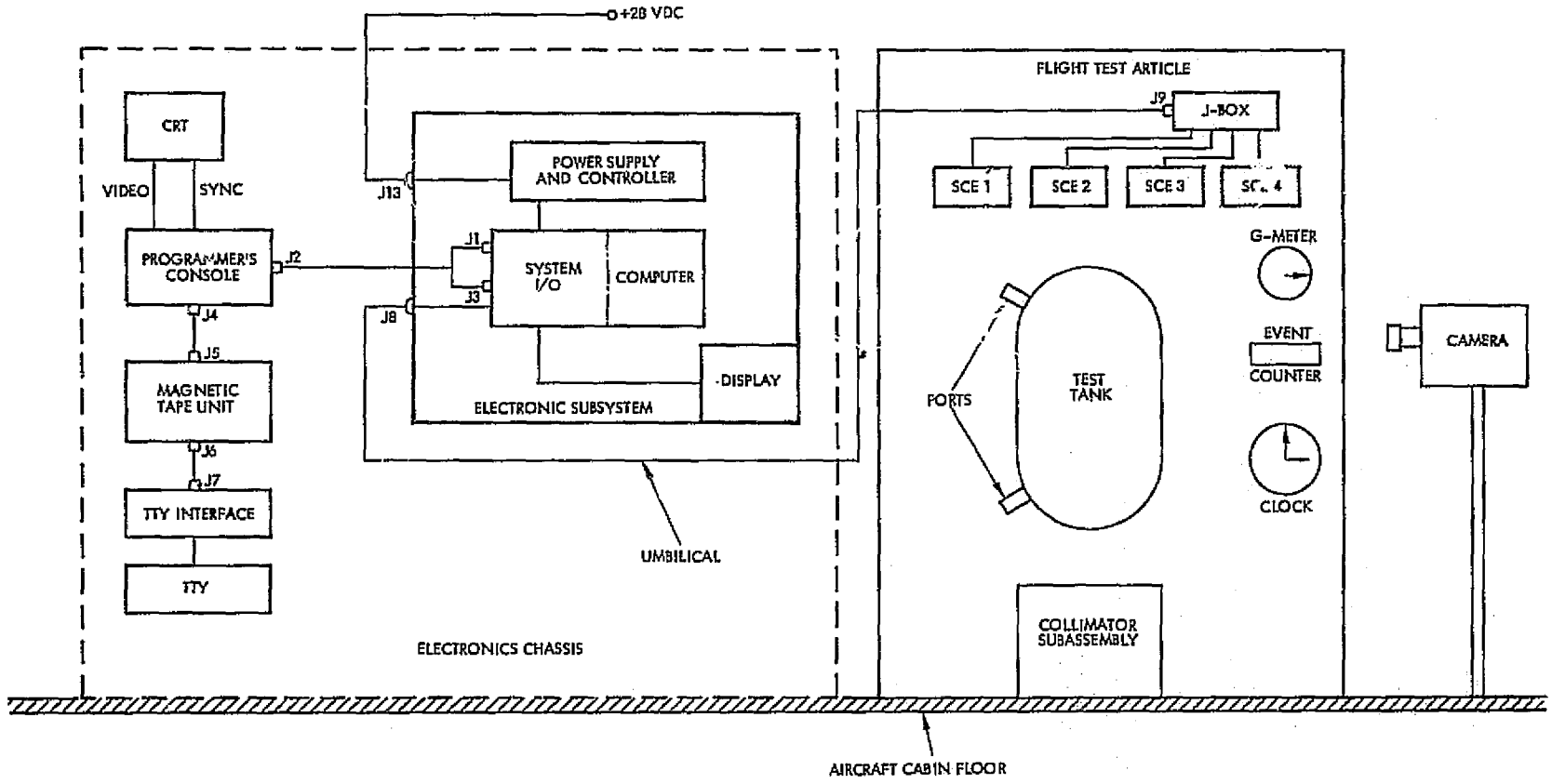

Figure 2-4. Experimental Arrangement

At no time during any of the zero-g parabolas did the propellant ullage interface reach the stable, zero-g equilibrium configuration. Rather, the propellant was more appropriately characterized as turbulent or, at the least, in a high degree of low-g slosh. Figures 2-5 through 2-8 are photographs of the typical propellant behavior at various times during a zero-g parabola. The photographic coverage also revealed that the propellant invariably remained in (or near) a one-g configuration for the first 4- to 6- seconds, and the last 1- to 2- seconds of each parabola; consequently, the first 6, and the last 2, 1-second gauging intervals were deleted from each zero-g parabola.

Despite the erratic behavior of the propellant during the zero-g parabolas, the nucleonic gauging system was capable of gauging the propellant content for any particular day's flight (consisting of 24 to 32 zero-g parabolas) to a total system accuracy of 2.05 percent or better; a typical result is shown in Figure 2-9. When all three flights were considered in toto, the total system accuracy was 2.76 percent; this result is shown in Figure 2-10 along with the quadratic expression relating the mass, M, in grams as a function of the Z-length in centimeters.

During the course of this program, a total of eighteen people were issued film badges to monitor any radiation dose that might be received from the nucleonic gauging system; those people whose jobs involved physical contact with the gauging system were also issued ring badges. The minimum detectable dose for these badges is 10 millirems. During the entire program, only one ring badge was reported to have received this dose or more; this ring badge recorded a dose of 0.04 rem during the same period that the worker's regular film badge recorded "minimal." Since the standard permissible dose rate for the general public is 7.5 rems per year, it was concluded that the nucleonic gauging system presents no undue radiation hazard to operating personnel in either ground or flight testing.

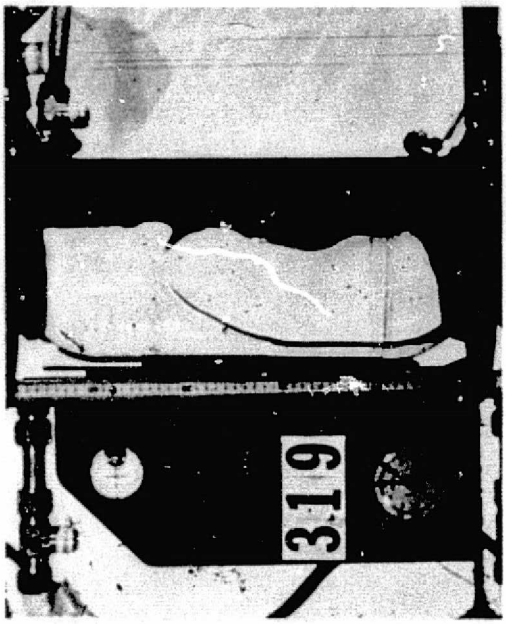

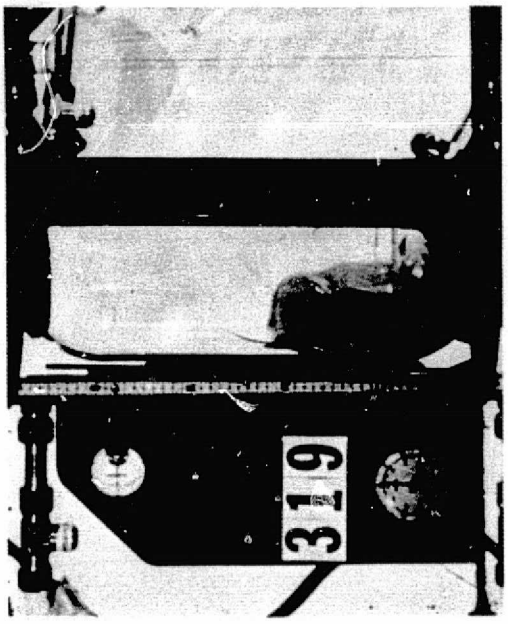

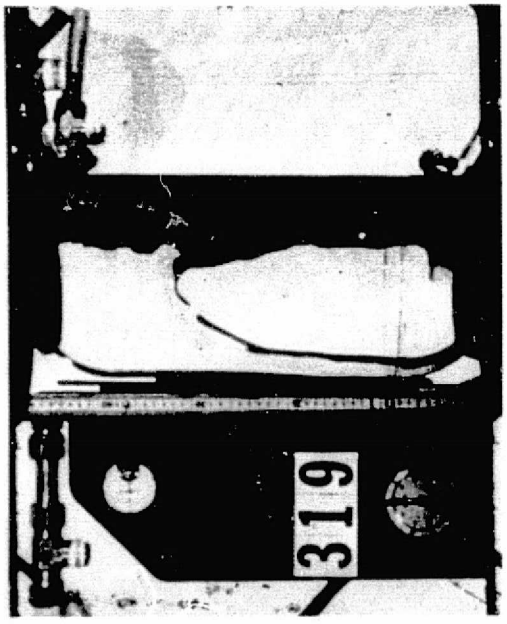

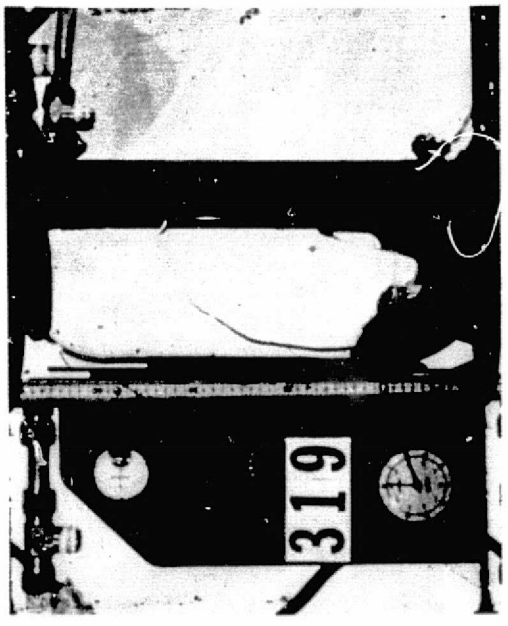

Figures 2-5 through 2-8. Propellant Behavior in the FTA

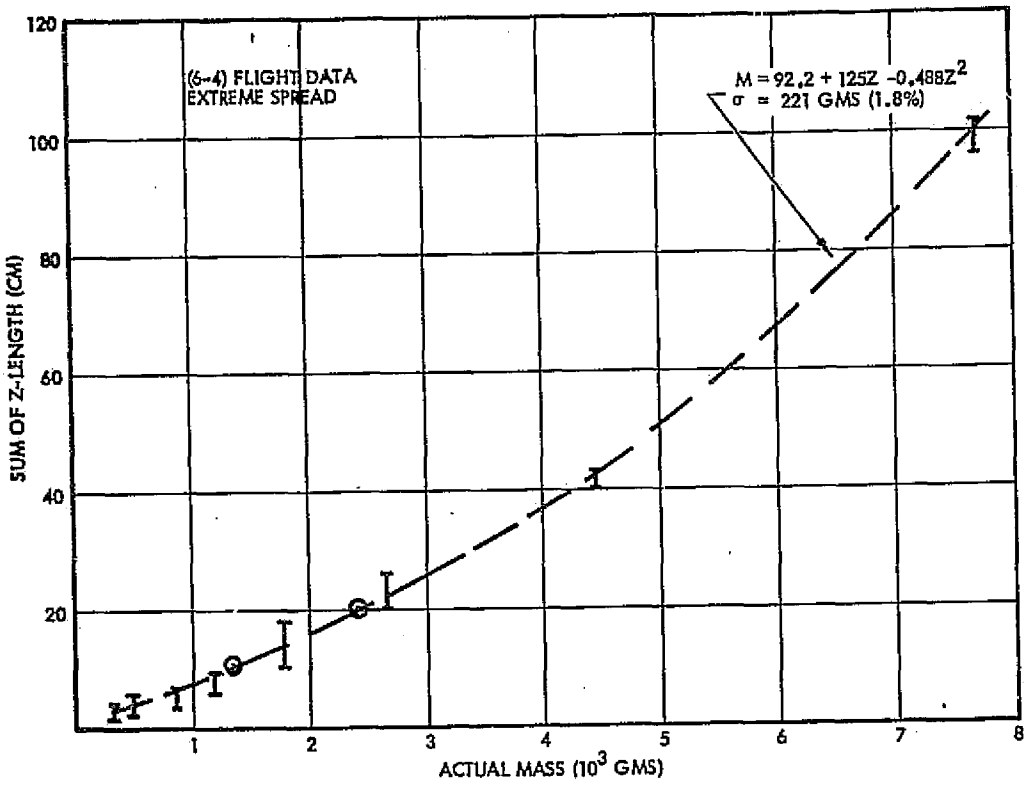

Figure 2-9. Mass Versus Z-Length for (6-4) Flight Data

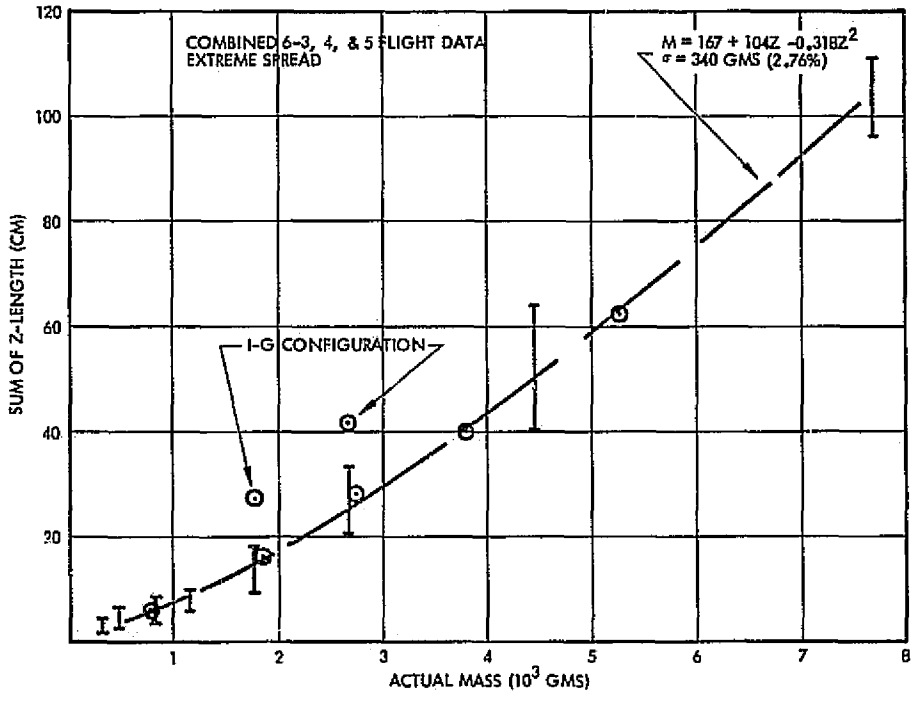

Figure 2-10. Mass Versus Z-Length for all Flight Data Combined

SECTION III

TECHNICAL PRESENTATION

3.1 GENERAL DESCRIPTION OF THE NUCLEONIC GAUGE CONCEPT

In its most general form, a nucleonic gauge is comprised of an array of gamma ray emitting radioisotope sources positioned on one side of a (propellant) tank, and an array of radiation detectors positioned on the other side of the tank opposite the sources; the concept is illustrated in Figure 3-1. Although all the elements and subsystems of the gauge are external to the tank, gamma rays that are emitted toward the detectors will penetrate the tank walls and be partially absorbed by the intervening fluid (fuel) within the tank. The amount of radiation which emerges on the detector side of the tank is then proportional to the mass of the intervening propellant.

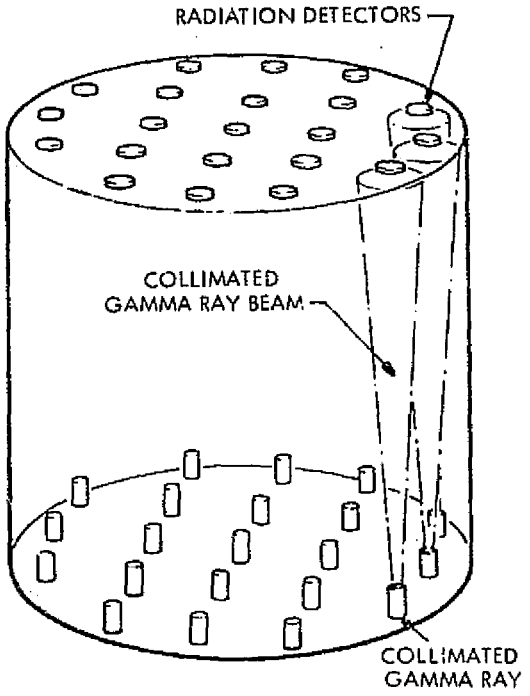

Figure 3-1. Typical Source-Detector Configuration

In practice, there are two basically different methods of mechanizing a nucleonic gauge: one mechanization is based on the natural — i. e., exponential — gamma ray absorption characteristics of the propellant while the other is based on obtaining a linear gamma ray absorption relationship. The latter technique is accomplished by selectively employing a window discriminator in the detection circuitry to accept only those photons which fall within a narrow energy range, thus making the gamma ray absorption a linear function of the absorber thickness. Although the linear system is the easier of the two systems to construct (at least from a hardware point of view), it is severely limited to tank dimensions the order of 8 feet or less; this limitation precluded the linear system from further consideration for the envisioned application and hence it was not subjected to rigorous study during this program. This report discusses only those systems based on exponential absorption.

For a propellant gauge employing the exponential principle of gamma ray absorption to operate properly under low Bond number regimes and/or zero-g conditions, it must first be insensitive to the fuel orientation within the tank. This is accomplished by judiciously distributing the detectors and radioisotope sources opposite each other and assuring that the detectors and sources are configured into a suitable array which covers a substantial portion of the entire projected area of the tank. The source-detector array is absolutely necessary unless the fuel is constrained by

some means (such as centrifugal force) into a known geometric distribution. For example, it would not be possible to use a single radioisotope source in the (central) interior of the tank and an array of radiation detectors on the exterior. If such a system were used to gauge propellant that may assume a random distribution (as in zero-g), a large error in propellant quantity measurement would result as is clearly envisioned in one case where the propellant is distributed along the walls of the tank, whereas in another case it is concentrated around the source in the center of the tank. The mean propellant thickness is the same in both cases. Since gamma ray absorption is a function of the thickness of the absorber, there will be equal amounts of gamma radiation absorbed within the propellant in both cases, and equal amounts of radiation will reach the detectors despite the fact that the first case has perhaps nearly an order of magnitude more propellant than the latter case. Needless to say, an attempt to use such a system for gauging the propellant quantity will produce a very large error.

To overcome this problem of random fuel orientation, the sources and the detectors are configured into arrays and distributed on a (nearly) planar surface, thereby creating a uniform gamma ray field within the boundary of the tank. In this gamma ray field, an element of propellant, may be moved anywhere within the boundary of the tank and, regardless of its position, will absorb the same amount of gamma radiation.

Due to limitations on the number (and distribution) of sources and detectors that can practicably be employed, nucleonic gauging invariably depends upon discrete sampling of the tank interior; a typical configuration is illustrated in Figure 3-1.

As shown, the gauge consists of individual gamma ray radioisotope sources, each of which is external to the tank and collimated to produce radiation in a narrow cone. On the opposite side and also external to the tank, a single detector is positioned in the center of each of the cones of radiation. Each source is sufficiently collimated so that it essentially illuminates only its opposing detector. The combination of each source and its opposing detector comprise a "source-detector pair", thereby providing a discrete "sample column" through the interior of the tank. By configuring a number of such source-detector pairs into an appropriate "sampling array", the entire contents of the tank can be sampled.

In general, the requirements for a radioisotope source for propellant measurement are high energy penetration capability to permit source-detector installation external to the tank, a comparatively long half-life to minimize calibration, and a source strength consistent with the accuracy and resolution requirements without compromise to personal safety.

3.1.1 Principle of Operation

In the nucleonic gauging system, the mass sampled by the i^{th} sample column due to the exponential attenuation of primary radiation from a radioisotope source when an absorber and/or fuel intervenes the

gamma ray beam will be proportional to the number of photons received at the i^{th} detector, N_{R_i}, according to:

$$N_{R_i} = N_{o_i} e^{-\left(\frac{\mu}{\rho}\right) \rho \ Z_i} \tag{3-1}$$

where

N_o = number of counts received in the absence of an intervening mass

$\left(\frac{\mu}{\rho}\right)$ = mass absorption coefficient

ρ = density of the intervening mass

Z = thickness of the intervening mass

In the event of a tank containing both fuel (liquid) and gas (ullage), the number of counts received by the i^{th} detector is simply

$$N_{R_i} = N_{o_i} e^{-\left(\frac{\mu}{\rho}\right)\left[\rho_L \ Z_{L_i} + \rho_G \ Z_{G_i}\right]} \tag{3-2}$$

where the subscripts L and G refer to the liquid and gas, respectively, within the i^{th} sample column.

The mass, M_i, in the i^{th} column is given by

$$M_i = (W_i) A_i \left(\rho_L Z_{L_i} + \rho_G Z_{G_i}\right) \tag{3-3}$$

$$= (W_i) A_i \left(\frac{\mu}{\rho}\right)^{-1} \ln\left(\frac{N_{o_i}}{N_{R_i}}\right) \tag{3-4}$$

where A_i is the area associated with the i^{th} sample column and W_i is the weighting factor associated with the i^{th} source-detector pair. In the typical situation where the sample columns are parallel,

$$A_i \approx \frac{A_T}{k} \quad \text{and} \quad W_i \approx 1 \text{ for all } i \tag{3-5}$$

where A_T is the total projected cross-sectional area of the tank and k is the number of sampling columns.

Thus, the total mass sampled by the k sample columns is

$$M = \sum M_i = \frac{A_T}{k} \sum_{i=1}^{k} \rho_L Z_{L_i} + \rho_G Z_{G_i} \tag{3-6}$$

or:

$$M = \frac{A_T}{k} \left(\frac{\mu}{\rho}\right)^{-1} \sum_{i=1}^{k} \ln \left(\frac{N_{o_i}}{N_{R_i}}\right) \tag{3-7}$$

This technique for computing propellant quantity is graphically illustrated (in two dimensions) in Figure 3-2.

It is now noted that the number of sample columns are finite and, hence, the "calculated" mass will not (necessarily) be precisely the "actual" mass. Also, the calculated mass will depend upon the configuration (spatial distribution) of the sample columns and the tank size and geometry. What is required, then, is a conversion — or, more correctly — a calibration curve from which the actual mass can be determined from the calculated mass, i.e.,

$$M_{act} = f\,(M_{calc}) \tag{3-8}$$

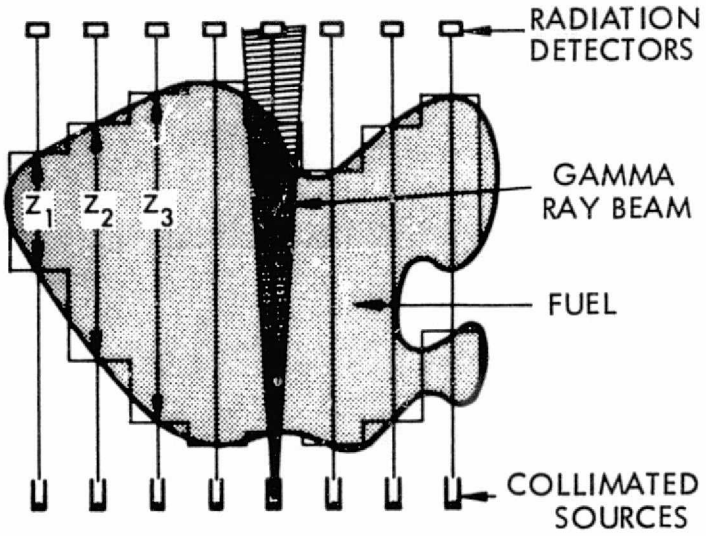

Figure 3-2. Two-Dimensional Area-Weighting for Computing Propellant Quantity

In practice, Equation (3-8) is solved with a computer simulation wherein the propellant can assume random orientations within a propellant tank under zero-g conditions. (See Reference 1.) However, Equation (3-7) is very easily mechanized with a small capacity digital computer and, a priori, so too are the functions represented by Equation (3-8).

3.2 SYSTEM DESCRIPTION AND DESIGN FEATURES

3.2.1 System Block Diagram

The system block diagram of the nucleonic gauging system is presented in Figure 3-3. As indicated, the system is comprised of two major assemblies:

1) The Flight Test Article (FTA)

2) The Electronic Subsystem (ESS).

In turn, the FTA is comprised of four collimated radiosiotope sources, the test tank and supporting cradle, and four Signal Conditioning Electronics (SCE) units. The ESS consists principally of the system's power supply and data processing electronics and is electrically interfaced to the SCE units of the FTA by means of a multiconductor umbilical cable.

3.2.2 The Flight Test Article (FTA)

As schematically depicted in Figure 3-4, the FTA consists of three major subassemblies:

1) Electronics Shroud. This subassembly contains the Signal Conditioning Electronics units (for detection, conditioning, and transmission of the diagnostic signals), the SCE mounting plates, and the junction box which interfaces the SCE unit's wiring harness to the Umbilical.

2) Tank/Cradle Subassembly. This subassembly consists of the optically clear test tank and a supporting cradle which

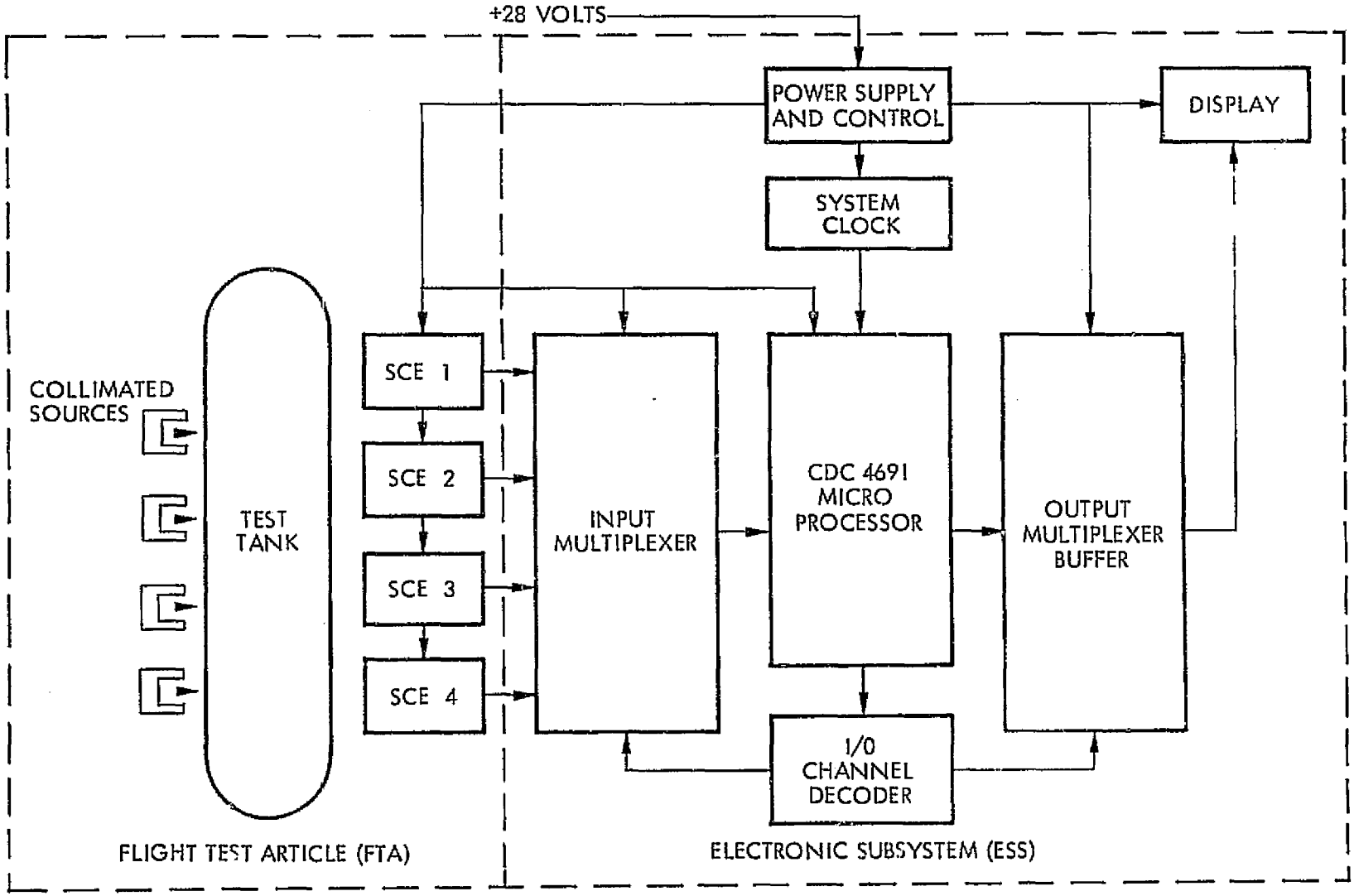

Figure 3-3. System Block Diagram

retains the test tank under both axial and longitudinal compression.

3) Collimator Subassembly. This subassembly contains the four Cs-137 radioisotopes mounted in the depicted uranium collimators.

As designed, the three subassemblies are rigidly bolted together as depicted in Figure 3-4, permitting the FTA to be free-floated within the aircraft cabin during the zero-g parabolic trajectory of the aircraft. The FTA has no sharp corners or projections and, when equipped with the two guard rails, damage to the FTA or the aircraft is minimized. During this program, however, the FTA was not free-floated, but was hard-attached to the cabin floor by bolting the base of the FTA directly to the floor. Additional rigidity was achieved by means of three guy-wires bolted to the floor and attached to the fittings which are welded to the three vertical support bars of the tank cradle as shown in Figure 3-5.

3.2.2.1 The Electronics Shroud

The Electronics Shroud contains the Signal Conditioning Electronics (SCE) units, associated support plates, and the junction box; Figure 3-6 presents photographs of the physical arrangement.

The arrangement shown permits the SCE units to be adjusted in the plane perpendicular to the gamma ray beams, thereby assuring that the detectors internal to each SCE unit intercept the beam at full intensity.

3.2.2.2 Tank/Cradle Subassembly and Propellant

The test tank employed in the FTA has a cylindrical center section 12 inches in length by 8 inches in diameter and is capped on either end by a hemisphere. The tank is fabricated from plexiglass and is polished inside and out to provide optically-clear tank walls.

The tank is fitted with two access ports — one for adding propellant (simulant) and the other for draining it. Each port has a V-flange to which is attached an aluminum screw-valve by means of a V-groove, quick-connect retaining ring. Pre-measured increments of propellant are introduced into the tank through the top valve via gravity from a polypropylene bottle. When the valve is open, water flows from the bottle, through the valve, and into the test tank. Closing the valve causes the access port to be sealed with a flush-fitting plastic plug which maintains a continuous, uniform interior surface. To drain the tank, the bottom valve is opened, and propellant flows via gravity through the valve to a catch-bottle (which can subsequently be weighed). When the tank is not in use, the valves are removed and both ports are sealed with matching plastic plugs.

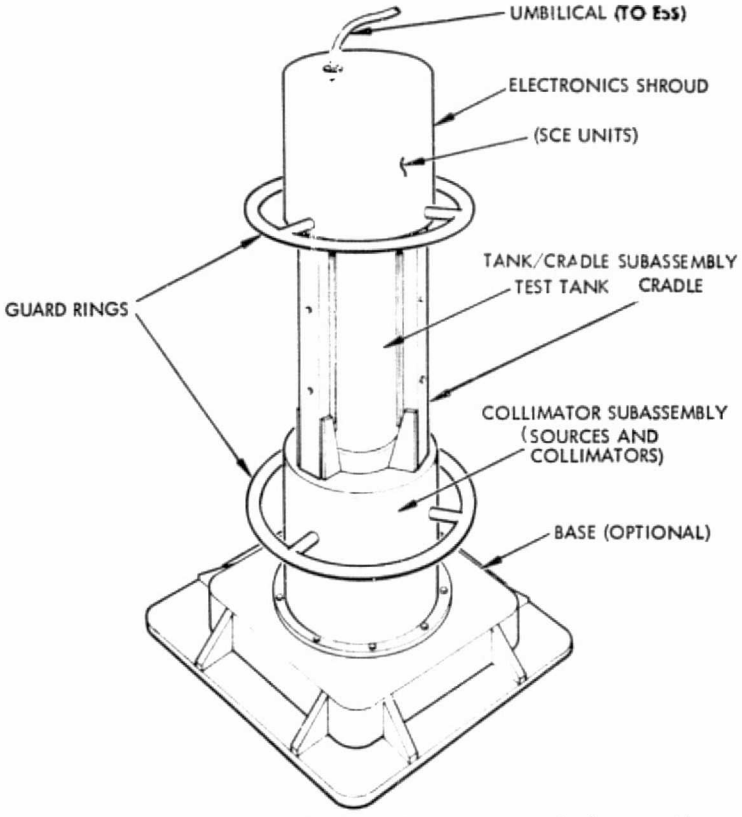

Figure 3-4. Flight Test Article Schematic (Free-Float Configuration)

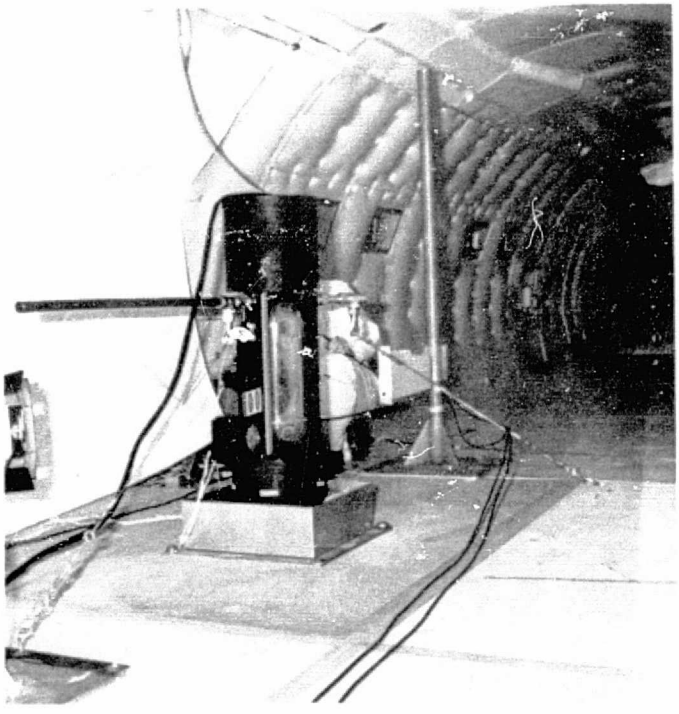

Figure 3-5. Flight Test Article (Bolted-Down Configuration)

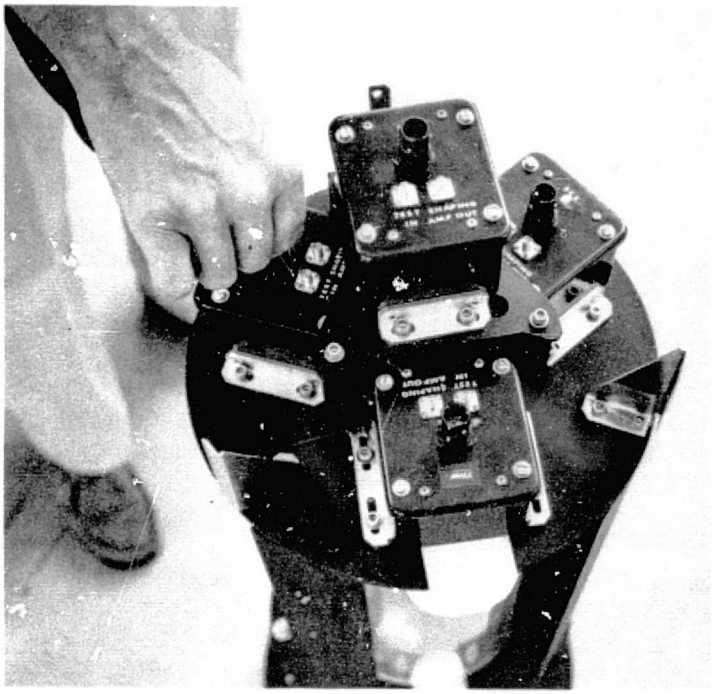

Figure 3-6a. SCE Units (Shroud Removed)

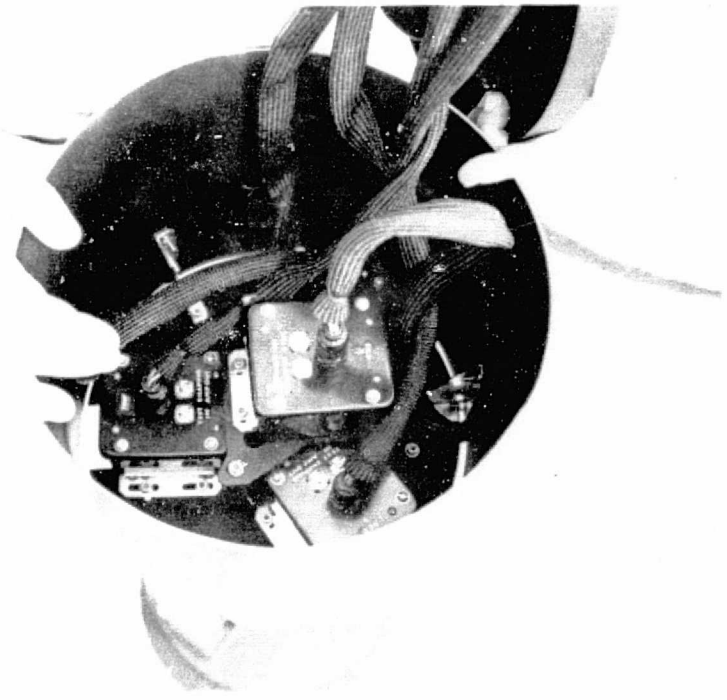

Figure 3-6b. SCE Units (Top Cover Removed)

The propellant simulant recommended for use in the test tank is water ($\rho/\sigma \approx 0.014$ sec^2/cm^3) which yields a time response in the test tank upon entering weightlessness of slightly greater than 1.5 seconds. During the program, the water was dyed with TBS to enhance the photographic coverage of the propellant behavior; no attempt was made to determine the effect of the dye on surface tension (or contact angle).

The test tank is restrained in a three-legged cradle as shown in Figure 3-4. One leg of the cradle is adjustable such that the tank can be retained under axial compression by torquing compression bolts in the cradle leg. Similarly, the tank is retained under longitudinal compression by torquing three compression bolts (on the SCE mounting plate) which causes the top cap to compress longitudinally the test tank. For servicing the tank is simply removed from the FTA by removing the three-leg retaining bolts and raising the tank vertically out of the cradle.

3.2.2.3 Collimator Subassembly

The collimators used in the FTA are shown in Figure 3-7. These collimators are fabricated from depleted uranium and then nickel-plated. Each collimator contains 7.5 Ci of Cs-137 double-encapsulated in stainless steel. The source capsule is retained in the collimator by the depleted uranium plug in the base, and by the bore diameter of the collimation channel being less than the capsule diameter. For shipping and storage purposes, the collimators are plugged with a depleted uranium plug which is inserted in the collimation channel and retained there by a B-nut screwed directly onto the collimator "nose". For operations within the aircraft, the depleted uranium plugs and B-nuts are replaced by the steel plug-plate shown in Figure 3-8 which is sandwiched between the Tank/Cradle Subassembly and the Collimator Subassembly as shown in Figure 3-9. When source activity is required, the Tank/Cradle Subassembly is unbolted (from the Collimator Subassembly) and removed to the side. This permits the plug-plate to be raised vertically, drawing the plugs simultaneously out of the collimation channels. The plug-plate is then stowed, the Tank/Cradle Subassembly reinstalled, and the FTA is then ready for gauging operations.

The comparatively large size of the collimators is the result of two design criteria. The first was to provide a high level of radiation shielding (in all directions) and, hence, biological protection for operating personnel. The second criterion was to maintain the level of intra-tank crosstalk (i.e., the amount of radiation "seen" by the j^{th} detector due to the i^{th} source) at the optimum level; in a reduced-scale tank where the source-detector channels are closely spaced to one another, the crosstalk criterion results in collimators with what appear to be inordinately long and slender "noses".

It is now noted that three of the collimators have a radius cut into their cylindrical side whereas the fourth collimator is completely circular. When assembled, the three collimators with the radius are clustered about the circular collimator and mounted in a "rosette" recess of the Collimator Subassembly base-plate. The collimators are retained

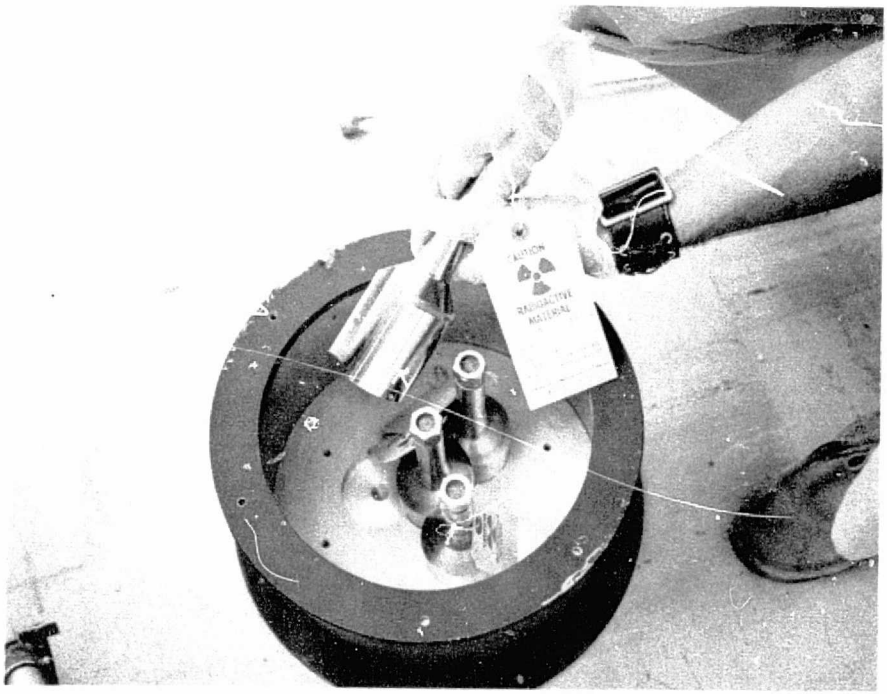

Figure 3-7a. Collimator Installation

Figure 3-7b. Completed Collimator Subassembly

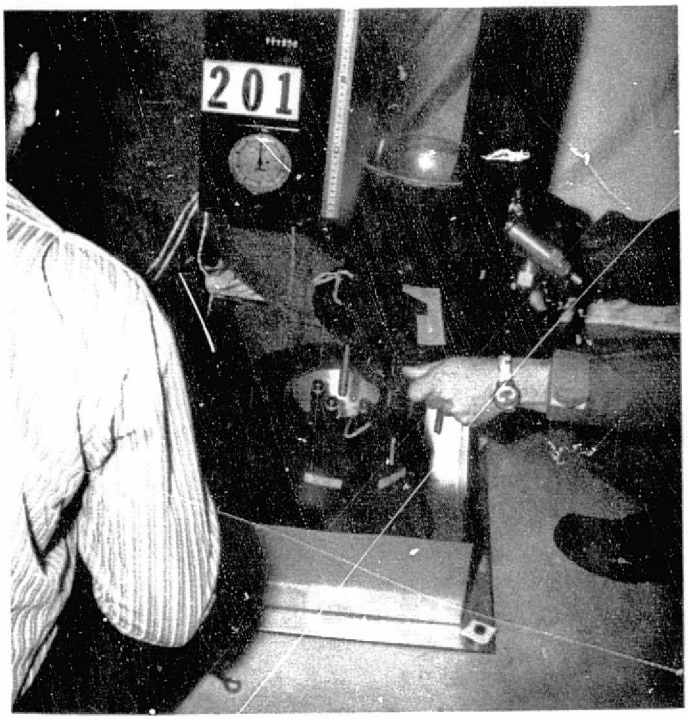

Figure 3-8. Plug Plate

Figure 3-9. Plug Plate Installed

rigidly on the base-plate by means of a retaining "hat" which is bolted directly to the base-plate. A compression gasket between the retaining hat and the collimators offsets dimensional tolerances and assures that the collimators are rigidly seated. The completed Collimator Subassembly is shown in Figure 3-7b.

3.2.3 The Electronic Subsystem

3.2.3.1 Signal Conditioning Electronics

The signal conditioning electronics consist of three distinct circuits, each with its own circuit board: (1) detector and charge sensitive preamplifier, (2) pulse shaping amplifier, and (3) pulse height window discriminator-monostable multivibrator-logic level converter as shown in Figures 3-10a and b.

The signal conditioning electronics are operationally illustrated in Figure 3-11.

The charge sensitive preamplifier converts the charge/γ generated within the integrally mounted CdTe detector to a charge-proportional voltage pulse by the following transform:

$$\frac{e_o}{q_d}(s) = \frac{1}{sC_d}\left[\frac{sC_d}{C_1\left(s + \frac{1}{R_1C_1}\right)}\right]$$

where

$q_d = 2 \times 10^{-8}$ coulomb for the photopeak of ^{137}Cs in CdTe

C_d = internal capacitance of Hughes 500 mm^3 detector and mounting hardware

R_1 = high megohm resistor selected for dc feedback stabilization

C_1 = low picofarad capacitor selected for desired conversion gain.

Inspection of the preceding transform indicates that all terms containing the detector capacitance, C_d, cancel leaving the charge conversion gain dependent solely upon the value of the feedback capacitor, C_1. The single-pole time-dependent response is thereby:

$$\frac{e_o}{q_d}(t) = \frac{1}{C_1}\left(e^{-\frac{t}{R_1C_1}}\right) \qquad (3\text{-}9)$$

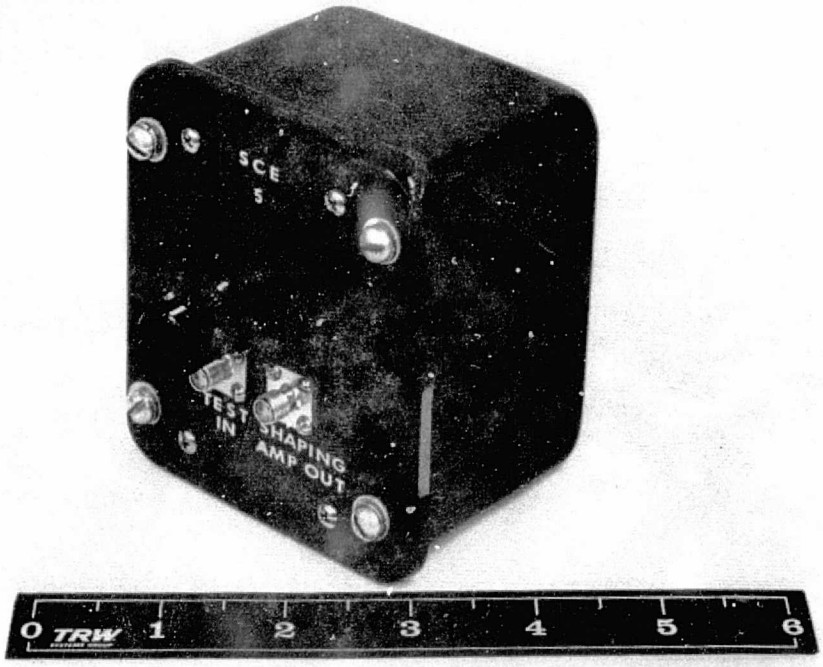

Figure 3-10a. SCE Unit

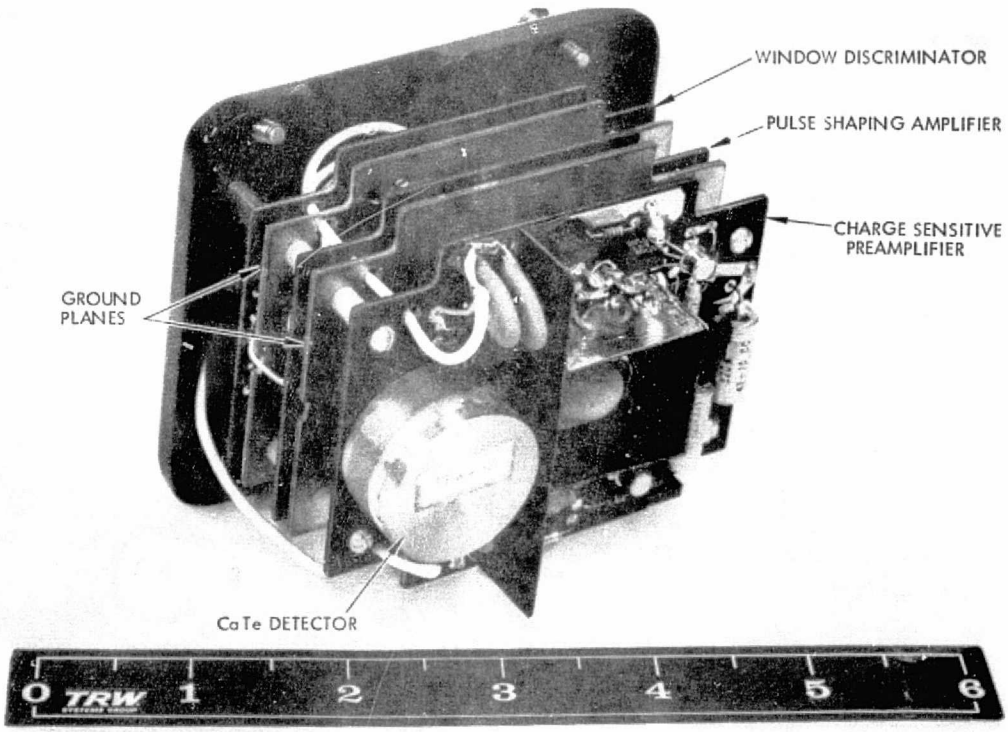

Figure 3-10b. Uncased SCE Unit

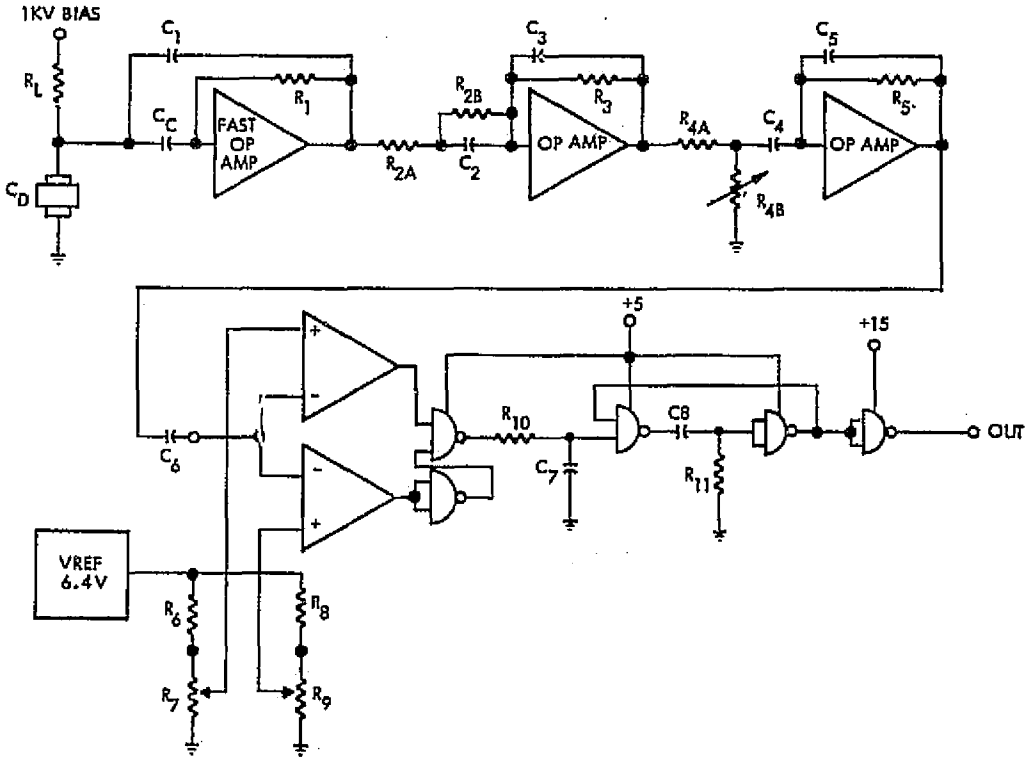

Figure 3-11. Zero-G Signal Conditioning Electronics Diagram

The preamplifier, shown in Figure 3-12, due to a unique design consisting of a minimum number of active components in the signal path, exhibits an extremely fast risetime (10 ns), and low noise (5.5 kev FWHM CdTe). When used with CdTe detectors of 5 pf capacitance the resolution of the detector-electronics system becomes completely dependent upon the quality of the CdTe detector used.

Provisions are incorporated to allow for bias voltages as high as 3 kilovolts to ensure an adequate voltage breakdown safety margin when used with large volume CdTe devices.

The shaping amplifier is formed by two active bandpass filter stages providing double differentiation-double integration (DDDI) pulse shaping. Bipolar shaping was selected over unipolar shaping since pulses processed by former method are more symmetrical about the base line, therefore allowing smaller count-rate dependent base-line shifts than less-symmetrical equal area pulses. Pole-zero compensation (unit step restoration) of the preamplifier decay time constant is achieved by setting $R_1C_1 = R_{2b}C_2$. The differentiation and integration time constants are made equal and set at 0.25 μsec based primarily on coincidence probability and impact on circuit complexity.

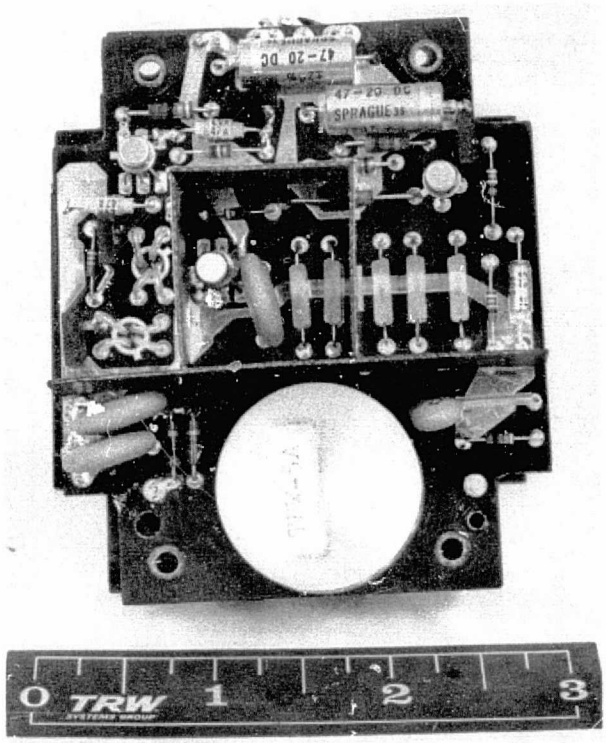

Figure 3-12. Uncased Preamplifier

Figure 3-13 shows the pulse shaping amplifier, $\tau = 0.25\ \mu s$, as configured for the zero-g gauge. Pole-zero compensation of the preamplifier decay time constant is achieved by setting $R_1C_1 = R_{2b}C_2$. The differentiation and integration time constants were set at 0.25 μs as determined by coincidence probability and circuit speed. The shaping amplifier transfer function is

$$\frac{e_o}{e_i}(s) = \left[\left(\frac{S + \frac{1}{R_{2b}C_2}}{R_{2a}C_3\left(S + \frac{1}{\frac{R_{2a}\cdot R_{2b}}{R_{2a}+R_{2b}}C_2\right)\left(S + \frac{1}{R_3C_3}\right)}\right) X \right. \qquad (3\text{-}11)$$

$$\left. \frac{S}{\frac{R_{4a}\cdot R_{4b}}{R_{4a}+R_{4b}}C_5\left(S + \frac{1}{\frac{R_{4a}\cdot R_{4b}}{R_{4a}+R_{4b}}C_4\right)\left(S + \frac{1}{R_5C_5}\right)}\right)\right]$$

where

$$\tau_{diff} = \tau_{int} = 0.25\ \mu s = \frac{R_{2a} \cdot R_{2b}}{R_{2a} + R_{2b}} C_2 \simeq R_3 C_3 = \frac{R_{4a} \cdot R_{4b}}{R_{4a} + R_{4b}} C_4 = R_5 C_5 \qquad (3\text{-}12)$$

Gain control is achieved by varying the value of potentiometer R_{4b}.

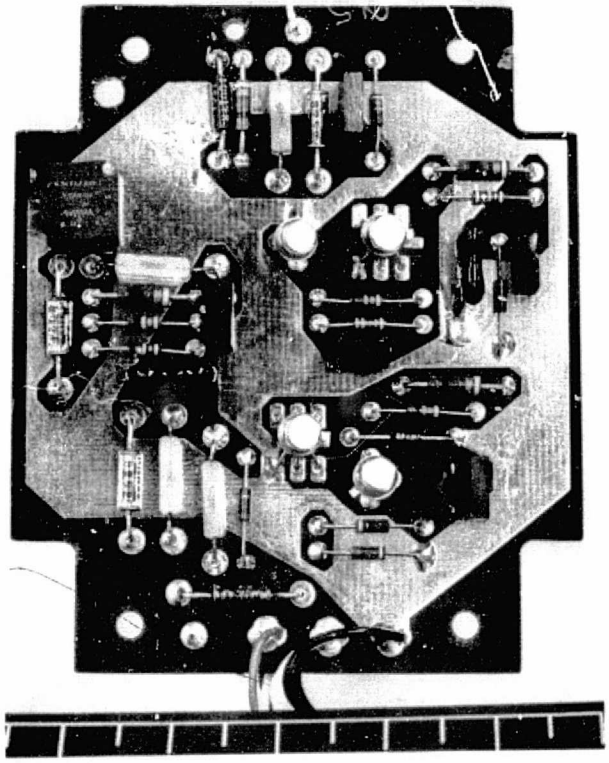

Figure 3-13. Uncased Pulse Shaping Amplifier

The closed-loop dc and ac gain curves for the pulse shaping amplifier are given in Figure 3-14.

The pulse height discriminator is comprised of upper and lower pulse height threshold discriminators (high-speed, high-performance integrated operational amplifiers), a stable temperature compensated threshold voltage source, a decision gate, and a TTL monostable multivibrator. The discriminator "window" adjustments are described by the following relationships:

$$V_{LTH} = \frac{6.4\ R_9\ (\%)}{100(R_8 + R_9)} \qquad V_{HTH} = \frac{6.4\ R_7\ (\%)}{100\ (R_6 + R_7)} \qquad (3\text{-}13)$$

A single single-pole lag network consisting of R_{10} and C_7 has been provided to allow sufficient time for both thresholds to be encountered prior to the monostable triggering decision.

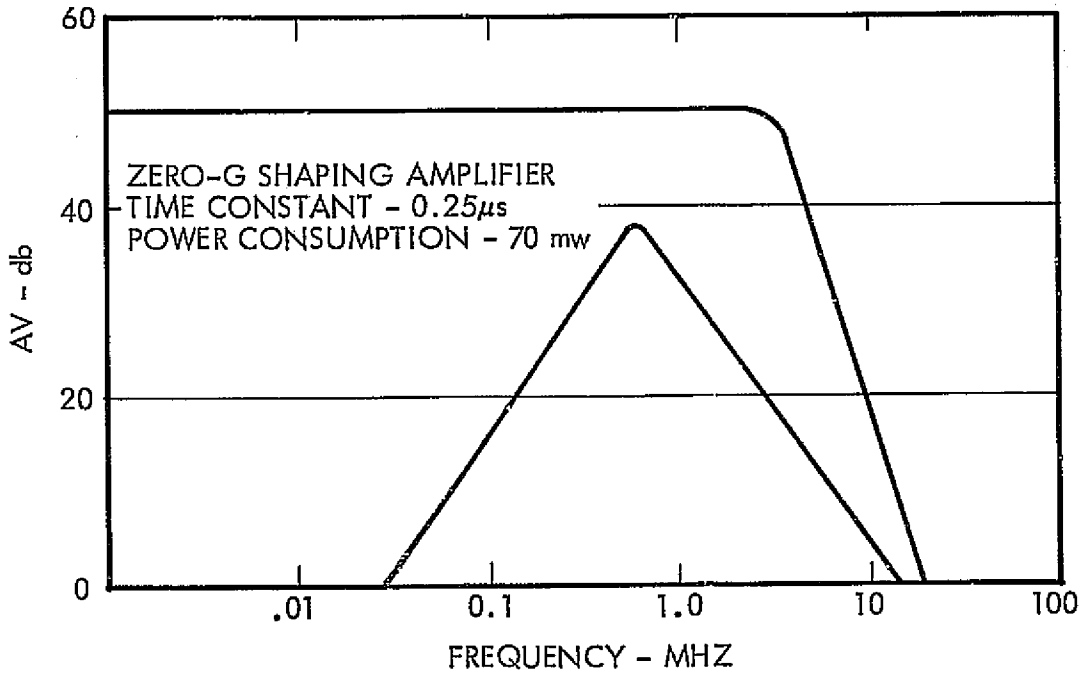

Figure 3-14. Closed Loop Gain for Pulse Shaping Amplifier

Overall performance of the signal conditioning electronics is given by Figure 3-15. As can be seen, the lower threshold stability (most critical due to its position in the spectrum "valley"), is essentially perfect over a temperature range from +10°C to +50°C. Outside this region, sufficient variation in CdTe performance will mask the effects of any energy threshold variation.

The output of the signal conditioning electronics (discriminator) is a series of rectangular pulses — each corresponding to one detector count — of 15 vdc amplitude and 0.25 μs width. These pulses are CMOS compatible and designed to interface with the zero-g processor interface package separated by ≤100 feet of coaxial cable.

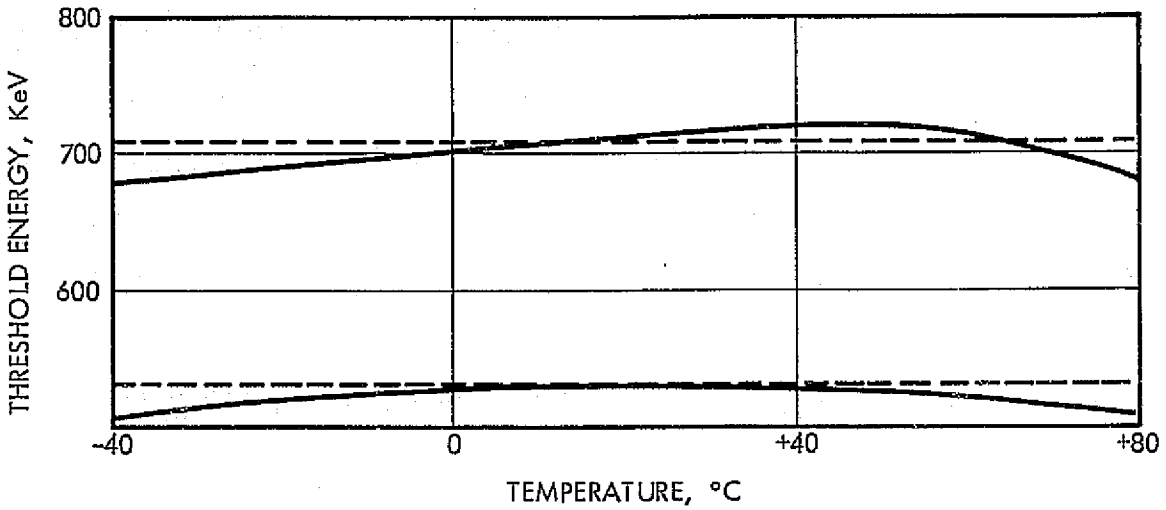

Figure 3-15. Zero-G Gauge Discriminator Threshold Versus Temperature

3.2.3.2 System Processor, Control, and Interface

General Method of Operation

The output of each SCE is directly inputted to a 21-stage binary counter; each of the CMOS counters has a capacity of 2^{20} counts and is associated with a particular source detector pair. These counters, along with the system clock and computer scratch pad, are initially reset during the power-up operation by a master reset line from the power supply. When all power is nominal, this line goes to a low state (logic level) which initializes the system clock at t = O and allows the counters to begin accumulating pulses. At the end of the 1-second accumulator cycle, the system clock, by means of a computer interrupt, causes the processsor to initiate the mass computation program. When, as part of the program, the computer I/O addresses the pre-assigned input channels, all of the count accumulators are inhibited, and the count data retained therein are stored in the processor memory along with the corresponding channel status. Because 0.1 percent count accuracy is required, all 21 bits of binary count data must be stored in core, requiring the use of double-precision input words (32 bits). The count accumulators are reset and restored to an accumulation mode by a "data acquired" pulse provided by the processor when the least significant half-word of the last channel (i.e., source-detector pair) has been read and stored. The processor then tests (a word derived from the failure input data) for a channel failure and automatically selects the appropriate software (loaded and internally stored during system calibration), computes the propellant mass, and updates the mass display while the counters are acquiring count data for the next measurement iteration. Iterations subsequent to the first occur every second; i.e., mass is recomputed every second.

The processor is interfaced to the display by means of a channel decoder and buffer electronics. A subroutine incorporated within the processor creates the BCD format required by the display drivers. Output buffering is accomplished through the use of Type "D" flip-flops which are updated by an output timing command from the processor.

The display for the mass readout is a Dialco seven segment LED featuring a 0.625-inch character height. Additionally, status of individual channels are indicated by special film masks contained in rear projection displays.

Input Multiplexer

As previously described, the output of each SCE unit is a series of CMOS-compatible rectangular pulses — each pulse corresponding to one detector count — of 15 vdc amplitude and 0.25 μsec width. The number of these pulses accumulated over a prescribed time interval constitutes the count data on which the central processor calculates the propellant mass. Since the processor obviously cannot accept count data indiscriminately, a level of logic must be established between the output of each individual SCE unit (the count data) and the input buss of the processor. This logic, which must also be communicative with the processor, is accomplished by the "Input Multiplexer".

The Input Multiplexer is shown physically in Figures 3-16a and b. As shown, the Input Multiplexer consists of four 21-stage CMOS counters — one for each SCE unit — whose outputs are paralleled via CMOS bilateral switches which are connected directly to the input buss of the 469I processor. Counter control and logical input of accumulated count data are established by means of the processor's I/O Channel Select Register, the I/O Channel Decoder, and the various decision gates shown.

It is now noted that the method of operation of the Input Multiplexer is fundamentally identical for each of the 4 SCE outputs; therefore, in the interest of brevity (and clarity), the operation of the input Multiplexer will be described for only one SCE channel.

It will be recalled that the counters, system clock, and computer scratch pad are initially reset during the power-up operation by a master reset line from the power supply. When all power is nominal, this line goes to a low state (logic level) which starts the system clock and allows accumulation of pulses from the SCE output. Pulses, i.e., the count data, are accumulated in a 21-stage binary ($2^{20} - 2^{0}$) counter. Seven other stages are available: four for the system status, two as spares, and one connected to ground (indicating sign positive). At the end of the prescribed accumulation cycle (e.g., 1 second) the system clock, by means of a computer interrupt, initiates the mass computation program. This interrupt is accompanied by a processor command which transmits a hexadecimally coded word via the I/O Channel Decoder, physically

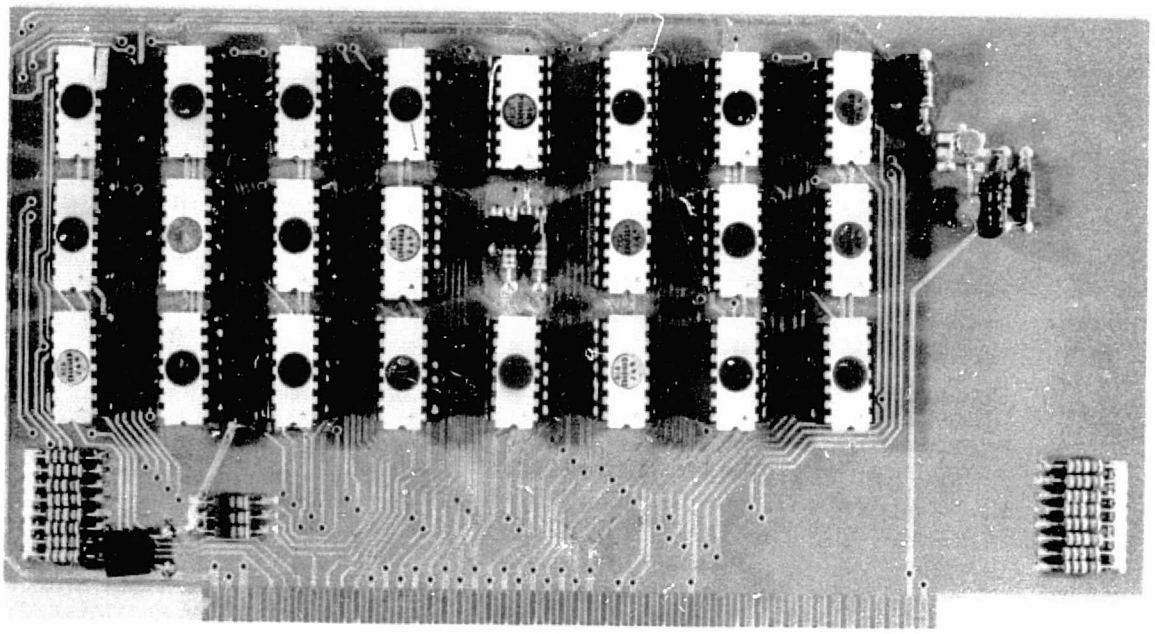

Figure 3-16a. Input Multiplexer (A-Board)

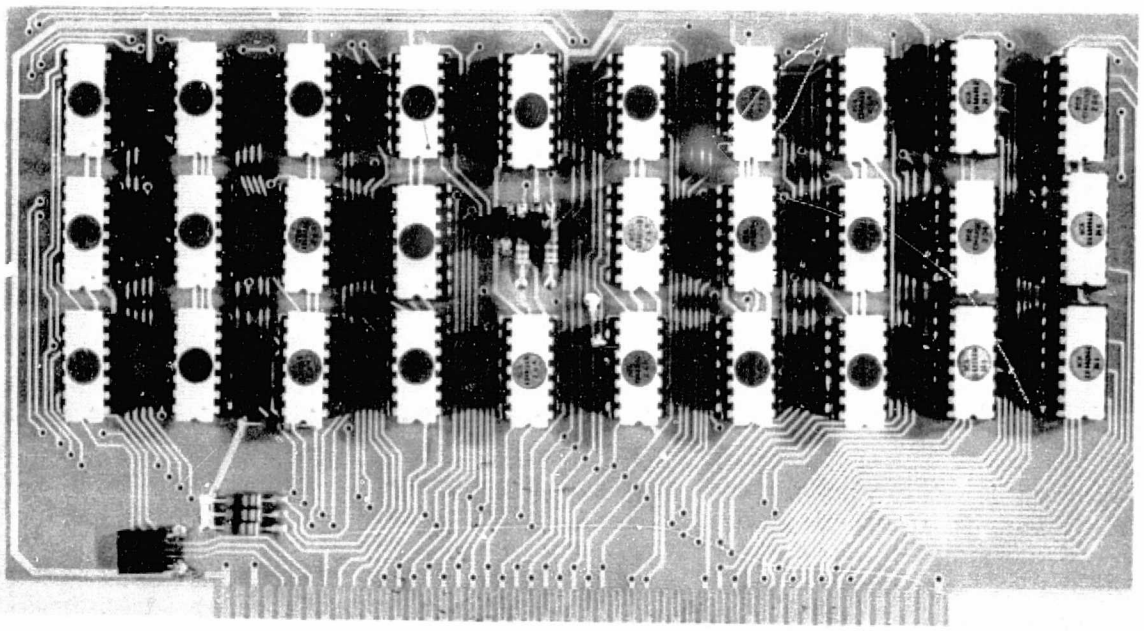

Figure 3-16b. Input Multiplexer (B-Board)

shown with the System Clock and Output Multiplexer in Figure 3-17. The I/O Channel Decoder operates on the hexadecimally coded word to decide which one of the 16 I/O channels is activated. It should be noted that in this activation process, if any of the channels 6-15 (octal) are activated, i.e., raised to a high logic level, then all pulse accumulation ceases. In the case at hand, the process is initiated with the activation of Channel 6_8 — which corresponds to SCE unit No. 1 — and all count accumulation will cease. Simultaneously, activation of Channel 6_8 applies the most significant number of counts (sign plus bits 2^{20} to 2^6) that were accumulated in the counter to the 16 lines of the processor input buss. When this input word has been stored, the processor advances the I/O Channel Select Register to the next higher channel (e.g., Channel 7_8). Since this channel — at a high logic level — is within 6-15 (octal), note that all the count accumulators will remain inhibited. Simultaneously, with the activation of Channel 7_8, the least significant numbers of counts (bits 2^5 -2^0) plus the system status (a 4 bit word) — also corresponding to SCE unit No. 1 — are applied to the most significant lines of the input buss and subsequently stored in the processor. Thus, each SCE unit output requires two "stepping functions" from the processor: the first to acquire the most significant count data and the second to acquire the least significant count data and system status.

After the count data are acquired for SCE unit No. 1, the processor continues to advance the I/O Channel Select Register sequentially until the following sequence has been completed:

SCE No.	Channel No. (Octal)	Data Acquired
1	6	Most Significant Bits (MSB)
1	7	Least Significant Bits + Status (LSB+S)
2	10	MSB
2	11	LSB+S
3	12	MSB
3	13	LSB+S
4	14	MSB
4	15	LSB+S

The sequence is "closed" when the data on Channel 15_8 are applied to the input buss, accepted by the processor, and a "data accept" pulse is applied simultaneously with the high logic level Channel 15_8 line to the decision gate to reset the counters. Concurrent with the resetting of the counters, the processor automatically switches the I/O Channel Select Register to a standby input channel (Channel 0). The input buss is then effectively in an "idle" mode, and the counters again begin to accumulate pulses until the system clock initiates the cycle again from the beginning.

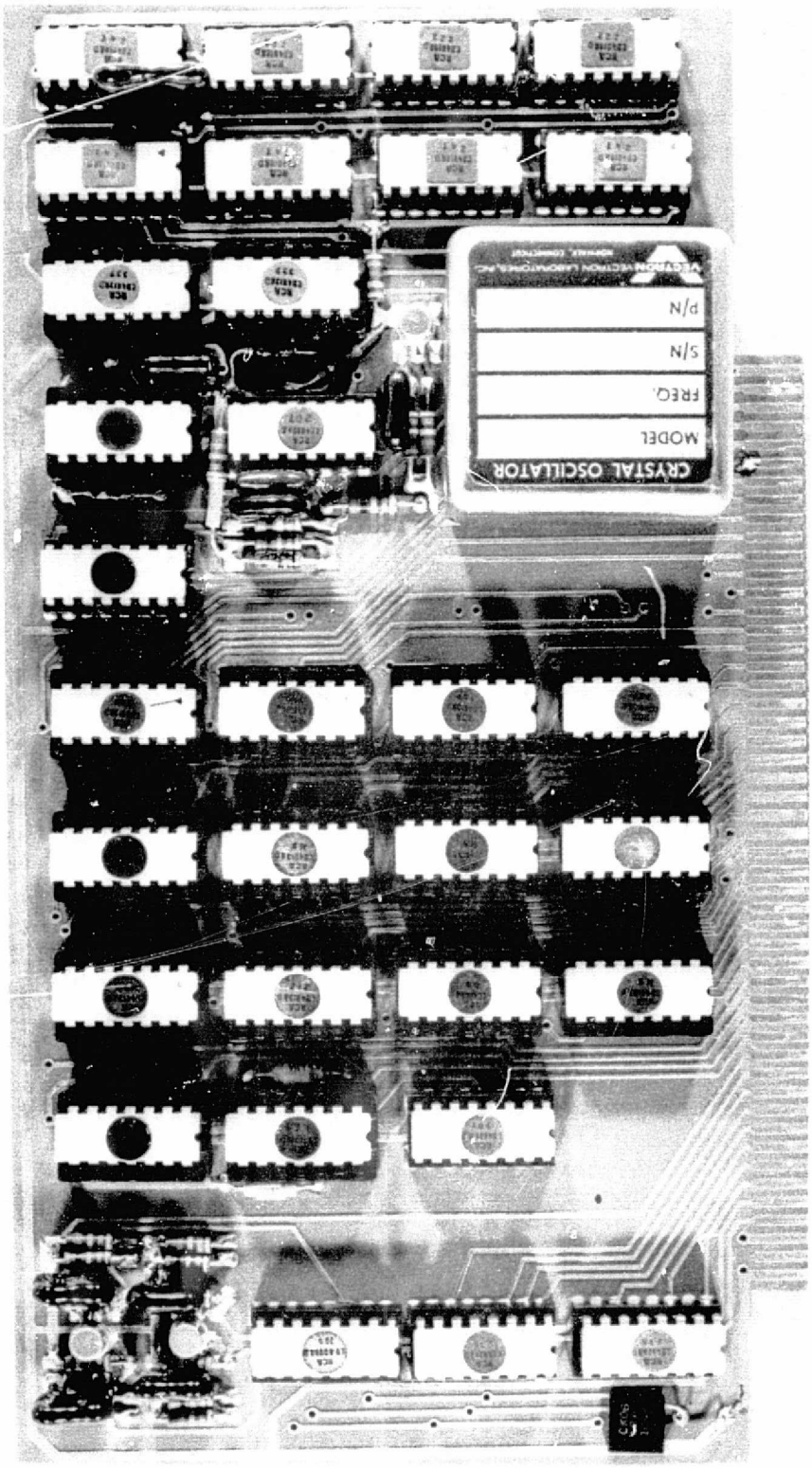

Figure 3-17. Output Multiplexer, I/O Channel Decoder, and System Clock

Count Accumulators

The count accumulators consist of 21-stage binary counters having a per accumulator capacity of $2,097,151_{10}$ counts and an accumulator speed of 10 MHz. Each of the accumulators is comprised of three CMOS integrated circuits (RCA Type CD4024AD), consisting of an input pulse shaping circuit, reset line driver, and seven binary counter stages. The entire accumulator is reset to "zero" by a high level on the reset input. Each counter stage is a static master-slave flip-flop. The counter state is advanced one count on the negative going transition of each input pulse. Logic is provided (RCA Type CD4011AD) to allow inhibition from continuous counting at the completion of the accumulation cycle upon command from the system processor. Due to the static nature of the binary counting elements, the accumulated count is retained in, and available at, the outputs of the binary counters until such time as they are reset.

System Processor

The Control Data Corporation 469 Digital Computer selected as the system processor is a fourth generation, state-of-the-art metal oxide semiconductor (MOS) large scale integrated (LSI) digital computer designed to operate reliably in areas of applications where small size, light weight, low power, and existence in a severe environment are imperative. Physical and electrical characteristics for the 469 Computer are presented in Table 3-1; Figure 3-18 is a photograph of the 469 Computer.

The memory used in the 469 processor is constructed with plated wire elements and is typically referred to as PWM (plated wire memory). This type of memory allows random access, is word organized, and does not require rewriting after a read cycle. Because of this nondestructive readout characteristic, the operating mode of the system is much faster. The basic word length is 16 bits with a read cycle time of 1.6 microseconds, a write cycle time of 2.4 microseconds, and an access time of 900 nanoseconds.

The operational registers of the 469 central processor reside in a set of MOS/LSI devices called the register file. This register file contains sixteen 16-bit registers composed of four MOS/LSI devices, each containing eight words of 8 bits each. The file registers are addressable as the first 16 words of memory for upward references and are used as accumulators for operation executed from the program stored in the write-protected portion of the PWM.

Along with the central processor, the following peripherals are available:

a) Programmer's console

b) Magnetic tape memory loader

c) Controller interface

d) ASR 33 TTY or 733 KSR

Table 3-1. CDC 469 Characteristics

Word Length	16 Bits
Memory Size	8192 Words
Interface Levels	0 to 5 Volts
Weight	2.75 Pounds
Volume	60 Cubic Inches
Power	15 Watts
Cooling	Conduction and Radiation

Central Processor

- o General purpose, binary, parallel, single address
- o Logic: High level P-MOS/LSI
- o Hardware registers: 16
- o Arithmetic: fractional, fixed point, two's complement
- o Clock: 4 MHz (1 MHz cycle rate)
- o Instructions: 42 total

Input/Output

- o Input channels: one, 16 bit, parallel
- o Output channels: one, 16 bit, parallel
- o Interrupt levels: 3 plus direct execute
- o Serial I/O: 1 In: 1 Out

The programmer's console is connected directly to the central processor and displays instantaneously the contents of the register files. The user has the option of controlling the execution of the object code either under a step-by-step execution mode or a normal execution mode. If a certain instruction need be changed, the new instruction and the related data word can be entered onto the console and entered directly into the object code from the console.

Output Multiplexer/Buffer

The Output Multiplexer, shown in Figure 3-17, is designed to accept mass and status data from the processor and store said data for constant display until such time as it is updated by the processor as part of the gauging cycle. Thirteen RCA CD4013AD dual Type "D" flip-flops are used to accept and store data made available by the processor on I/O Channels 16_8 and 17_8. Channel 16_8 contains BCD coded mass data and is "written" on eight CD4013ADs when the hexidecimal code

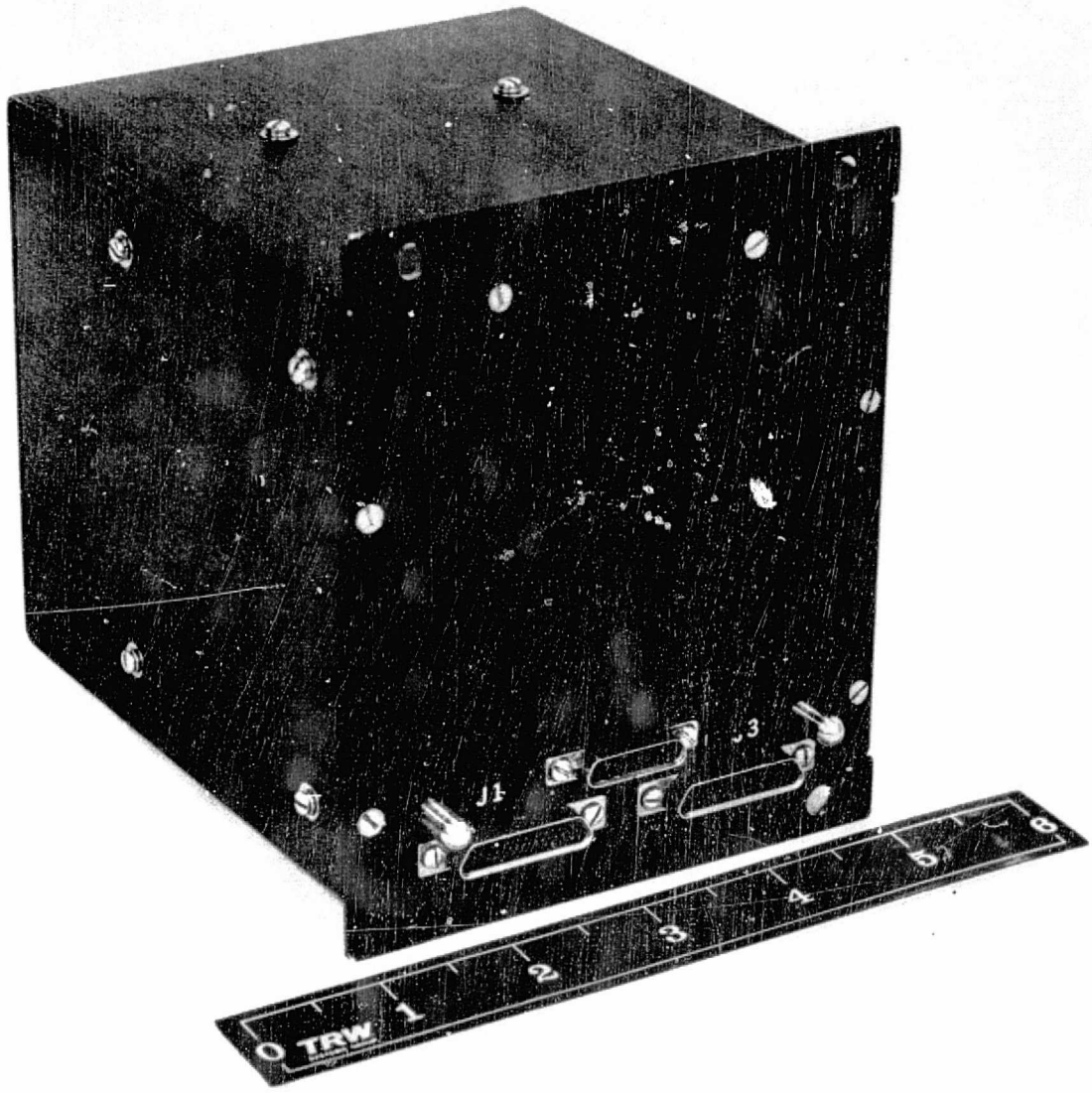

Figure 3-18. CDC 469I Computer

for 16_8 is placed on the I/O select buss and the output timing line from the CDC469 is strobed. System status information is stored in the remaining five CD4013ADs in an identical manner, with the only exception being that 17_8 is placed on the I/O select buss prior to the output timing strobe pulse.

System Clock

The system clock (shown in Figure 3-17) provides all timing signals necessary for proper gauge operation. Extreme timing accuracy is imperative as the mass calculation is based on counts accumulated during a precise time interval. To achieve the desired accuracy use of a temperature stable crystal controlled clock oscillator was required. For this purpose a CMOS compatible 4 MHz (±0.001 percent) clock manufactured

by Vectron Laboratories was selected. The output of the crystal clock is used to perform two functions: (1) to slave the internal CDC469I 4 MHz clock to a more accurate timing source (more stable operations and sequence timing), and (2) provide the reference clock signal to the system timing count-down logic for interrupt generation.

The system timing cycle is initiated by a low logic level applied to the master reset line. A count-down chain consisting primarily of RCA CD4013AD and CD4018AD counter ICs is used to generate a processor Level 1 interrupt 1 second after the initial power-up sequence and every second thereafter.

3.2.3.3 System Display

The System Display is mounted in the Display Console shown in Figure 3-19; the face of the Readout Display as viewed from the console is also graphically depicted in this figure.

To power the system, the Power Control Switch—mounted in and an integral part of the Readout Display—is depressed. Being a "screen-switch," the face of the Power Control Switch will immediately illuminate indicating "Power-On" and power status "Not Nominal". When power reaches nominal, the power status is grounded and the Not Nominal indication will extinguish. In fact, the Not Nominal indication is not visible during power up due to the short duration (the order of milliseconds) required to reach nominal status.

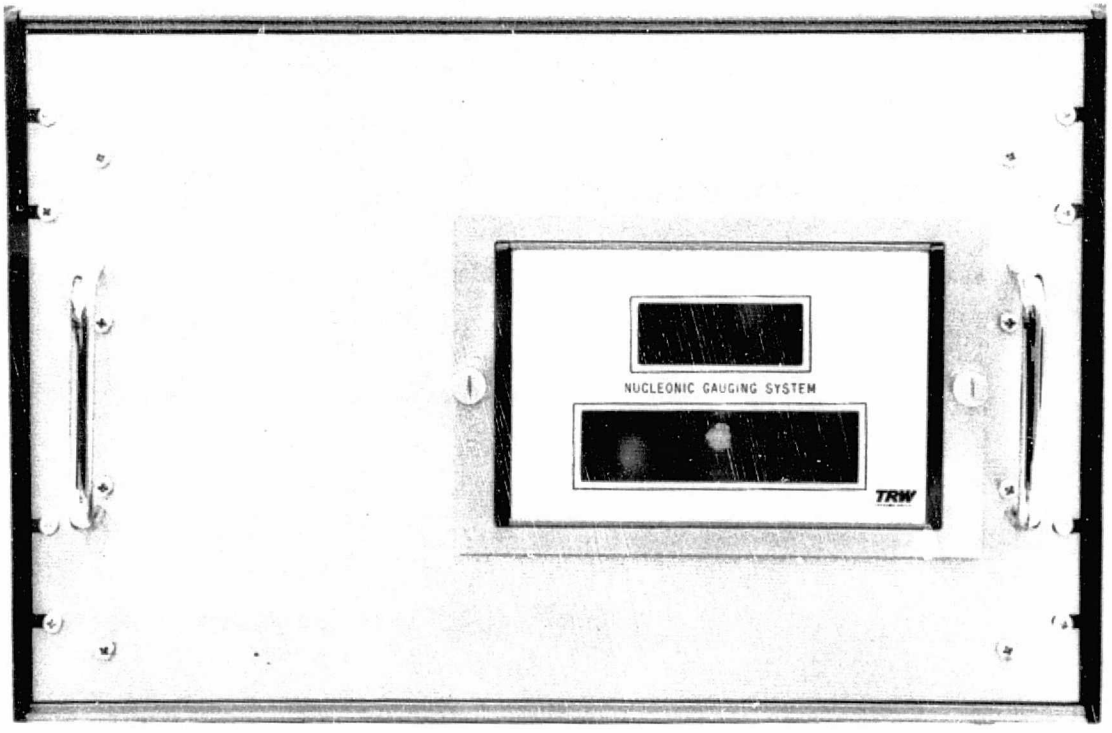

Figure 3-19. System Display Console

For the first second after application of power, the mass display is blanked by the logic level on a line which is derived from the system clock. Likewise, the mass display will blank at any time the system power is not nominal. After the inital 1-second (count accumulation) period, the mass display is unblanked, and the numeric characters representing the mass in pounds are illuminated.

The mass display is a Dialco 4-character, 7-segment solid state (LED) readout assembly with 0.625-inch character height. The 4 characters indicate mass digits in thousands, hundreds, tens, and units, respectively. The appropriate mass digit as computed in the processor is transmitted (Channel 16_8) via the output Multiplexer to the mass display as a 16-bit word. The display converts the 16-bit word to the 7-segment readout by means of an integral BCD to 7-segment decoder.

System status is transmitted (Channel 17_8) via the output Multiplexer to the Channel Status which is also located on the Readout Display. The Channel Status consists of 4 rear-projection display units—one for each SCE unit—equipped with film masks designating the nature of the failure in each channel, and also the degradation in the accuracy of the displayed mass due to the failure. For example, if the detector fails on (SCE) unit No. 3, this is automatically sensed electronically and, by means of decision "logic" in the Processor, the failure is indicated by applying power to one of the lamps of the No. 3 Channel Status (rear-projection) display unit. The failure will be indicated by the face of the display unit being illuminated — in this case with the color red — through a red film mask. Similarly, the accuracy degradation in the indicated mass due to the failure of SCE unit No. 3 is also displayed on the (now red) No. 3 Channel Status by powering another lamp within the rear projection display; the face of the display will not contain (additionally) a numeric value for the system accuracy.

In the unlikely event of a catastrophic failure — loss of all SCE units, total power failure, etc. — a logic line is activated, the mass display is blanked, and all Channel Status units are illuminated.

3.2.3.4 System Controller and Power Supply

The system low voltage power supply provides +15, +5, and -3 volts for operation of the computer and interface circuitry. The high voltage power supply provides bias for the CdTe radiation detectors located in the SCEs.

The power supply controller continuously monitors the outputs of the low voltage power supply. It provides "stop" and "clear" signals to the computer in the event that any or all of the supplies drop below 1 percent of their nominal values. If any or all of the supplies rise to greater than 1 percent of their nominal values, the controller stops and clears the computer and then removes power from the entire system.

The low voltage power supply consists of two sect. ns—the oscillator/ rectifier portion and the regulator section; Figures 3-20 a and b present the physical layout of these two circuits, respectively. In the oscillator/ rectifier section, +28 volts is used to power a square wave oscillator that drives the primary of a toroid transformer. The ac voltages derived from the multiple secondary windings are rectified by bridge rectifiers and filtered by 100 mf capacitors. Motorola MC1561R monolithic regulators are used to provide a high degree of line and load regulation. Because of the limited amount of current available on the output of the regulators, series pass transistors are used on the +15, -15, and +5 volt supply. Reduced load requirements on the -3 volt supply made a pass transistor unnecessary.

Figure 3-21 shows the electrical schematic of the power supply controller.

The operation of the power supply controller is as follows: transistor Q1 and associated circuitry provide approximately 14.5 volts to power the controller. Integrated circuit Z1 and transistor Q2, diodes CR1 and CR2 produce an extremely stable and temperature compensated 10-volt reference voltage for comparators Z2, Z3, Z4, Z5, Z8, Z9, Z10, and Z11. These comparators are connected such that in the case of an over- or under-voltage condition, a logical one (~15 volts) appears on the output of the 8-input "OR" gate formed by diodes CR4 through CR11. This high voltage passes through a CMOS buffer and turns on transistor Q3 which stops the computer. In a similar manner of the computer is cleared by transistor Q4, except that the signal is delayed approximately 100 microseconds by R46 and G31. This sequence of stopping and then clearing the computer is necessary to prevent the memory of the computer from being scrambled when the power supplies are non-nominal or when powering down normally.

If an over-voltage condition exists on any of the supplies, there is a high voltage on the output of the 4 input "OR" gate formed by diodes CR13 through CR15 and also on diodes CR4 through CR11. This stops and clears the computer and causes the flip-flops in Z15 to reset which makes transistors Q6 and Q7 turn off, thereby removing the 28 volts from the low voltage oscillator previously described.

The on-off switch located on the display unit triggers a monostable multivibrator formed by cross-coupled gates in Z15; this provides a noise-free pulse to turn the supply on and off.

The high voltage power supply is shown in Figure 3-22.

3.2.4 Subsystem Assembly

All four power supply circuit boards previously described are stacked atop each other with a copper shield between each board. All interboard connections pass through ceramic EMI filters. This assembly is mounted on spacers and fastened to its own self-contained box.

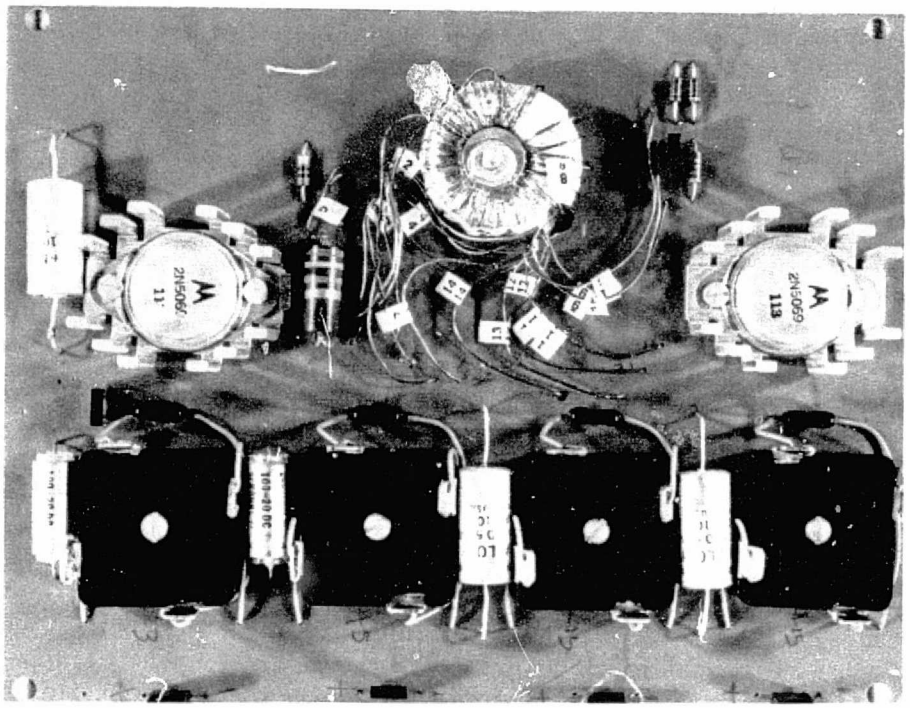

Figure 3-20a. Low Voltage Power Supply: Oscillator/Rectifier Section Assembly

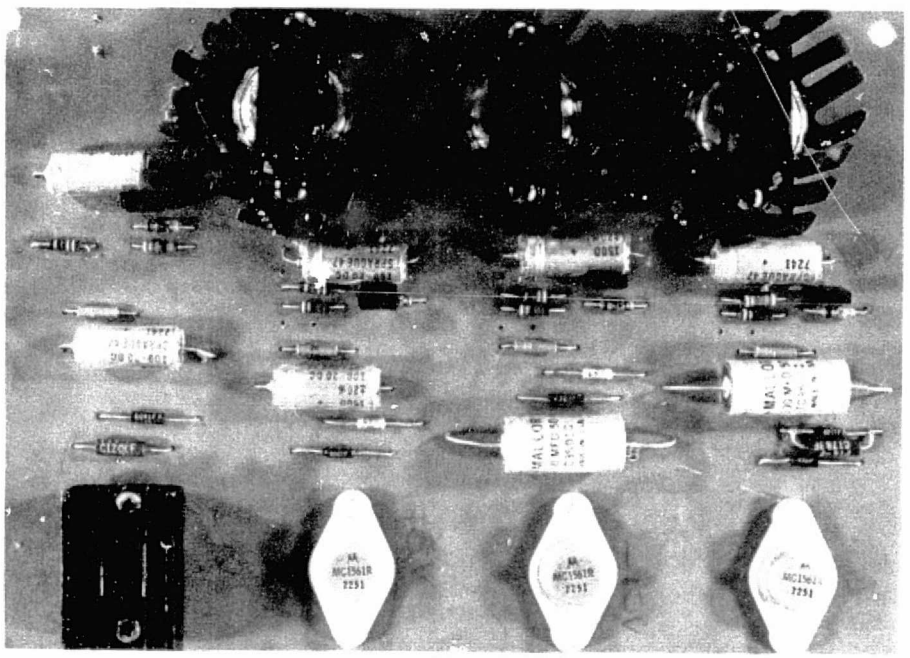

Figure 3-20b. Low Voltage Supply: Regulator Section Assembly

FOLDOUT FRAME

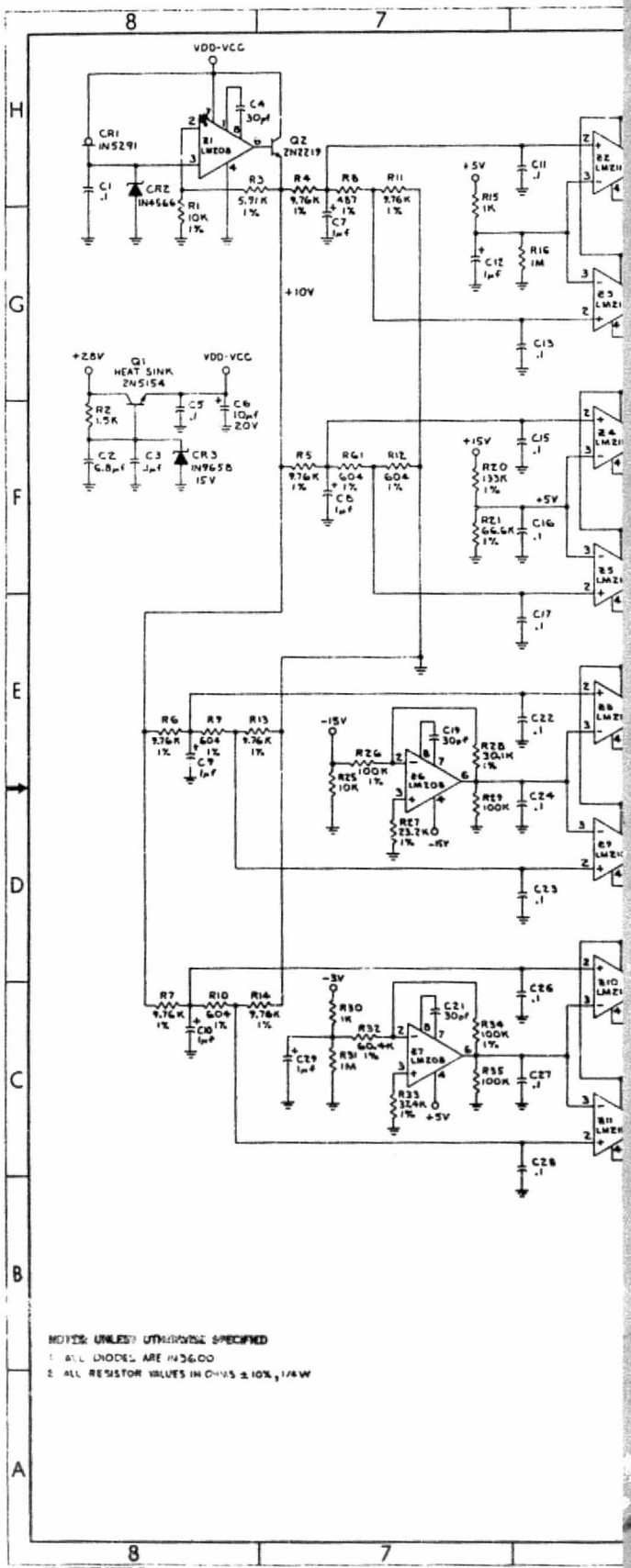

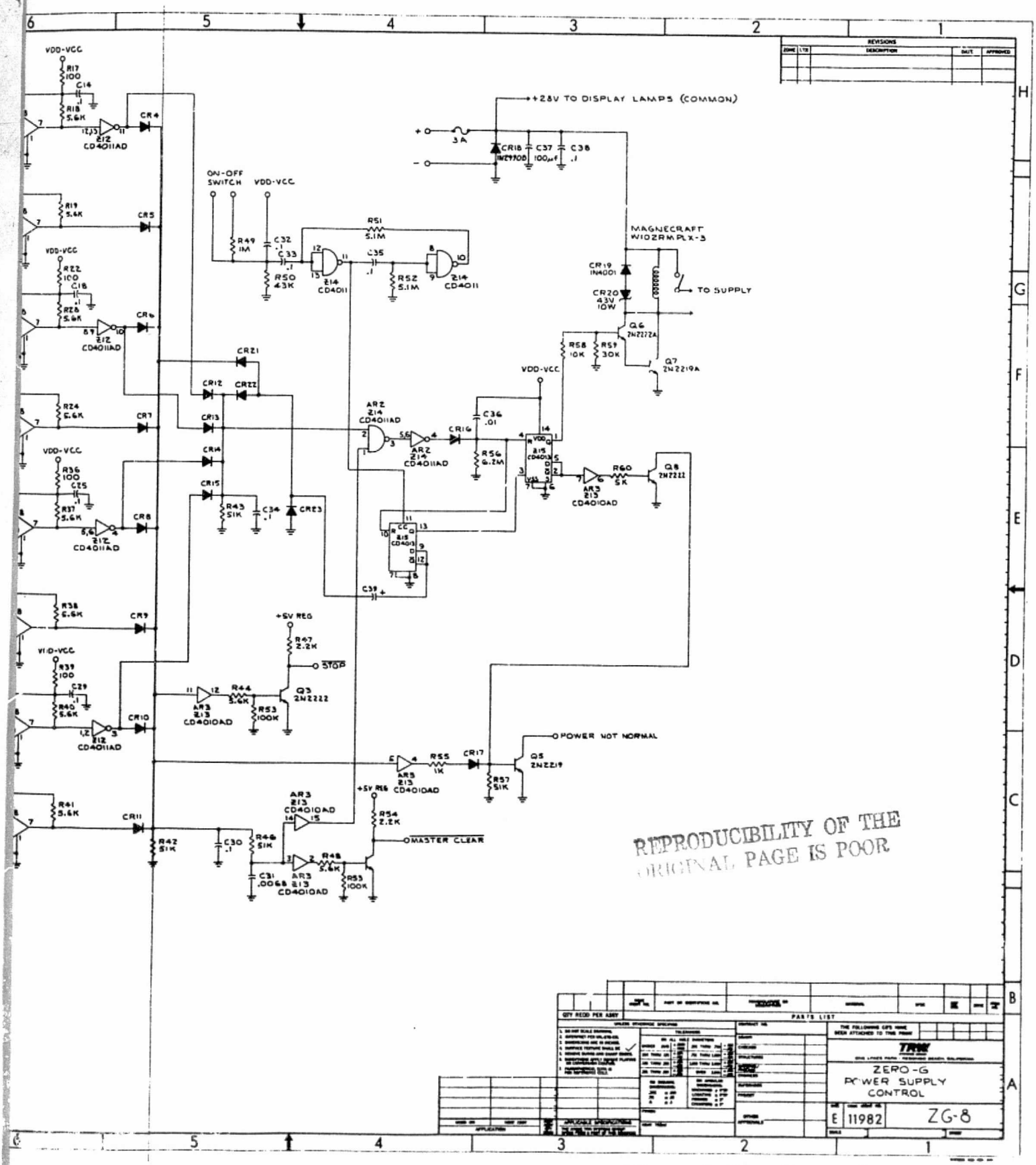

Figure 3-21. Power System Controller Schematic

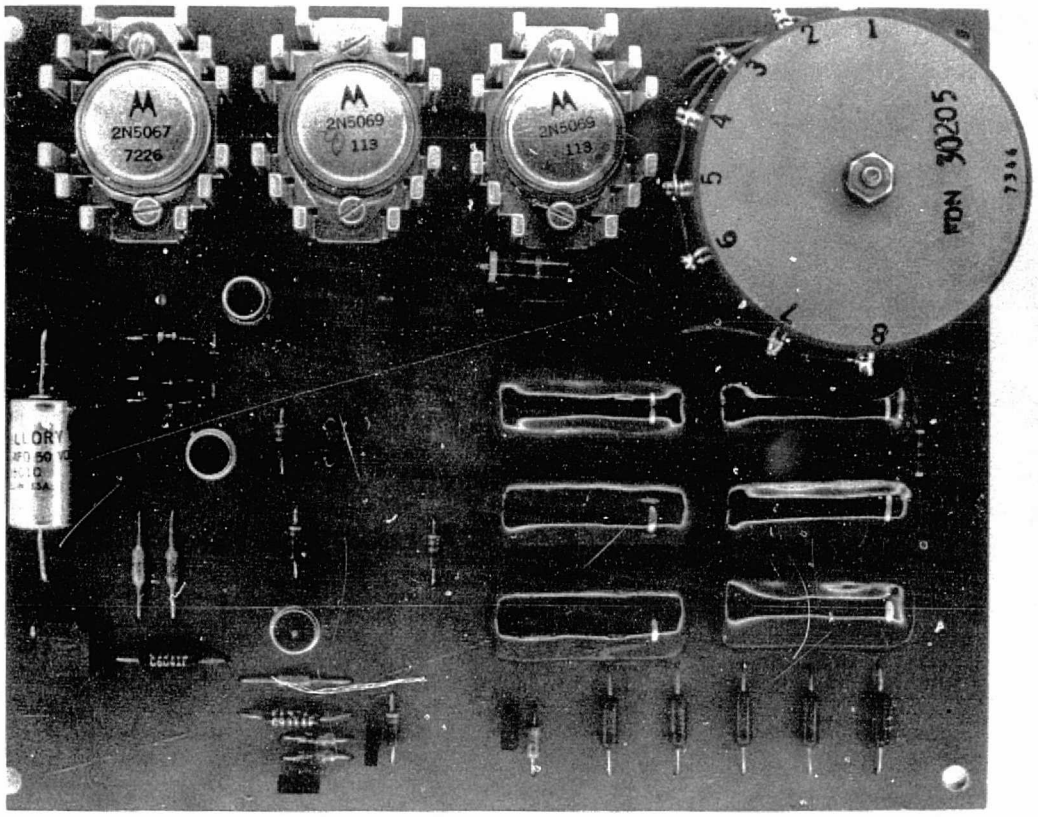

Figure 3-22. High Voltage Power Supply Assembly

The three circuit boards comprising the computer interface circuitry shown in Figures 3-16 and 3-17 plug into the "mother board" shown in Figure 3-23. This four-board assembly is mounted on spacers and fastened to its own self-contained box.

The system display, which includes the digital readouts, on-off switch, and channel failure indicators, is housed in a self-contained box shown in Figure 3-19.

3.2.5 System Assembly

Exclusive of the radioactive sources and SCEs the entire nucleonic gauge mounts in a 13-inch high by 19-inch wide deep enclosure; i.e., the System I/O, Computer, and Power Supply bolt to the chassis of the enclosure. Slides are provided to pull the chassis away from the enclosure thus providing easy access to the circuitry within. Figure 3-24 presents the chassis fully extended while Figure 3-25 shows the assembled system. As can be seen from the figures, the system display is visible through a cut-out in the front panel of the main enclosure. The system may be operated in this configuration, or, if desired, by loosening the quick disconnect screws on either side of the display, the display box can be removed and located up to 20 feet from the main enclosure. Carrying handles and tilt stand are provided on the display box.

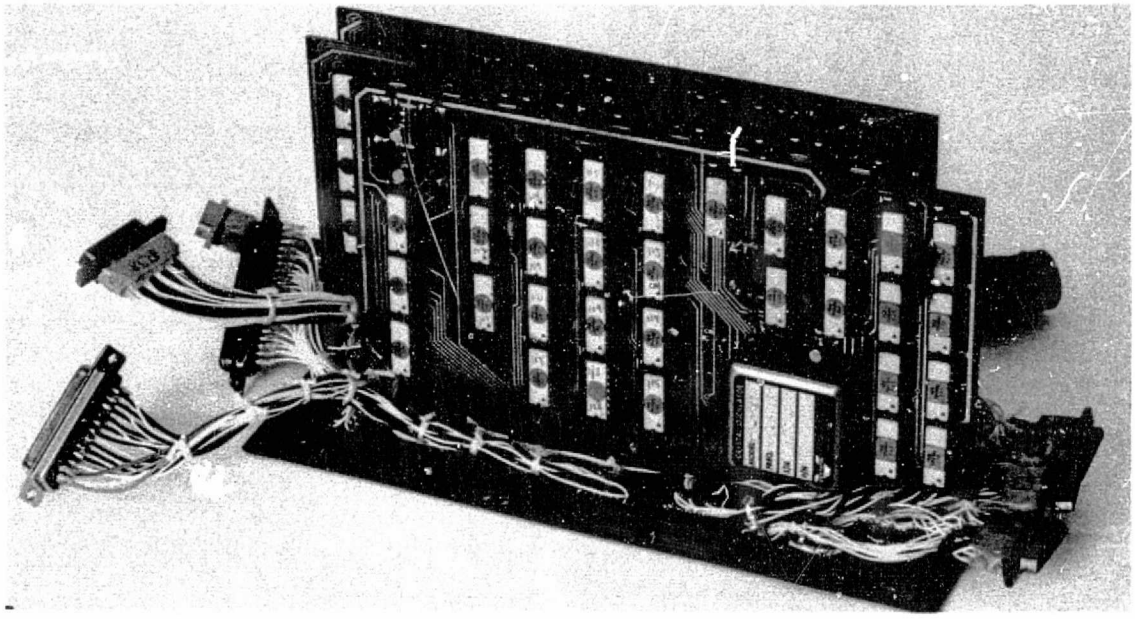

Figure 3-23. Mother Board (Assembled)

3.2.6 System Software

Two software packages are available for the 469 computer. The first package, the 469 computer assembly program, converts programs written in assembly language into binary machine language for execution by the 469 computer software simulator or on the 469 computer itself. The assembly program itself is written in Fortran to provide a certain degree of computer independence. The second package, the 469 computer software simulator, processes the binary object deck generated by the 469 assembler on a CDC 6500 series computer. This enables a program to be coded and debugged prior to the delivery of the actual computer hardware.

The assembler program has two major functions. The first is to allow the programmer to use meaningful names for instructions rather than the equivalent octal numeric identifier. The assembler translates these mnemonic operation codes directly into machine code. The second and most convenient function is to allow the programmer to assign labels or names to specific locations in the memory. This alleviates the necessity to change the memory reference statement every time the symbolic code is changed. The assembly program takes care of the assignment of symbols to locations and the resultant translation by constructing a symbol table which gives the absolute location and the symbol to which it has been assigned.

The assembler accepts symbolic instructions for the 469 computer as an input. This input may either be punched cards, or a file generated by a terminal. The latter method was chosen for this application, because of the many advantages and conveniences that are characteristic to a timesharing system. Any reference made to a timesharing system,

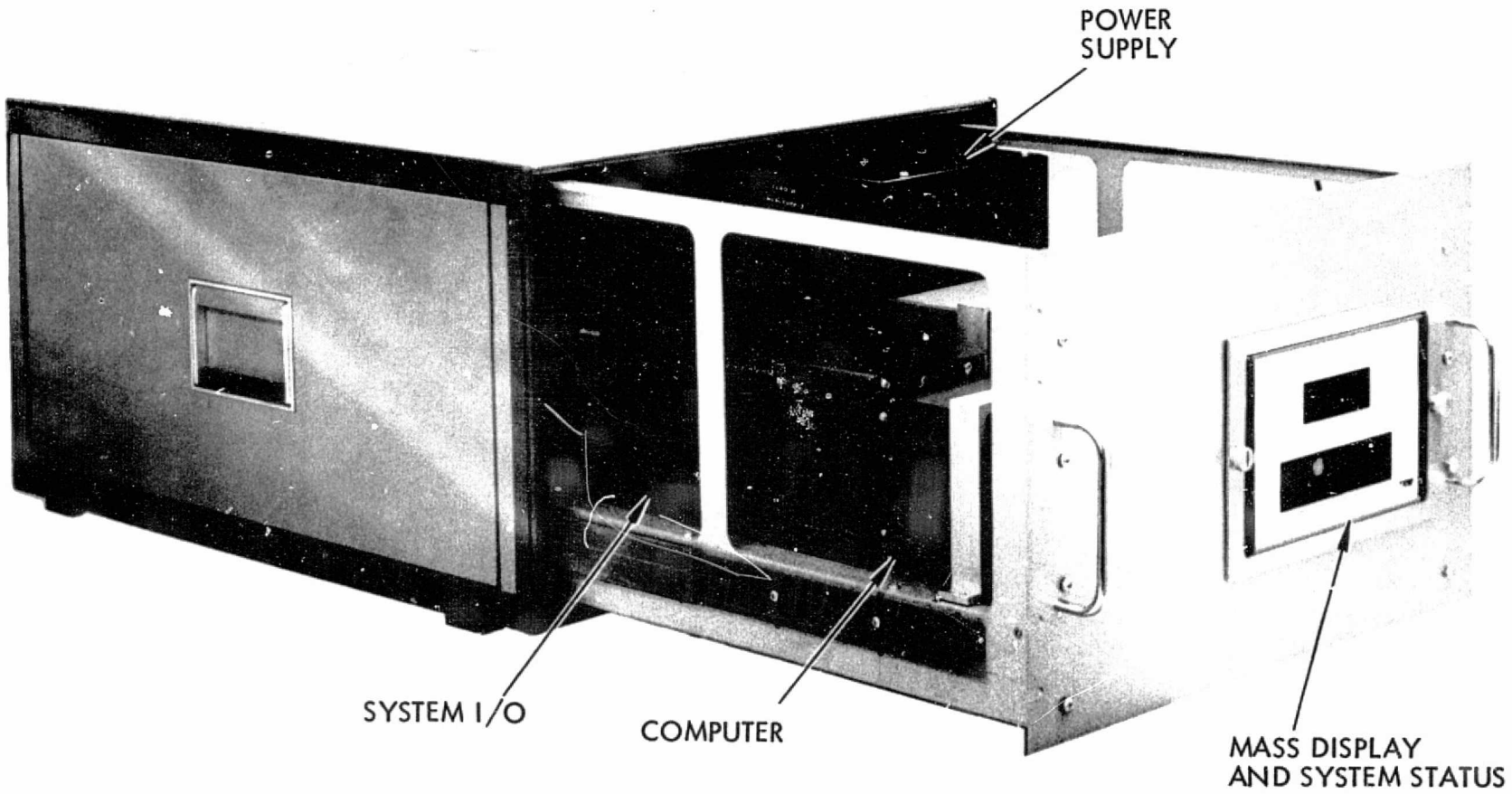

Figure 3-24. Assembled Electronic Subsystem: Chassis Extended

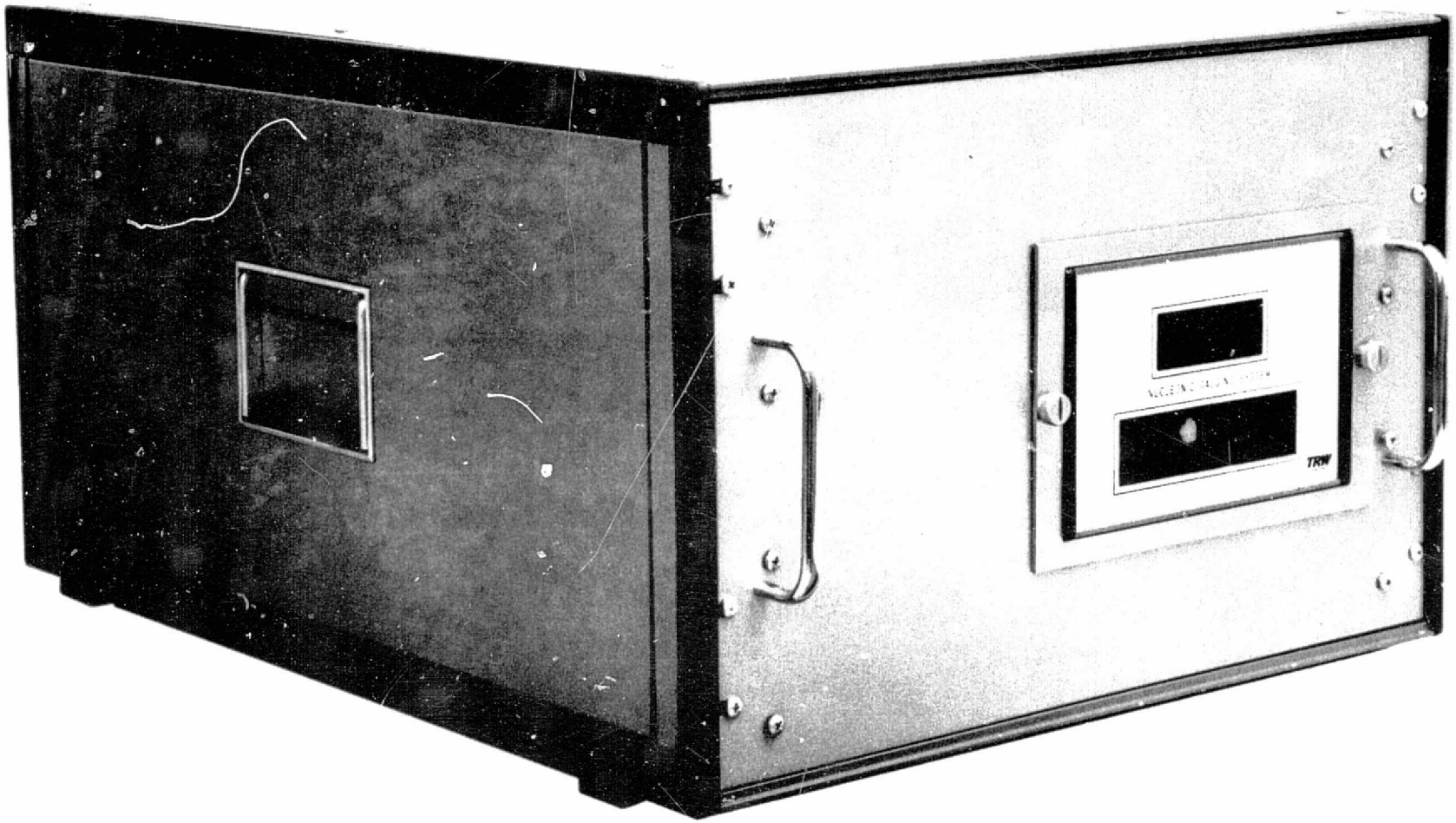

Figure 3-25. Assembled Electronic Subsystem

heretofore, is assumed to be that of the TRW/TSS 6000 series available throughout the TRW Systems' facility.

Assuming a program has been written and stored on disk, only a few simple instructions are required to process the code. If the 469 assemble code is stored under the file name ASSEM, and the test program is stored under TEST, the following control cards are necessary:

```
RFL, 50000.          Request Field Length

REWIND, TEST

ASSEM, TEST, LOUT1.
```

LOUT1 is an output file assumed to be empty at the start of execution; if LOUT1 is omitted, the output file is, by default, the terminal.

The output generated consists of error messages, contents of each machine word, a mnemonic listing, memory allocations, and other useful information that may provide help in debugging a program. The actual object machine language code is deposited onto two files: TAPE 69 and TAPE 70. If at any time a program must be recompiled during one "sitting" at the terminal, both files should be rewound to assure proper simulator execution. These two files provide the necessary communication between the assembler and the simulator or actual 469 computer.

The 469 Simulator (SIM/469) provides the capability of instruction-by-instruction simulation of the 469 object language program created by the assembly program. The simulator can be used to assemble and simulate a 469 program in one computer run, or the simulator can be used to simulate the object language programs that have been generated by the assembler on a previous run.

The simulator provides the following debugging aids:

a) SNAPSHOT DUMPS – allows a segmented dump of any area of memory at any point in the simulation of a program

b) TRACES – allows the user to reference the contents of the register files at any time

c) TIME and PAGE output limits

d) Write accessible memory bounds

e) Data file definitions and manipulations.

Three files must be made available at the start of the executions of the simulator. TAPE 69 and TAPE 70, both having been created by the assembler, must remain essentially untouched. The third file, TAPE 4, contains two parts; each performs a specific task and is created by the user. Part 1 contains any control cards that are to be processed during

the execution of the simulator. These control cards consist of any definitions of snapshot dumps, traces or time, and page or memory constraints.

Part 2 contains the input data required by the external peripheral and made available to the input channels. Since this is simulated, the data file is in the form of three parameters:

a) The time the data are available

b) The channel the data are available on

c) The actual data.

The input file, TAPE 4, as mentioned, consists of two parts separated by an EOF mark. Initially, the two parts are created separately and merged by means of a COPYBF command. Assuming the two parts are labeled PART 1 and PART 2, the sequence of command would be:

```
COPYBF, PART 1, MINIT 4

COPYBF, PART 2, MINIT 4.
```

MINIT 4 is the final file that contains both Part 1 and Part 2. MINIT 4 can be stored on disk, retrieved and used by the simulator, but only Part 1 will appear to be contained in MINIT 4. This is to say only Part 1 can be modified or even listed as the file exists. If at any time MINIT 4 is to be edited, the following sequence of commands must be performed:

```
REWIND, MINIT 4

COPYBF, MINIT 4, PART 1

COPYBF, MINIT 5, PART 2.
```

Part 1 and Part 2 are assumed to be empty previous to the execution of the commands.

Execution of the simulator can be processed by the following command:

```
SIM, MINIT 4, LOUT 2.
```

The 469 simulator has the file name SIM, and as before, the output is stored on the file name LOUT 2 unless the name is omitted; default causes the output to be generated on the teletype machine.

Along with the central processor, the following peripherals are available:

a) Programmer's console

b) Magnetic tape memory loader

c) Controller interface

d) ASR 33 TTY or KSR733.

The programmer's console which is connected directly to the central processor displays the contents of the register files. The user has the option of controlling the execution of the object code either under a step-by-step execution mode or a normal execution mode. If a certain instruction need be changed, the new instruction and the related data word can be entered onto the console and entered directly into the object code from the console. This is normally done to make temporary changes to the data. For larger code modifications the teletype can be used: this teletype, similar to the terminals available for TRW/TSS timesharing, generally has the function of controlling the entire system. The teletype is connected to a controller interface apparatus that provides the necessary interface between the universal teletype unit and the central processor. Figure 3-26 shows the interconnection between all equipment and the gauging processor.

Having processed a program by the 469 assembler and generated a magnetic tape containing the object deck, the magnetic tape memory loader provides the service of loading the object deck into the 469 memory. (See Figure 3-27.) This provides the only necessary interface between the service machine, the CDC 6500, and the 469 computer. Once the object deck is loaded, the 469 computer is completely independent of any other processor systems. At this point, control of the program is completelely monitored by the user through either the teletype or the programmer's console.

Assuming a program has been generated, loaded, and made operational on the 469 computer, the program operation commences as follows:

Data readings are taken directly from the propellant tank at four pre-specified locations. These data, in the form of radioactive binary "counts", are accumulated for an interval of 1 second. As this accumulation is being performed, the 469 computer, having processed earlier data, will be in a pause mode waiting for new inputs. Upon completion of the 1-second accumulation phase, an interrupt signal is issued to the 469, the inputs are made available to the system, and the program is placed into a mode of execution. Simultaneously, with the reading of the data, the accumulators are reset to zero and the process of summing the data is restarted.

The data read from the accumulators must be made available to the 469 computer in a very specific manner. The total counts received by each individual accumulator may range from 200 counts (a full tank) to a maximum of 1 million counts (on empty tank). Since a normal single precision data word represents 15 bits of information, a maximum data value $2^{15} + 1$ implies a need for double precision inputs. Therefore, two words of information and two input channels must be used for each accumulator. Double-precision is correct only in the sense of using two data words for input. In reality, a modified word organization is utilized here since the entire second word is not needed. Added status information

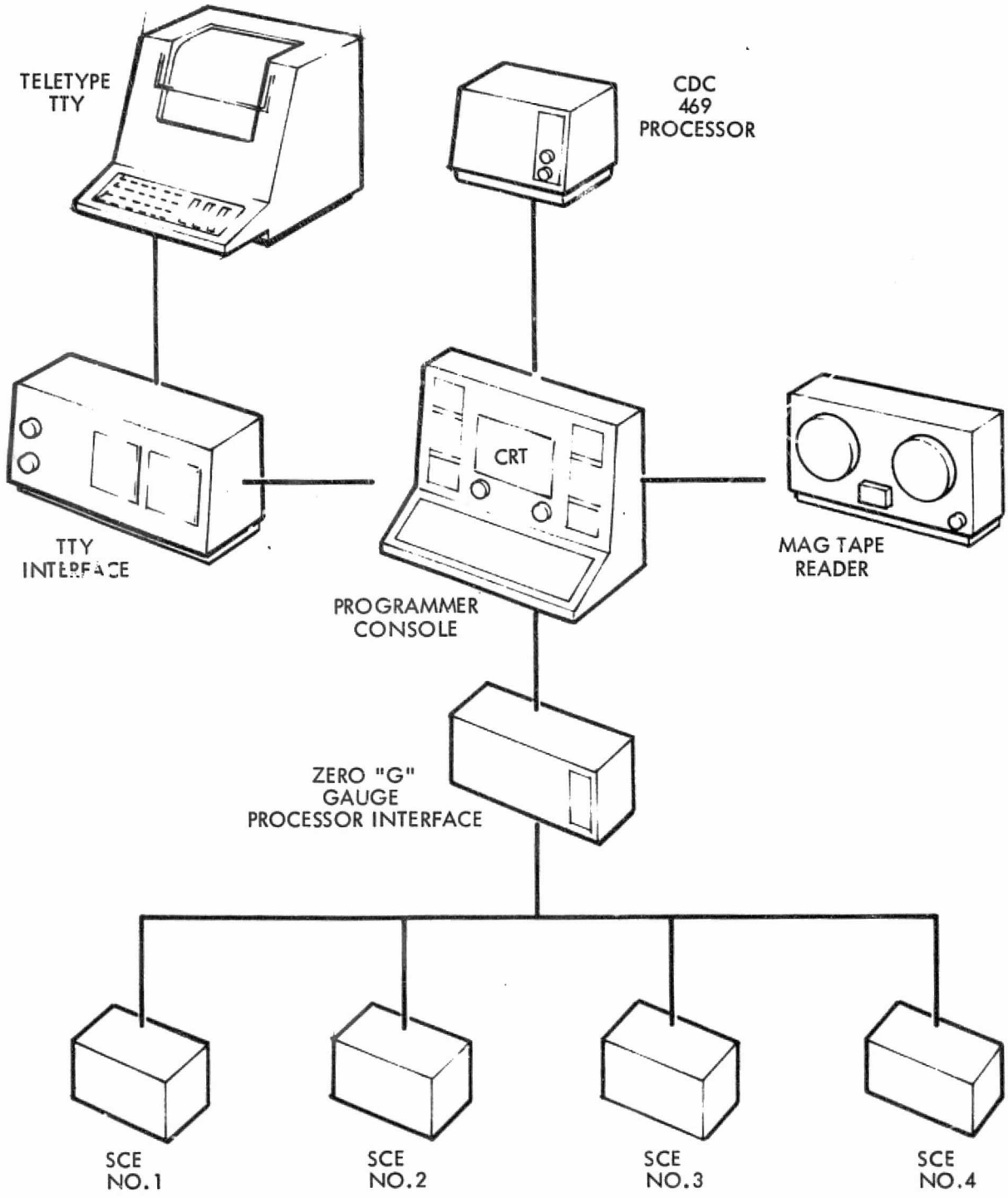

Figure 3-26. Processor Interconnection During Program Development

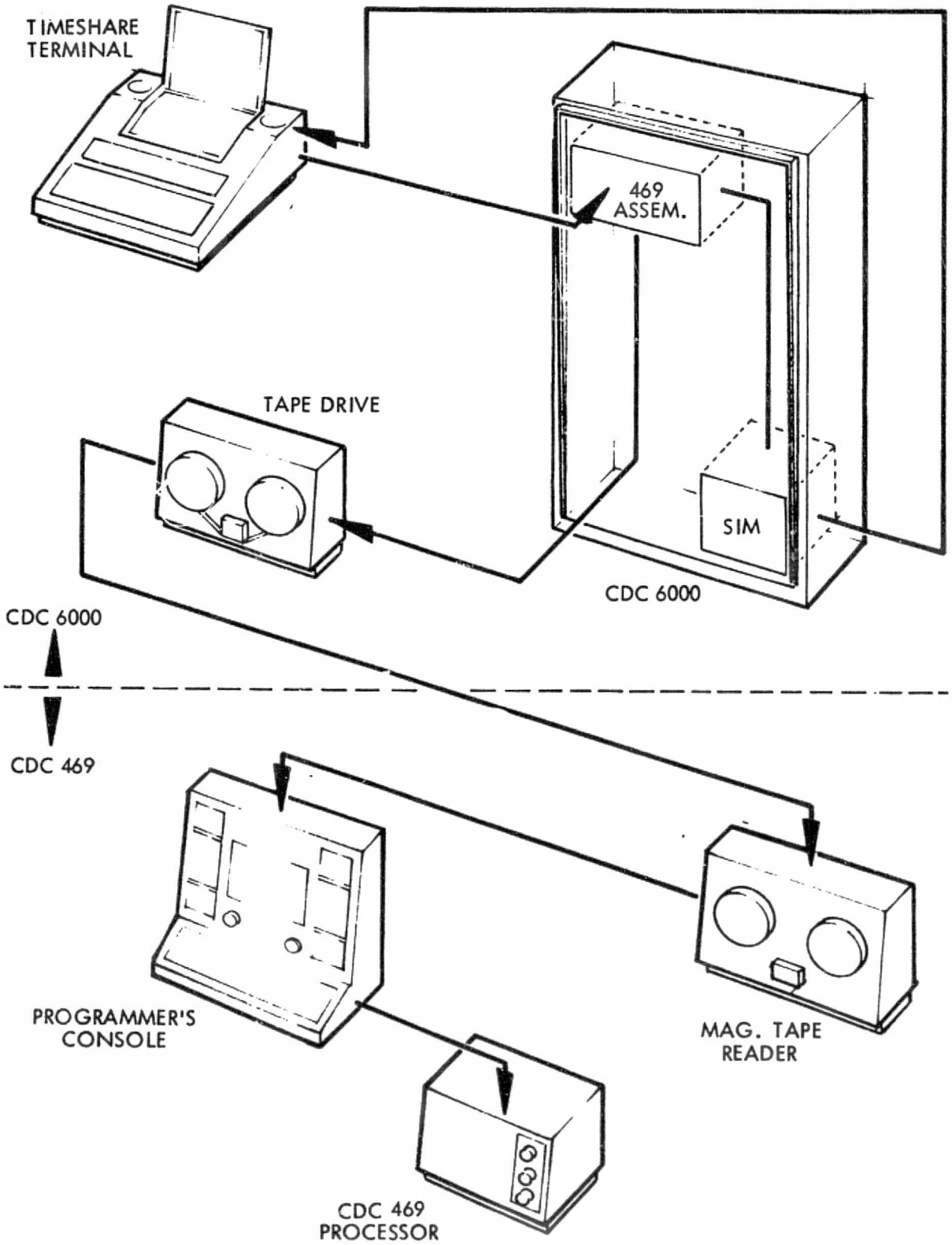

Figure 3-27 Loading of Assembled Programs

is inputted as an additional 4-bit piece of information. (See Figure 3-28.) (Notice that the sign bit in the second word is used as a data bit along with the next adjacent 5 bits.) This enables a maximum reading of $2^{20} + 1$ (1,048,577) counts to be processed. The next 4 bits represent a status flag, indicating the operational status of the four external accumulator devices. Modified program execution must be made as a function of the failure of any or all of the accumulators. The last six bits remain set to zero and serve no particular function at this time. The availability of these bits suggests the possibility of scaling the data inputs if at any time the data would exceed 1 million counts, but at this time the possibility of data overflow is somewhat remote.

Once these accumulator values are made available to the 469 computer on channels 6 through 15g, the program progresses from its pause mode into an execution mode. Each channel is sequentially read, checked against reasonable minimum and maximum limits, and stored for later use. From the first three accumulator data inputs only the 21 data bits are stored; the remaining 10 bits are masked off and lost. The last accumulator provides not only the data information but also the status information. This 4-bit status flag is now evaluated for the purpose of modifying the actual mass calculations. Obviously the failure of any of the accumulator devices would alter the mass calculations by a large factor. Since the mass calculation is performed by means of a logarithmic polynomial evaluation, it is possible to alter the coefficient as well as redistibuting the weighting of each accumulator to make up any deficiencies.

Additional and specific details on the system software are found in Volume II of this report which contains complete documentation.

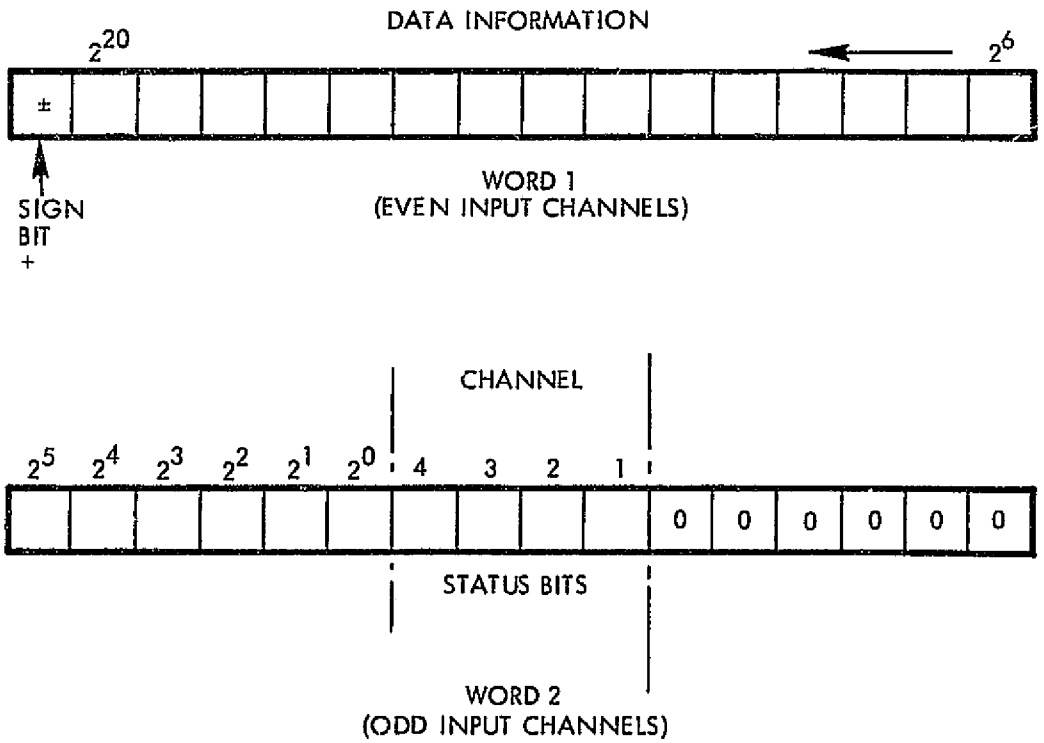

Figure 3-28. Data Word Structure

3.3 SYSTEM FLIGHT TESTS

3.3.1 Test Objectives

The overall objective of the flight test program was to demonstrate the capability of the nucleonic gauging system to gauge the content of reduced-scale storable liquid tanks in a zero-g environment as provided by a KC-135 zero-g aircraft. Also included within this objective were the following:

1) The gauging system would be compatible with the requirements for zero-g experiments to be conducted on the KC-135 zero-g aircraft and would operate reliably with the varying environmental conditions.

2) The gauging system would present no undue radiation hazard to operating personnel in either ground and/or flight testing.

3) The gauging data would be repeatable.

3.3.2 Test Arrangement, Equipment and Instrumentation

Figure 3-29 presents a diagram of the experimental arrangement that was used for the flight tests of the nucleonic gauging system. As indicated in this figure, the Electronic Subsystem (ESS) was mounted in an "Electronics Chassis" integral with the computer peripherals; although the peripherals were employed primarily for data acquisition, they also provided the capability to perform in-flight diagnostics and to effect in-flight program changes, if required. The Electronics Chassis was bolted directly to the cargo tiedowns in the cabin floor of the aircraft and electrically interfaced to the aircraft power supply and, via the multi-conductor umbilical, to the Flight Test Article (FTA). The Electronic Chassis is shown in Figure 3-30.

The FTA was additionally outfitted with a clock, an event counter, and a g-meter, each being positioned in close proximity to the test tank and within the field-of-view of the camera. This arrangement permitted the electrical output of the gauging system to be directly correlated over each 1-second gauging interval with the propellant behavior recorded by the camera. Pre-weighed quantities of propellant simulant (contained in plastic bottles) were introduced into the test tank via the "fill" port and could be drained from the tank via the "drain" port into empty catch bottles (and subsequently weighed). The base of the FTA was bolted directly to the cargo tiedowns with additional bracing being achieved with three guy-wires attached between the tank cradle legs and the cargo tie-downs; the installation is shown in Figure 3-31.

The aircraft employed was the NASA 930, a KC-135A equipped for zero-g flight tests; aircraft specifications, along with other data, are given in Reference 1.

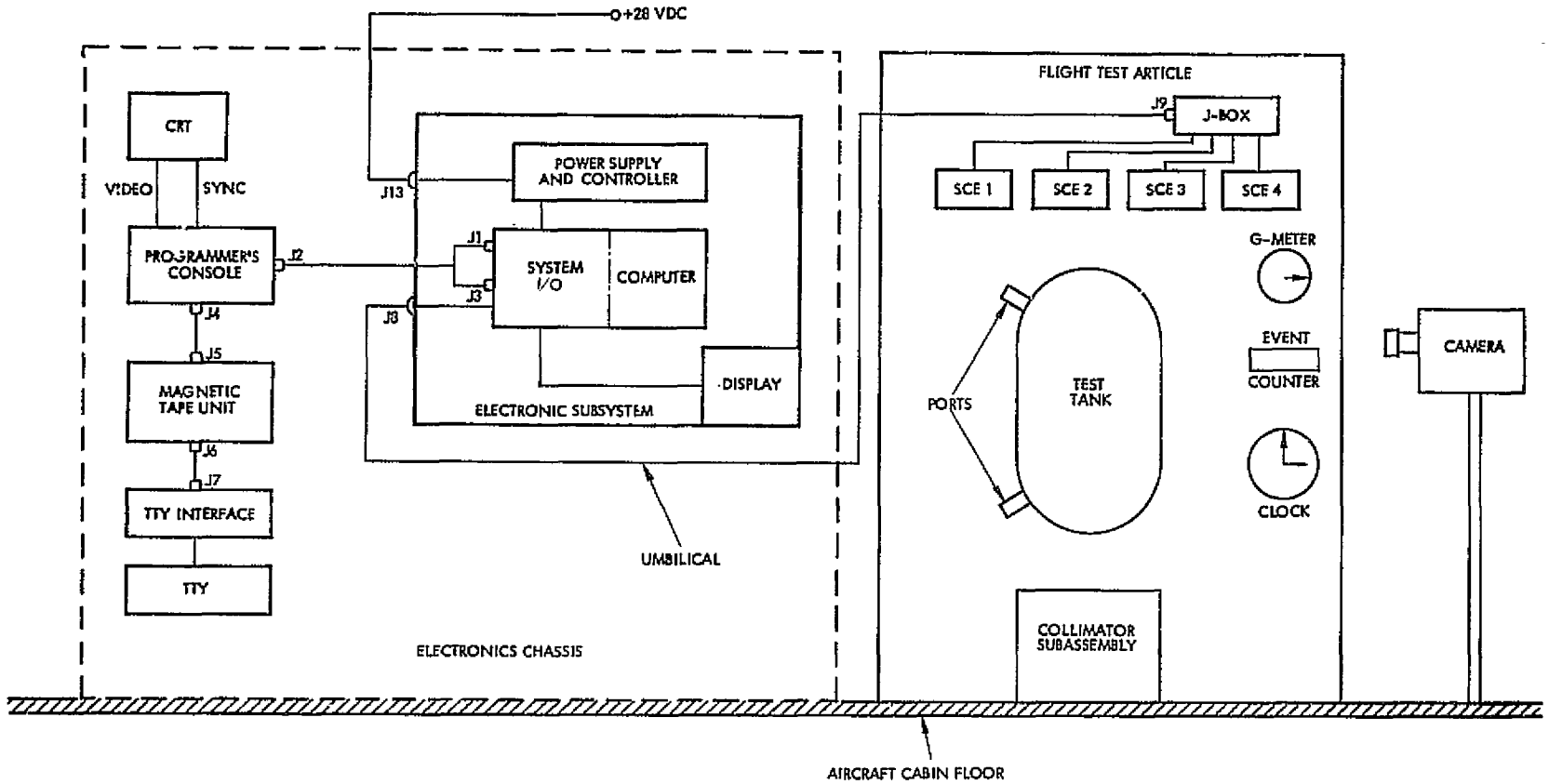

Figure 3-29. Experimental Arrangement

Figure 3-30. Electronics Chassis

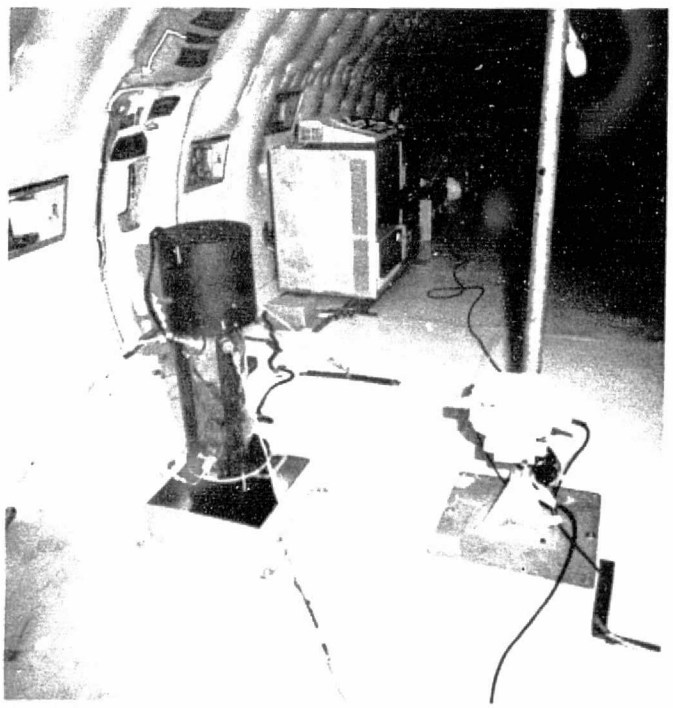

Figure 3-31. FTA in Tied-Down Configuration

3.3.3 Test Plans and Procedures

Detailed test plans and procedures are presented in References 2, 3, and 4; in the interest of brevity, only a generalized synopsis is presented in this report.

Test Plans; General

As originally conceived, the flight-test program was to consist of a series of individual flights with each flight encompassing a prescribed number of zero-g parabolas. The first flight in the series was a Flight Verification Test wherein proper function of all the electronic equipment in the configuration depicted in Figure 3-29 would be verified. This flight would also serve to familiarize the flight crew with certain in-flight operations/procedures, particularly the filling/draining of propellant simulant, operation of the data acquisition equipment, and handling procedures associated with the Flight Test Article. The radioisotopes were not to be installed for this flight, thereby eliminating any potential radiation hazard to the crew.

The second flight scheduled was a full-function gauging system test wherein gauging data would be acquired for various tank loadings under zero-g conditions (i. e. , during the zero-g parabolas) and under one-g conditions (i. e. , during the level flight portions between zero-g parabolas). The data obtained in this flight were to be utilized to generate a new set of system software relating count data to actual propellant mass. This new software would then be loaded into core, replacing the software that was based on a computer simulation of the idealized propellant quantity/behavior and the associated count data. In this manner, it was hoped to eliminate empirically (most of) the real external influences (e. g. , aircraft vibration, etc.) on the propellant behavior which is not accounted for in the idealized simulation.

The third flight was actually to be a repeat of the second flight, but with the gauging system employing the empirically-derived system software. This flight was truly to be the validation of the gauging system and, in particular, to assess system accuracy. In this flight the crew would be able to assess qualitatively the gauging system performance simply by visually observing the system's display and comparing the indicated value(s) (mass in grams) with the known mass within the test tank. Gauging data would also be acquired on the magnetic tape for subsequent reduction, analysis, and comparison with the data from the previous flight. If indicated, these data could also be merged with the previous data, thereby providing an even broader base on which to generate empirically the system software.

During the course of the program, scheduling of the aircraft was problematical. Consequently, after completion of the Flight Verification Test(s), the "second" flight was actually three individual flights on three consecutive days. Between these three flights, there was insufficient turn-around time to process the data and generate new system software.

Technically, this was of little consequence since all of the data could be processed "after-the-fact", i. e. , the first of the three consecutive flights could provide the data base for the software, and the data from all flights subsequent to the first could be evaluated "off-line" in a large scientific computer. Indeed, this is precisely how the gauging system's performance would be quantitatively assessed. Also, all the data from the three flights could be merged to provide an extremely broad software base for any future flight tests.

Test Procedures; General

Having made the installation indicated by Figure 3-29 on the aircraft, a pre-flight function test was typically performed using ground power to the aircraft. Essentially, this function test consisted of assuring that the ESS and the peripherals were operating nominally, and that the software was properly loaded in the 469 computer. This was accomplished by powering the peripherals and the ESS and observing the system display for a nominal condition (i. e. , the NOT NOMINAL indicator extinguished). Communication was then established with the computer via the TTY, verifying the software by visually observing on the CRT the prescribed outputs of selected registers. Invariably, the gauging system operated in the nominal mode during these pre-flight function tests. The ESS and peripherals would then be powered-down and the aircraft/crew prepared for takeoff.

Once airborne and in level flight, the pre-flight function test was repeated to verify nominal system operation. A fresh, blank DATA TAPE was loaded onto the tape transport, the plug-plate was removed from the FTA, and gauging commenced via a command executed on the TTY.

Several files of gauging data were first obtained in the level flight condition with the test tank empty (zero-point calibration). These files could then be outputted and printed on the TTY for visual observation. This output consisted of the (octal) counts received by each of the four SCE units and the resultant mass of propellant simulant in the tank for each 1-second interval during the entire gauging period (typically 10 to 15 seconds). The count data were visually reviewed to assure that they were (approximately) of the proper magnitude, and that they were consistent over the consecutive (1-second) gauging intervals.

The aircraft would then execute the first zero-g parabola, with gauging initiated on entry into the parabola and terminated at pull-out. The data obtained over this parabola were then outputted on the TTY for visual observation.

An increment of propellant simulant was introduced into the test tank at this time and gauged for a 10 to 15 second interval while in level flight; these data would be outputted and observed for consistency. The

aircraft then executed several (3 or 4) zero-g parabolas during each of which the simulant was again gauged. After the last parabola and with the aircraft in level flight, the simulant was gauged and the resulting data outputted. These data were compared for consistency with the data obtained during level flight prior to the zero-g parabolas. Another increment of propellant simulant was then introduced into the tank and the sequence repeated in accordance with the schedule of Table 3-2.

When the schedule of Table 3-2 was completed, the DATA TAPE was removed from the transport and stored in a canister. The ESS and peripherals were powered down, and the FTA "safed" by reinstalling the plug-plate. No attempt was made to drain propellant simulant from the test tank as it was deemed unnecessary on the basis of safety, and that sufficient data would be generated on just the (tank) "fill cycle". The aircraft/crew then prepared for landing.

After the aircraft was parked, the DATA TAPE was off-loaded and shipped to TRW Systems for subsequent reduction and analysis.

Flight Verification Test: Equipment and Procedure Changes

Upon completion of the installation indicated in Figure 3-29 (less the radioisotopes) and using ground power to the aircraft, the ESS and peripherals were powered and the gauging system indicated nominal operation. Communication was established via the TTY with the computer and several dummy data files were generated on the magnetic tape. The gauging system and peripherals appeared to be operating nominally in every respect. The ESS and peripherals were powered down in preparation for takeoff.

Table 3-2. Tank Loading Schedule

Bottle No.	Weight of Simulant (grams)	Total Weight of Simulant (grams)	Percent of Tank Capacity
1	310.6	310.6	2.5
2	168.7	479.3	3.9
3	355.1	834.4	6.8
4	342.9	1177.3	9.6
5	598.6	1775.9	14.4
6	888.0	2663.9	21.7
7	1776.0	4439.9	36.1
8	3262.1	7702.0	62.6

Once airborne and in level flight, the ESS and peripherals were again powered and the "pre-flight" function test indicated all systems in the nominal operating mode. The first zero-g parabola was then executed. Sometime during this parabola, the voltage NOT NOMINAL indicator illuminated on the gauging system's display. All attempts to restore the system to a nominal operating condition during this flight were unsuccessful.

When the gauging system and peripheral were off-loaded from the aircraft and reinstalled in a laboratory environment, troubleshooting revealed that a stage of the (computer) electronic protection circuitry had failed-safe; in particular, that stage which monitors the +28 vdc aircraft-supplied power and all other voltages derived from the +28 vdc. The failed components were replaced and the system was reinstalled on the aircraft. A pre-flight function test indicated nominal operation in every respect and no other component failures occurred during the flight program.

However, during a later flight verification test where the radioisotope sources were introduced (but not the propellant simulant), there was a large variability, observed in the count data over the 1-second gauging intervals; with no simulant in the tank, these data should have been very uniform. With the system installed on the aircraft, and the aircraft parked and on the ground power, output registers of the CRT were visually observed over extended gauging periods. The registers appeared to be aperiodic in the reset/pause cycle, suggesting that the LEVEL 1 interrupt was also aperiodic. This condition could be caused by a fault in the gauging system's timing, or by receipt of a false LEVEL 1 interrupt (due, perhaps, to a problem in supplied power and/or ground-loops). Suspecting the aircraft power, the ESS +28 vdc power line was removed from the aircraft's power buss and connected to a 24 vdc battery. (The ESS regulates between +22 vdc to +36 vdc). On battery supply, the gauging system functioned properly with the output registers, revealing a steady, rhythmic 1-second reset/pause cycle.

The aircraft power was then observed on an oscilloscope and was found to have many ac components, particularly 400 Hz; amplitude also varied with engine run-up and depending upon the location of the ground point. All attempts to "clean up" the +28 vdc aircraft power and/or establish a single-point ground were unsuccessful. To solve this problem, a regulated laboratory power supply (powered by aircraft-derived 110 vac) was used to derive the +28 vdc for the ESS. No further problems were encountered during the remainder of the flight program.

During this period, the flight crew reported that a more positive way (than a double-key entry on the TTY) to initiate gauging was desired. Consequently, a switch was built that, when open, inhibited the LEVEL 3 and LEVEL 1 interrupts; when closed, both interrupts would enable and gauging would commence. At this time, the event counter located on the FTA was also slaved to the LEVEL 1 interrupt, providing a one-to-one correspondence between the 1-second gauging intervals and the count number displayed in the photographic film.

3.3.4 Data Reduction

For data reduction, a large-scale CDC 6500 computer was selected. Since this is a 60-bit word machine, it was first necessary to develop a program to convert the 16-bit word of the gauging system's 469-computer to the 60-bit word of the CDC 6500. This program was denoted REDUCER and is described further (along with other programs for reduction and analysis) in Volume II of this report.

REDUCER generated two output files. The first of these is the total, unedited data after the word-length conversion; i. e., the count data (in octal) as it was written to the magnetic tape by the 469. In addition, this file also contains the Z-lengths (in decimal centimeters) corresponding the count data; an example of TAPE6 is shown in Figure 3-32. TAPE 6 was used as the primary basis for all subsequent analyses.

The second file generated by REDUCER — denoted TAPE7 — is basically a summary of TAPE6. This file averages the count data over each of the zero-g parabolas (or level flight) while gauging was active, and tabulates the corresponding calculated mass and the number of 1-second gauging intervals for which gauging was active; an example of TAPE 7 is presented in Figure 3-33.

3.3.5 Test Results

TAPE7 was used for making a quick, quasi-quantitative assessment of the overall gauging system performance. For example, the count data obtained during level flight before and after each series of zero-g parabolas should be relatively unchanged since the quantity of propellant simulant was unchanged, and the propellant was (reasonably) stable in the one-g configuration. This consistency in the count data is illustrated in Figure 3-33. Note also in this figure that the average count data are reasonably stable over each of the zero-g parabolas for which the tank loading was unchanged. This observation is not especially useful, however, in that it lacks uniqueness; i. e., the "propellant-ullage" interface could be relatively stable, relatively unstable (high degree of slosh and/or turbulence), or the electronics could be noise (near) saturated.

TAPE7 was also used to assess (quickly) the gauging system performance in a more quantitative manner. In this instance, the count data from the level flight portions of gauging — denoted the one-g data — and the corresponding Z-lengths were inputted into a generalized curve-fitting program. The Z-lengths were theoretically calculated from the known quantity of propellant simulant in the tank, the density of the simulant, and the geometry of the tank. The curve-fitting program generated the coefficients for a least squares curvefit to

$$N(R) = A \exp^{BZ}$$

FILE NO. 14

	Channel Number 1	2	3	4	Calculated Mass (lb)	Not Used	Z-Lengths (cm) for Channel 1	2	3	4
17	0C4695 1 G B1 2									
1	025777	014455	016032	033142	000C02	0C000C	1.2	1.0	2.1	1.2
2	024570	012522	014533	026377	0C0003	0C000C	1.8	2.7	3.2	3.1
3	024757	C13341	015226	030672	000003	0C000C	1.7	2.0	2.7	2.1
4	024766	013761	015553	032072	C00CC2	0C0000	1.7	1.5	2.4	1.6
5	024513	C13665	015343	035165	000002	0C000C	1.8	1.6	2.6	.5
6	025264	014076	015704	031726	000CC2	000C0C	1.5	1.4	2.3	1.7
7	024660	013347	015047	031451	C00C03	0C000C	1.8	2.0	2.9	1.8
8	025166	014322	015411	031364	000002	0C0000	1.6	1.2	2.5	1.9
9	024643	C14034	015565	033017	CC0C02	0C000C	1.8	1.4	2.4	1.3
10	024712	013474	015557	030374	000003	0C0000	1.7	1.8	2.6	2.3
11	022177	C12171	013565	030100	0C0003	0C000C	3.1	3.1	3.9	2.4

FILE NO. 15

20	C04606 1 G B 3									
1	023467	C12603	014334	026061	000C03	0C000C	2.4	2.6	3.4	3.3
2	C22372	C11404	012710	024635	000C04	0C0000	3.0	3.8	4.7	3.9
3	022267	012217	013540	027366	0C0C03	0C000C	3.0	3.0	4.0	2.7
4	022743	012074	013561	025121	000CC4	0C000C	2.7	3.2	3.9	3.7
5	022324	C12147	013525	027303	000C03	000000	3.0	3.1	4.0	2.7
6	022347	C12322	013530	026541	CC0C03	0C000C	3.0	2.9	4.0	3.0
7	022245	012230	013500	026067	000004	0C0000	3.0	3.0	4.0	3.3
8	C22301	012020	013450	030051	C00C03	0C000C	3.0	3.3	4.1	2.4
9	022213	012147	013605	026276	000C03	0C00CC	3.1	3.1	3.9	3.2
10	022535	C12032	013510	030674	000C03	0C000C	2.8	3.3	4.0	2.1

Figure 3-32. Sample Output Format of TAPE6

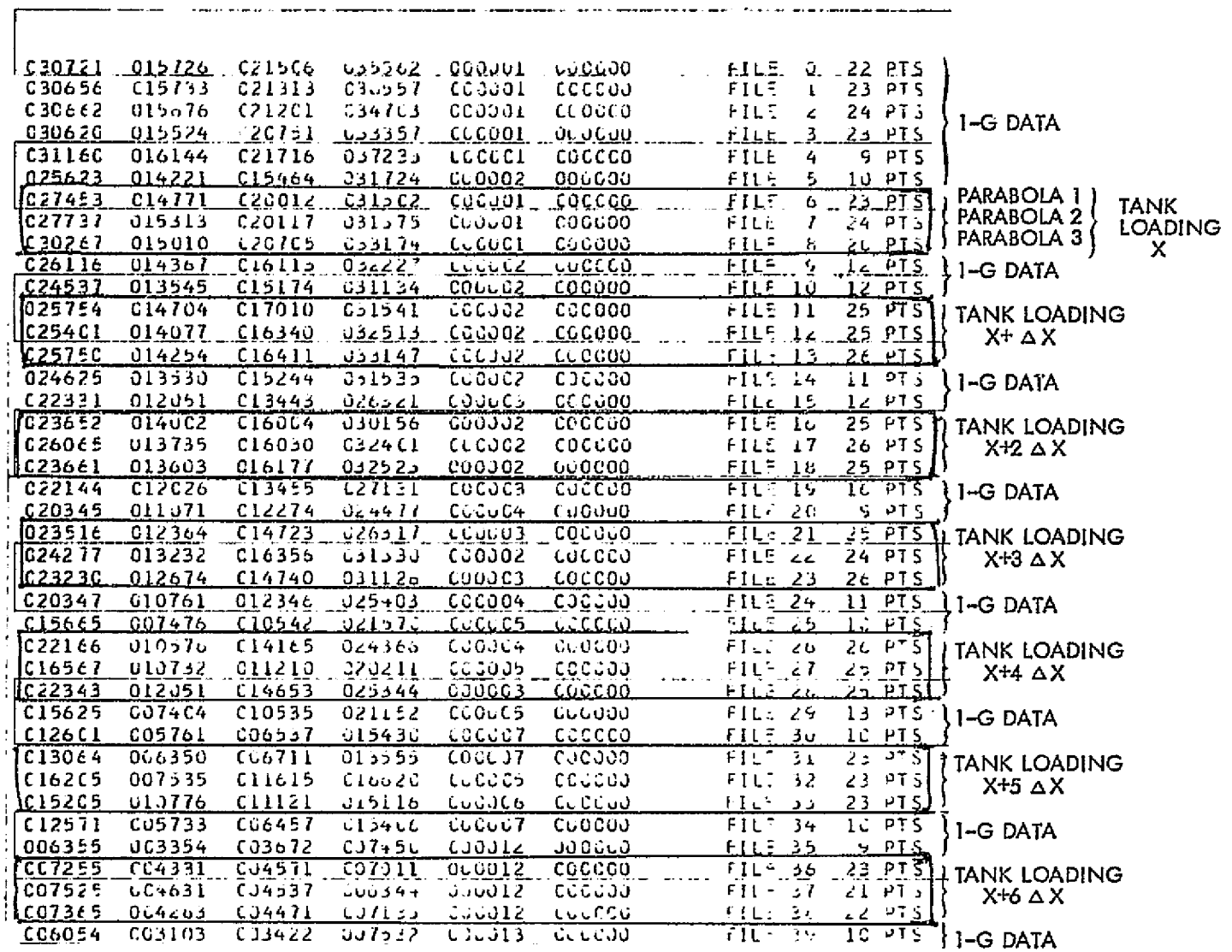

Figure 3-33. Sample of TAPE7

where N(R) are the counts received corresponding to the propellant simulant "thickness", Z. For the nucleonic gauging system, the coefficient A is actually the number of counts received when the tank is empty, and the coefficient B is actually the mass absorption coefficient, $(\mu/\rho)\rho$. It is noted that the count data for the empty tank condition (Z = 0) were not used as inputs to the curvefit.

A typical result is presented in Figure 3-34. As shown, the calculated value of the coefficient A is somewhat greater than the value measured during the flight tests. This result was observed on all four channels (SCE unit outputs) for the empty-tank condition; i. e. , the calculated "A" was always greater than the observed "A". This strongly suggested that the electronics were speed saturated (paralyzed) at the highest count rates associated with an empty tank condition. This phenomenon, which probably resulted from the system being optimistically designed to the upper speed limit of the electronics, was deemed inconsequential since it fell within a range readily corrected by the system software. (An alternative would be to insert a thin absorber; e. g. , a lead sheet, within the gamma-ray beams at a small penalty in count rate statistics.)

The calculated value of the coefficient A was typically higher than the observed value (the flight test data) on all four source-detector channels by about 10-percent (or less). In this regard, Figure 3-34 is a typical representative. In all instances, the calculated value of the coefficient B (actually $\mu/\rho)\rho$ fell within the range 0. 082-0. 84 cm^{-1}, and agreed quite closely with the design value of 0. 084 cm^{-1}. In all cases,

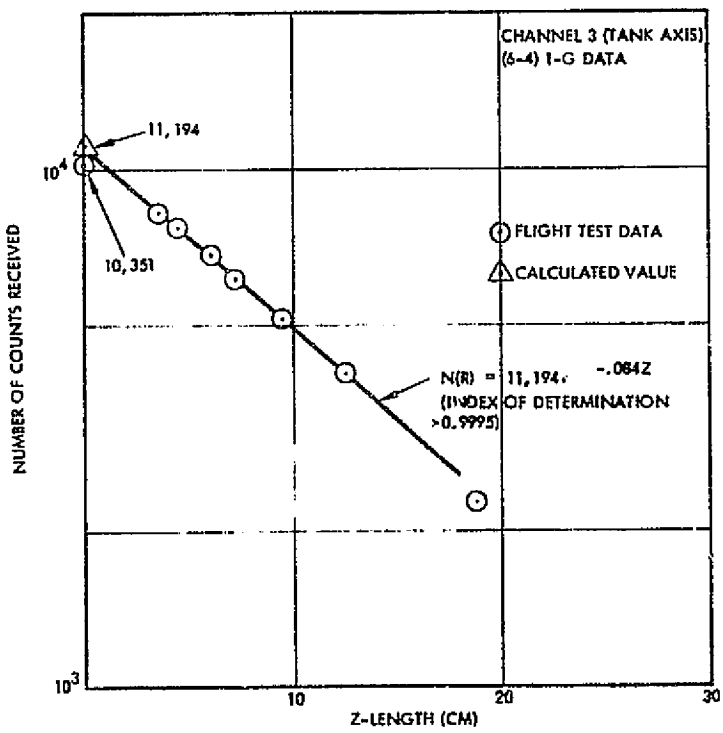

Figure 3-34. Curve-Fitted Count Data

the index of determination for the curvefits to the flight test data was greater than 0. 9995.

With the exception of the empty tank data, the foregoing results clearly indicated that the gauging system was performing essentially as designed for the level flight (one-g) conditions. This is clearly demonstrated in Figure 3-35 where the sum of the Z-lengths is plotted against the actual mass for the one-g conditions. The sum of the Z-lengths is obtained (TAPE6) by adding together the Z-lengths for each individual source-detector channel as computed from the count data and then taking the 1-second average over the gauging interval. The sum of the Z-lengths shown encompass the extreme spread over the three flights. It is noted in this figure that once the quantity of propellant simulant is sufficient to occupy the hemispherical end-cap in the base of the tank, then the mass should be a linear function of the sum of the Z-lengths. In particular, the slope is simply $4/\pi R^2$ where R is the radius of the tank and the factor 4 accounts for the four source-detector channels.

Assured on the basis of the level flight (one-g) data that the gauging system was functioning properly, a hard copy of TAPE6 (e. g. , Figure 3-32) was generated. These data were visually inspected on a point-by-point basis and revealed that the number of counts in the first 1-second interval of each gauging period (e. g. , a zero-g parabola) appeared inordinately high, being especially pronounced for the level-flight gauging periods. Furthermore, the number of counts received in

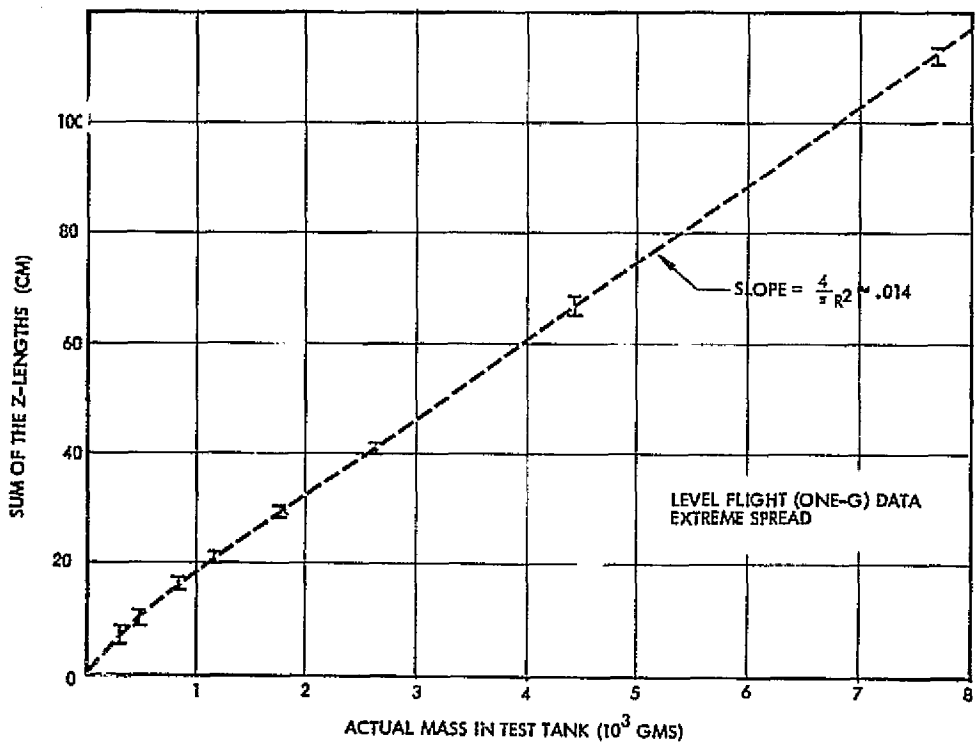

Figure 3-35. Mass Versus Z-Length for One-G Condition

the last 1-second interval of each gauging period appeared inordinately low, again being pronounced in the level-flight data. This "discrepancy" was attributed to the circuitry introduced during the Flight Verification Test wherein gauging initiation/termination was hard-wire designated via inhibiting the LEVEL 3 (and 1) interrupt(s). No tests were made to determine if this circuitry was faulty (e. g. , transient) in this regard since, as will be described shortly, it was decided to delete (at least) the first and last 1-second interval in each gauging period.

The hard-copy of TAPE6 also revealed a comparatively large variability in the count data (and, hence, corresponding Z-lengths) for the 1-second intervals while gauging in level-flight. This variability amounted to a few tenths of a centimeter in Z-length (noting that the resolution of the gauging system was approximately one-tenth centimeter). This was an unexpected result, particularly since it was contrary to the data of TAPE7 (the summary). Indeed, the data from TAPE6 were strongly suggestive that the propellant-ullage interface was unstable. Thus, it was concluded that the interface experienced a temporal surface instability of short-period which was detectable in the 1-second gauging intervals (as evidenced in TAPE6), but which was "integrated out" over a gauging period of several seconds or more (as evidenced in TAPE7). This conclusion was later confirmed when photographic films of the propellant-simulant behavior revealed small "fluctuations" at the interface; these were believed to be due to aircraft vibration being transmitted to the FTA through the hard-attached mounting.

A point-by-point visual inspection of the TAPE6 data for the zero-g parabolas was less revealing of the gauging system performance. If anything, these data indicated that the propellant simulant never reached a zero-g equilibrium; i. e. , there was a large variability of the count data for each 1-second gauging interval over the gauging period, and also between the four source-detector channels. Furthermore, hand calculations applied to the first several 1-second gauging intervals (the beginning of the zero-g parabolas) revealed that the simulant invariably appeared to be in a one-g configuration. These data were somewhat disconcerting since, at the time, the photographic films were not available, and the flight cre only reported their observations once the simulant began to move. gure 3-36 presents the typical history of the Z-lengths over a gauging period. As shown in this figure, there is a large variability not only in the Z-lengths for each individual source-detector channel, but also in the sum-of-the-Z-lengths. Note also the tendency of the Z-length data to peak at the beginning ($t \leq 2$ sec) and at the end ($t > 20$ sec) of the parabola at value(s) more descriptive of a one-g configuration.

All the gauging data for the zero-g parabolas clearly indicated that the propellant simulant never achieved a true zero-g equilibrium configuration. In fact, the data strongly suggested that the simulant behavior was more appropriately characterized as "turbulent", or at least, "a high degree of low-g slosh". Recalling now that the time response of the FTA was approximately 1. 5 seconds, and the gauging system was capable

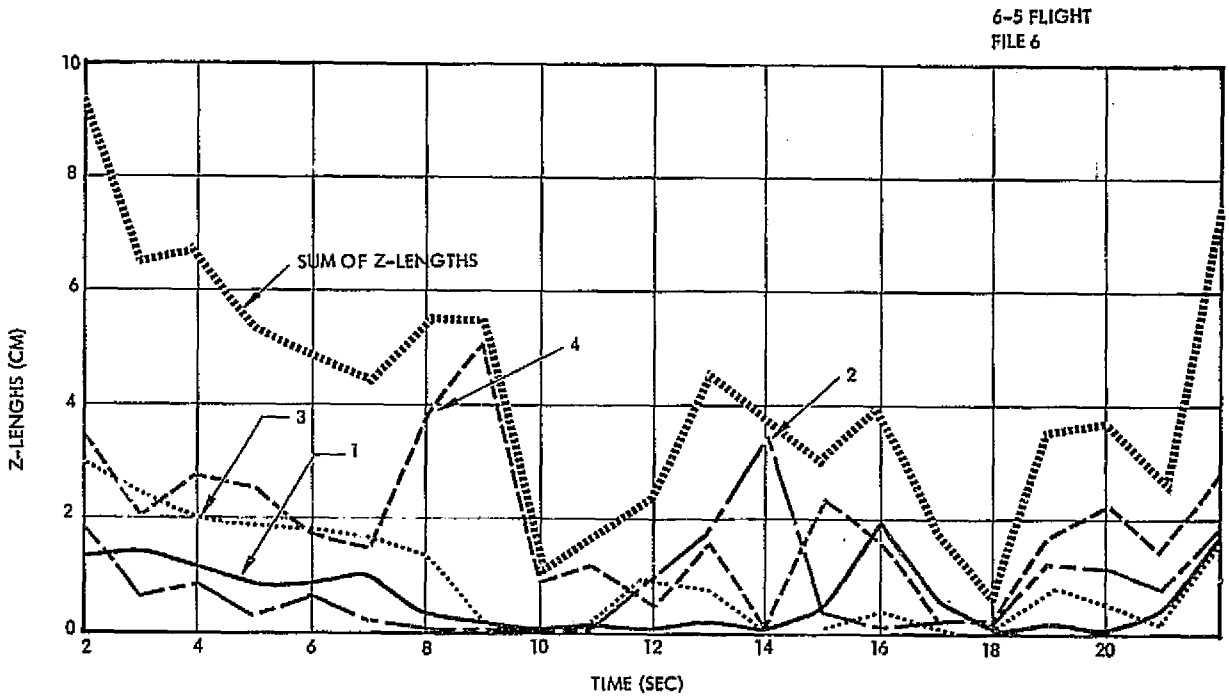

Figure 3-36. Z-Length Versus Time Over a Gauging Period

of a 1-second resolution, it was decided to investigate the effect of integration time. Basically, this was accomplished by forming a window of "n" seconds width and sliding it along each gauging period. Of interest was the quantity "n" and, in particular, what effect did "n" have on the average Z-lengths. For if the propellant simulant was turbulent, then there would be an "n" beyond which greater values of "n" would not (appreciably) affect the Z-length. In other words, given sufficient sampling time, the gauging system would perceive a truly turbulent condition of the simulant as a "bottle of seltzer water" – a truly random process; in which event the gauge output would remain invariant.

Using TAPE6 as an input, a digital computer program was written to vary the gauging system integration time. A typical result is presented in Figure 3-37. This figure plots the sum of the Z-lengths over the gauging period for a particular parabola (constant tank loading) for the four different integration times noted. As obvious, longer integration times smooth the data. The significance of the data of Figure 3-37, however, is where a comparison with similar data for other parabolas at the same tank loading is made; these comparisons are shown in Figure 3-38 and 3-39. Note in these two figures that as the integration time is increased,

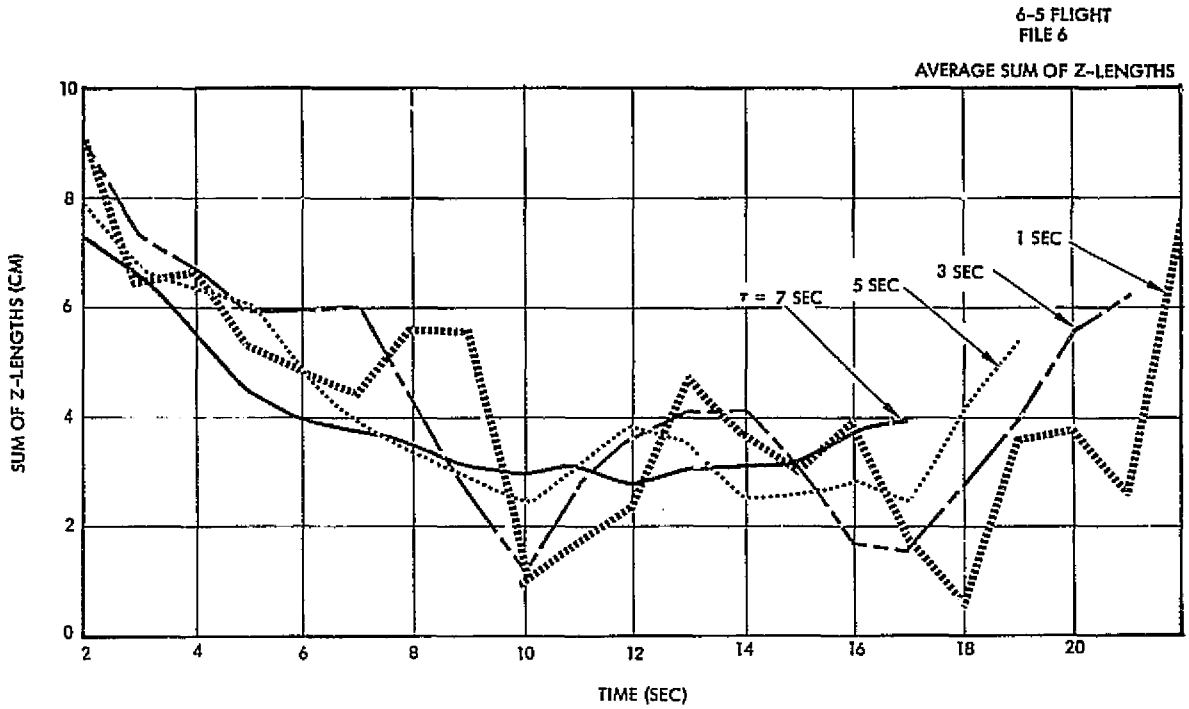

Figure 3-37. Effect of Integration Time, τ

not only are the fluctuations smoothed, but also the curves for the three files (parabolas) appear to be "drawing closer" together (as would be expected). In the limit — assuming perfect gauge performance — all curves for a given tank loading should merge into a common curve.

This limit was never achieved in the flight-test program due to a combination of factors, but primarily because the "turbulent" nature of the propellant simulant could not be treated as a truly random process. For example, Table 3-3 tabulates the average sum of the Z-lengths, for various integration times for eight files (parabolas). The tank loading was constant for files 13 through 16, and constant at some other value for files 25 through 28. As shown in this table, Z was less sensitive to the integration time than it was to the file (parabola) number, even though the tank loading was constant. The interpretation of the data in Table 3-3 required some assistance from the photographic films. A careful review of these films revealed the following:

1) The propellant simulant clearly remained in a one-g configuration for the first several 1-second gauging intervals; often this configuration was one where the interface of the simulant was "tilted" and precessed about the tank axis (g-vector).

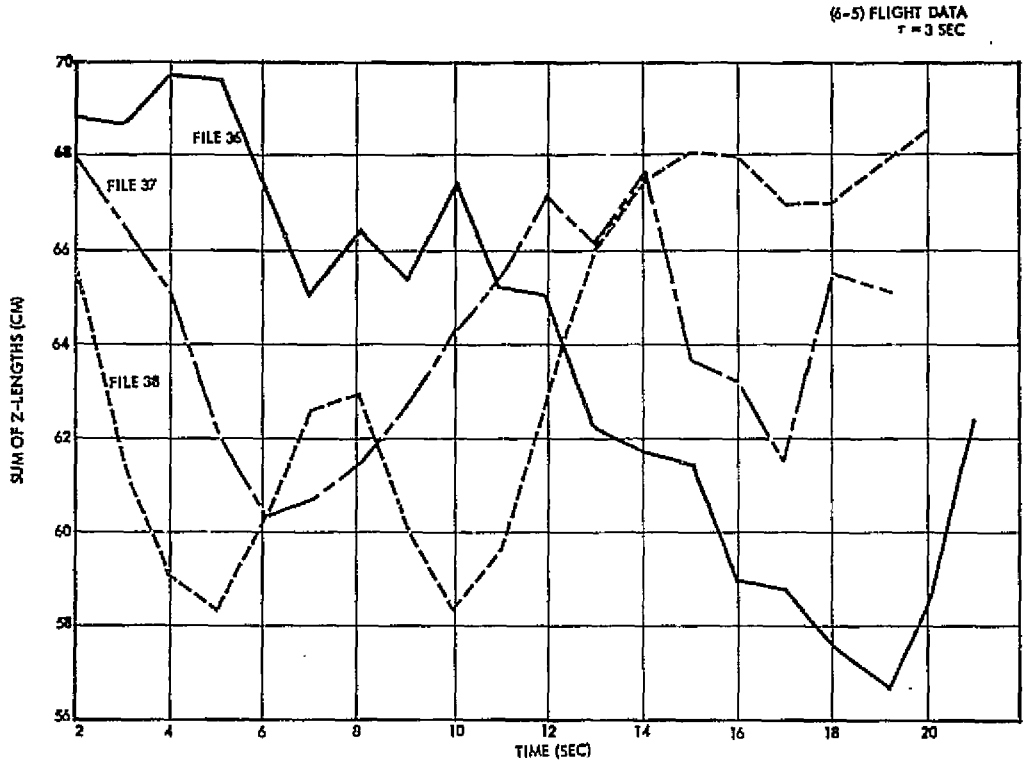

Figure 3-38. Z-Length for Three Different Parabolas (τ = 3 sec)

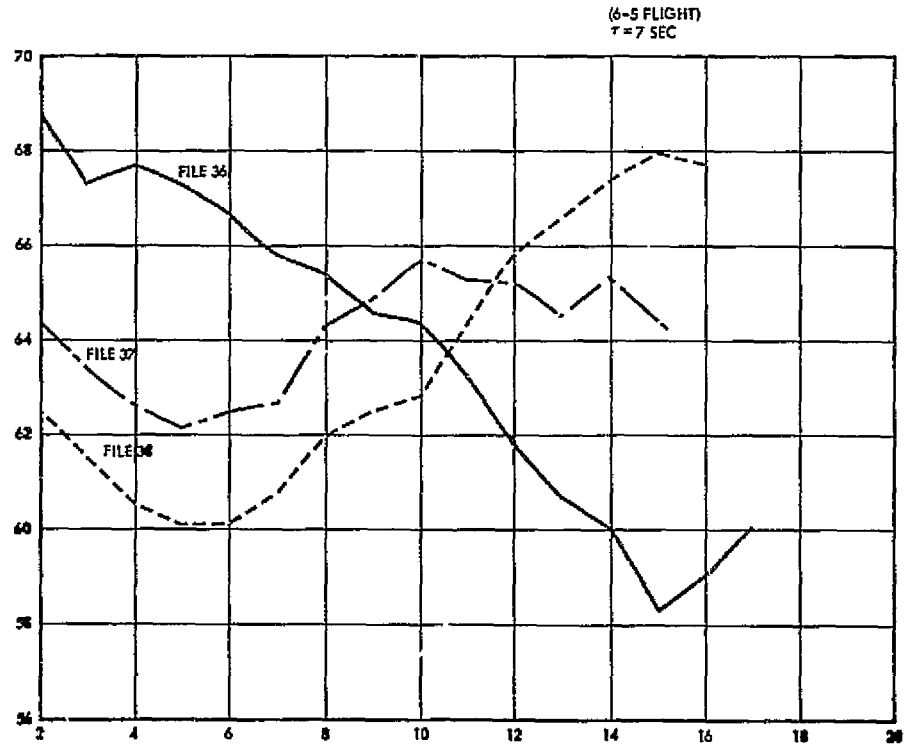

Figure 3-39. Z-Length for Three Different Parabolas (τ = 7 sec)

Table 3-3. Average Sum of Z-Lengths, $\overline{Z}$, Versus Integration Time, τ (6-4 Flight Data)

File	Z in cm; τ in Sec $\tau = 1$	$\tau = 3$	$\tau = 5$	$\tau = 7$
13	9.83	8.71	8.51	8.44
14	8.48	8.44	8.40	8.49
15	10.96	10.76	10.70	10.78
16	11.55	12.19	12.52	12.52
25	10.19	10.22	10.33	10.33
26	14.04	15.51	16.03	16.03
27	10.74	10.23	9.73	10.23
28	11.61	11.34	11.07	10.80

2) When, and if, the simulant did leave the one-g configuration, it occurred no later than about the sixth or seventh 1-second gauging interval (i. e. , about 6 or 7 seconds into the parabola).

3) Some parabolas were difficult to judge; i. e. , the propellant was not obviously in a one-g configuration, nor could it be characterized as low-g slosh, or turbulent, as was typical of most parabolas. In these instances, the simulant would appear as "tongues", climbing up the tank wall and (often) rolling over the top of the tank.

4) No two parabolas appeared to yield the same simulant behavior, even if the tank loading was unchanged. The simulant would usually leave the zero-g configuration by climbing the tank wall in the form of a large tongue. The direction of this tongue was usually rearward, although other directions were observed. In only a few instances, and at the highest tank loadings, did the propellant appear to climb the tank wall completely and uniformly around the circumference of the tank.

5) The speed at which the simulant left the one-g configuration varied. In most instances, it would "rush" up the rear wall in the form of a tongue, and burst over the top of the tank.

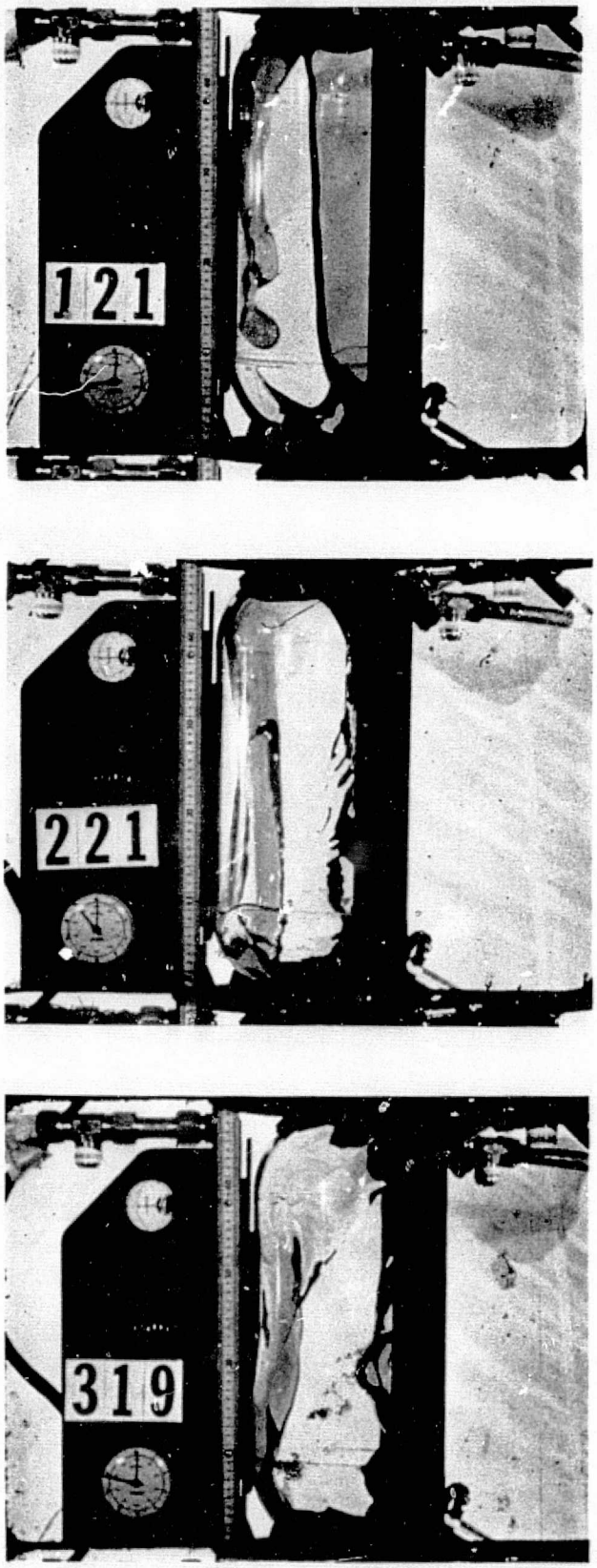

Figure 3-40. Propellant Behavior in Different Parabolas

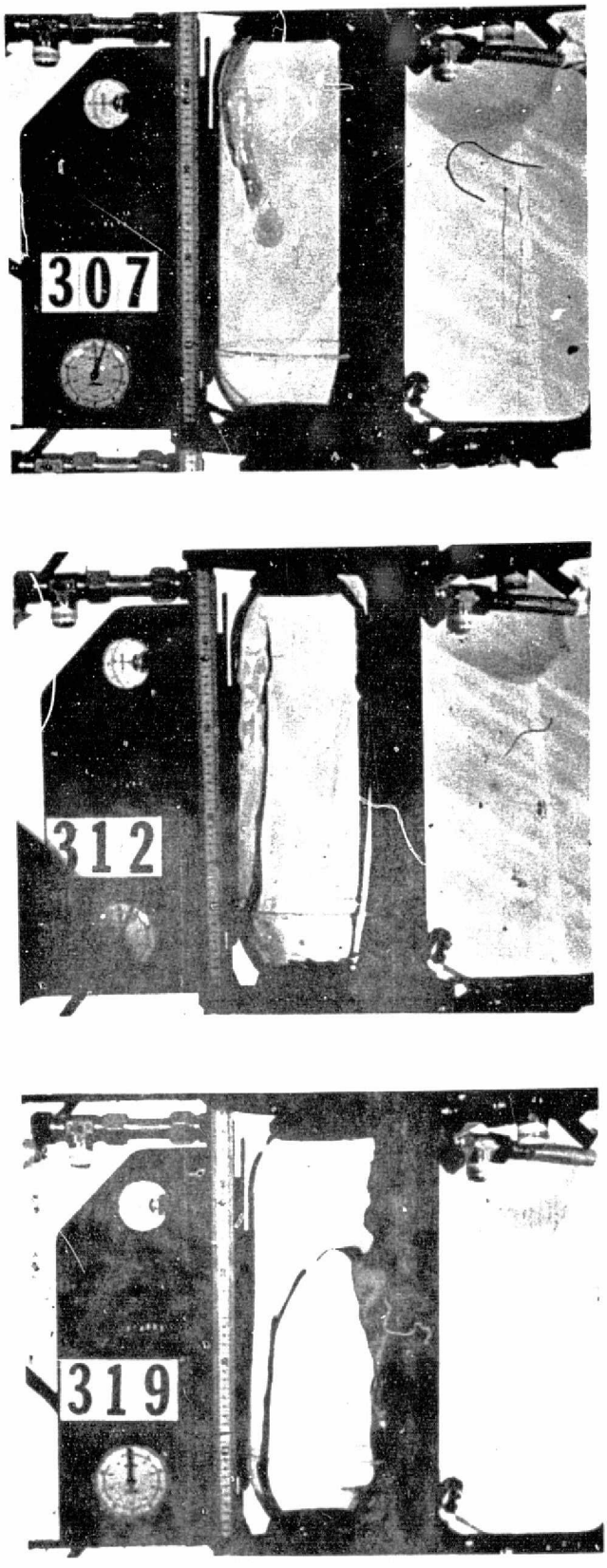

Figure 3-41. Propellant Behavior for Different Tank Loadings

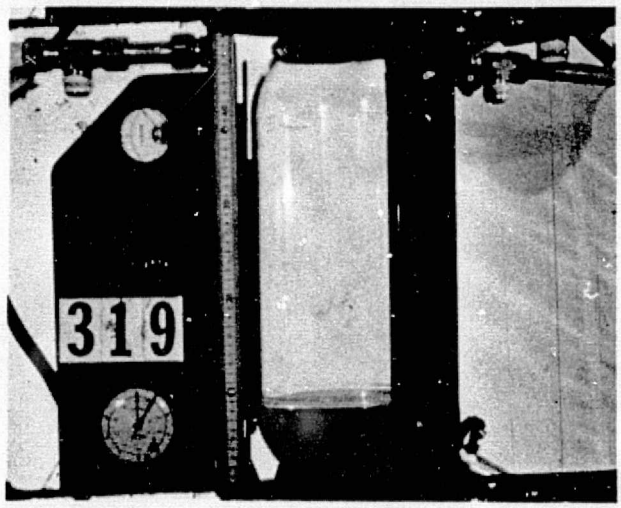

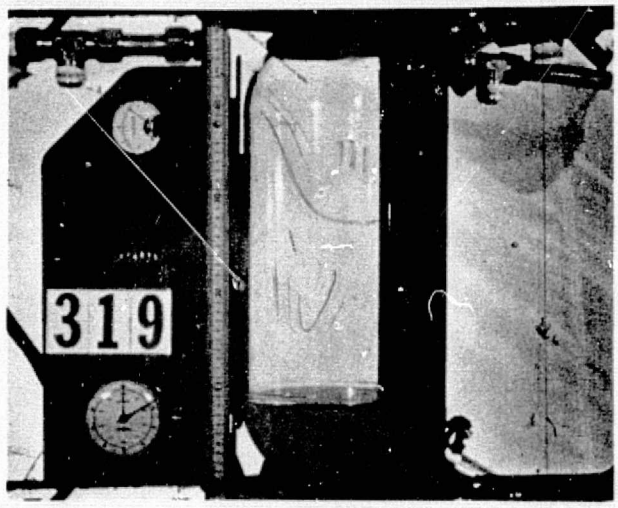

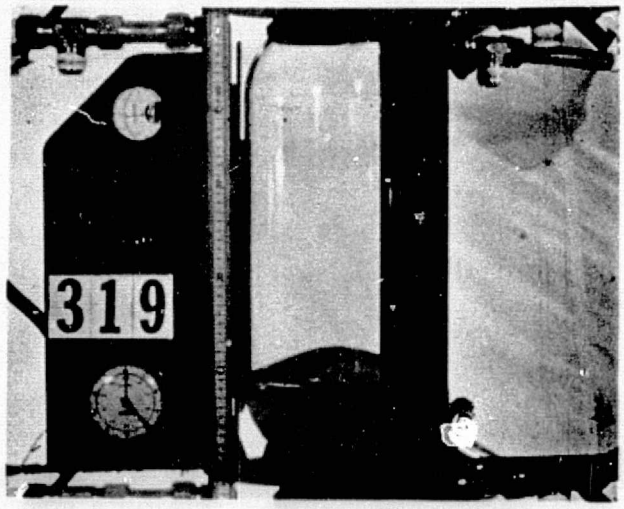

Figure 3-42. Propellant Behavior at 1-Second Intervals (Continued)

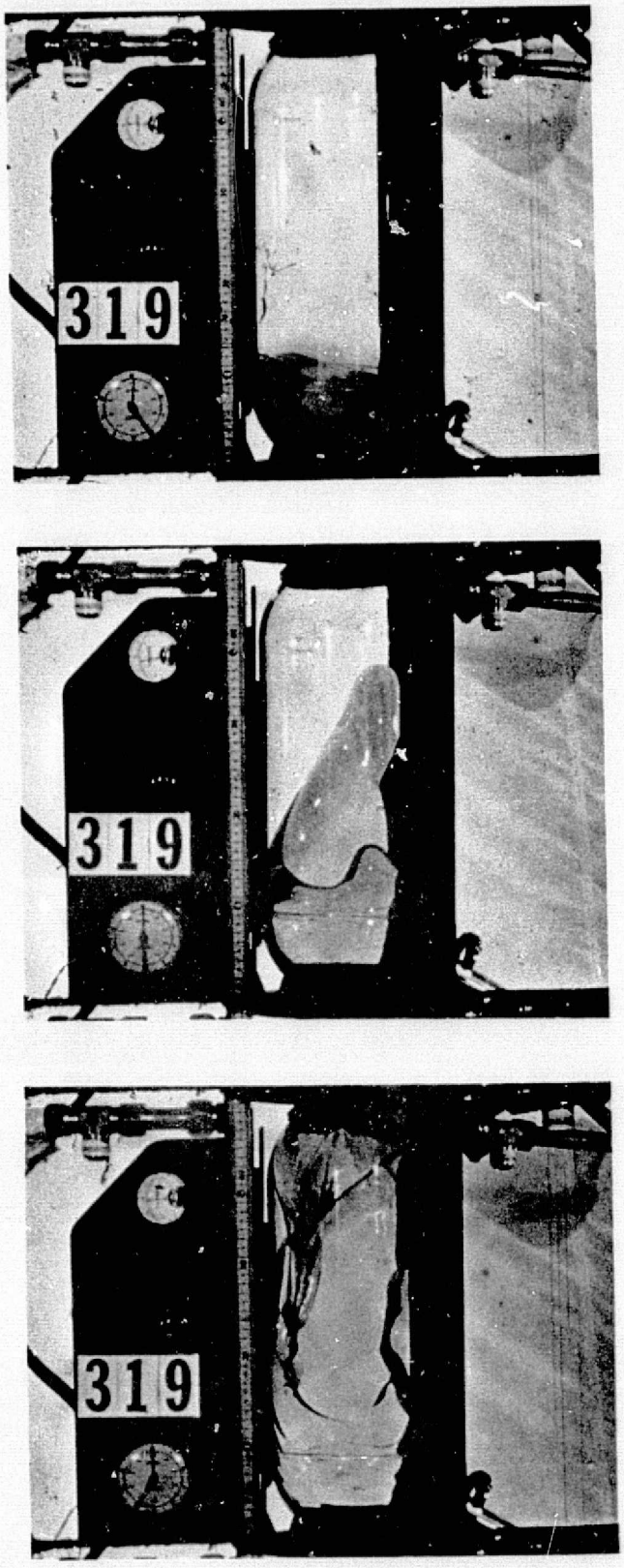

Figure 3-42. Propellant Behavior at 1-Second Intervals (Continued)

Figure 3-42. Propellant Behavior at 1-Second Intervals (Continued)

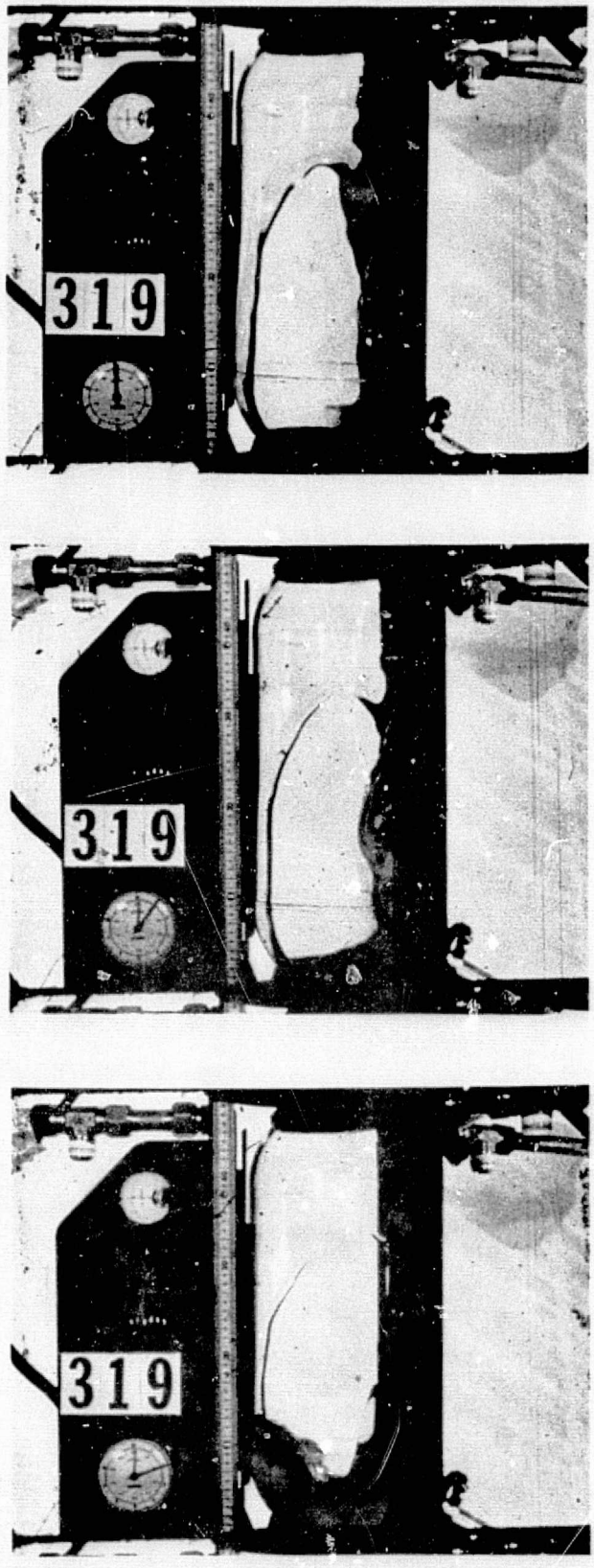

Figure 3-42. Propellant Behavior at 1-Second Intervals (Continued)

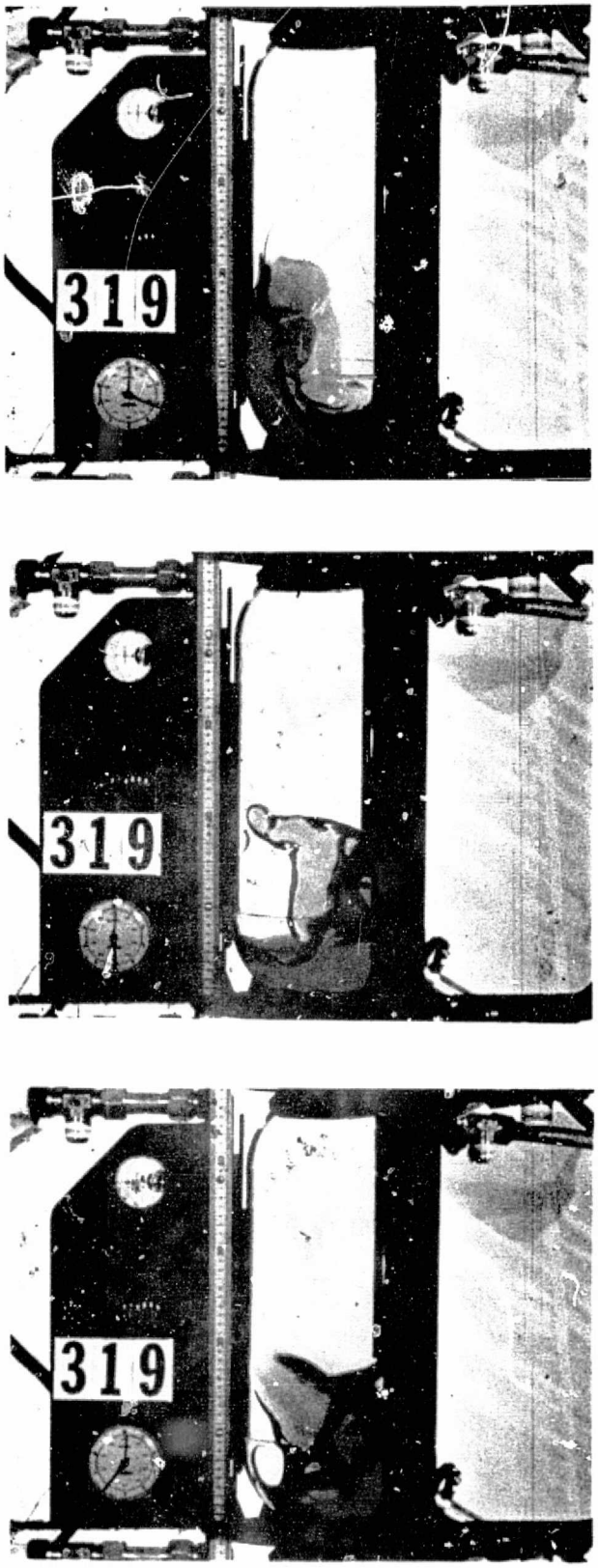

Figure 3-42. Propellant Behavior at 1-Second Intervals (Continued)

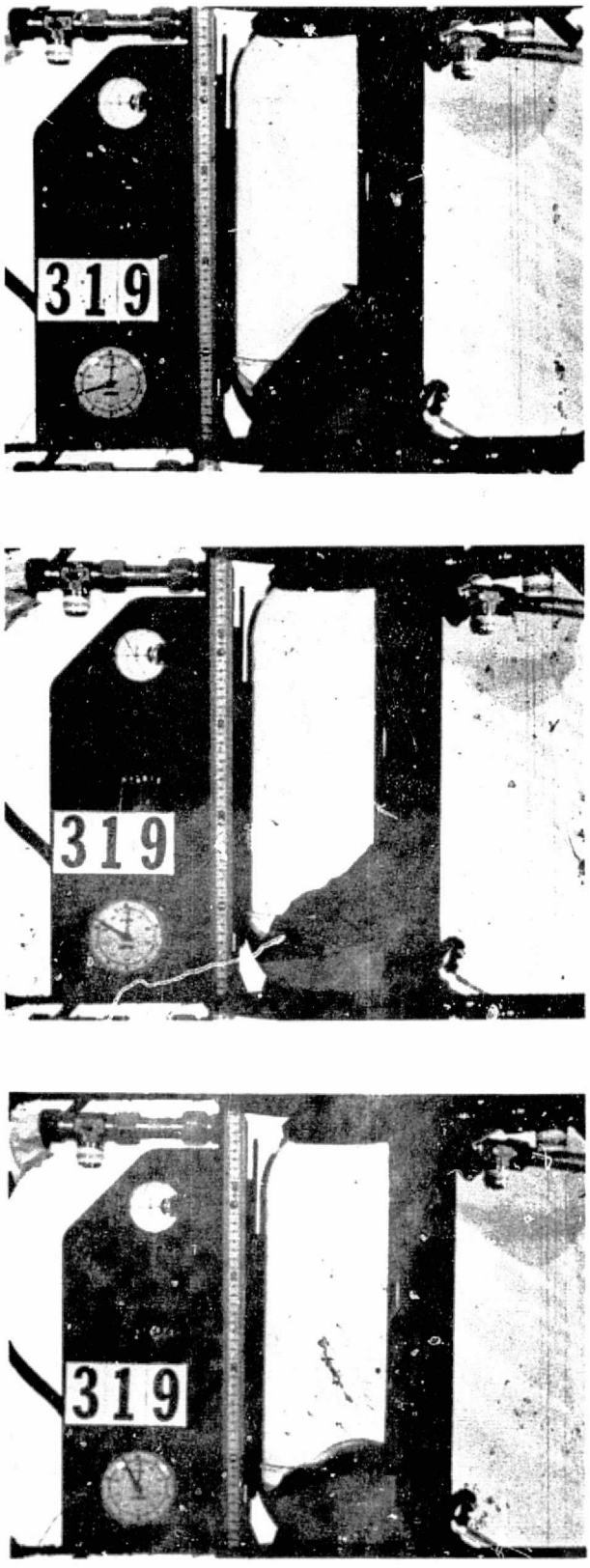

Figure 3-42. Propellant Behavior at 1-Second Intervals (Continued)

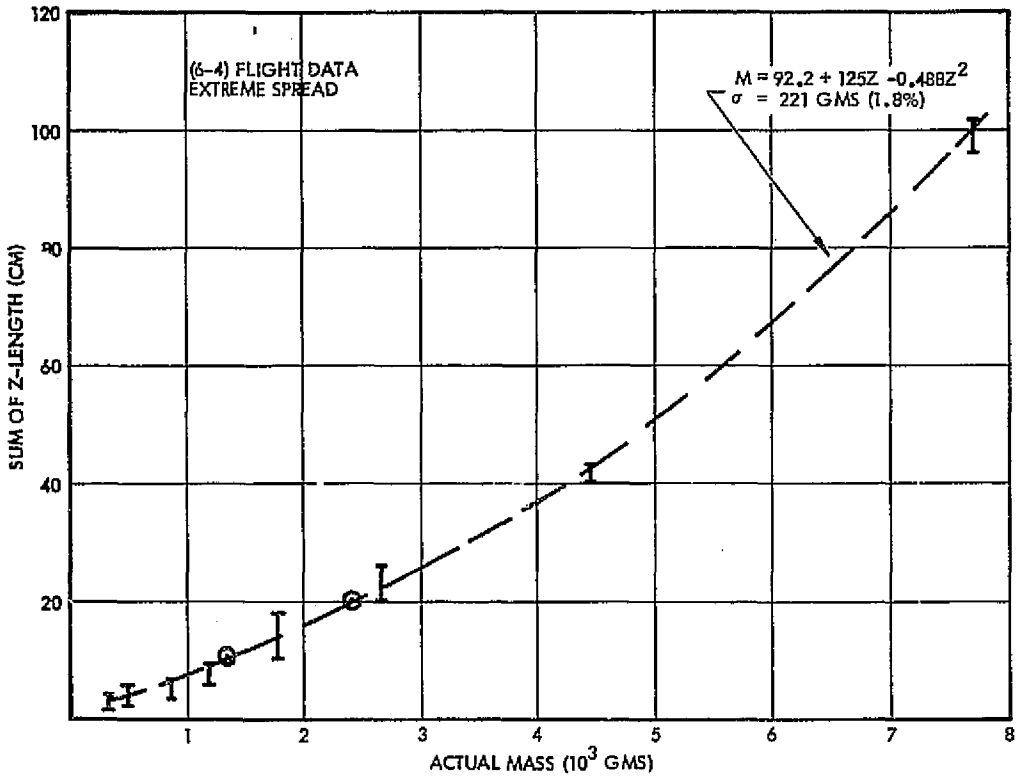

Figure 3-43. Mass Versus Sum-of-the-Z-Lengths, (6-4) Data

the test tank, this 221 grams translates to a total system accuracy of 1. 8-percent (123 grams = one percent).

This technique of polynomial curve-fitting was applied to all the data; i. e. , to the Z-lengths for each individual source-detector channel for the sum-of-the-Z-lengths, for all parabolas, for all flights, and for all flights combined. These data are summarized in Table 3-4. In this table, "CH" denotes the source detector channel number (channel 3 is on the tank axis and the other three channels are equi-distant from, and concentric about, channel 3, and the sum-of-the-Z-lengths denotes that all four channels have been combined. The standard error of estimate, σ , is in grams, and ΔM represents the maximum excursion (in grams) of the flight data away from the curve described by

$$M = A_0 + A_1 Z + A_2 Z^2$$

As shown in Table 3-4, the standard error of estimate (using the sum-of-the-Z-lengths) for the individual flights is comparable, ranging

Table 3-4. Data Summary

		σ (Grams)	ΔM (Grams)	Mass = $A_0 + A_1 Z + A_2 Z^2$ (Z in cm)		
				A_0	A_1	A_2
(6-3) Data	CH 1	236	-559	109	563	-21.2
	2	229	618	9.61	526	13.8
	3	393	1121	98.7	762	-82.0
	4	270	590	-16.6	542	-38.9
	Sum of Z-Lengths	232	533	-43.1	175	-3.40
(6-4) Data	CH 1	353	-757	264	491	-7.88
	2	514	-1142	261	412	-3.38
	3	339	-639	275	620	-12.9
	4	515	-1698	-13.5	395	-4.65
	Sum of Z-Lengths	221	444	92.2	125	-0.488
(6-5) Data	CH 1	344	638	264	299	-0.965
	2	281	672	211	332	-2.03
	3	369	839	300	272	-0.370
	4	421	-937	314	193	2.61
	Sum of Z-Lengths	277	508	251	68.9	-0.0081
(6-3, 4, 5) Data Combined	CH 1	413	-1177	278	393	-4.36
	2	446	1422	193	410	-4.43
	3	572	-1659	336	417	-5.28
	4	477	1826	151	314	-2.03
	Sum of Z-Lengths	377	-1166	195	97.5	-0.255

from 221 to 277 grams (1. 8 to 2. 3 percent). Similarly, the maximum excursion of the data ranges from 444 to 533 grams (3. 6 to 4. 3 percent). When all the data for the three flights are combined, however, the standard error of estimate increases to 377 grams (3. 1 percent).

Other polynomial curvefits were investigated extensively, and it was found that the decrease in the standard error of estimate for higher degrees was, for all practical purposes, negligible. Similarly, methods of segmenting the data into various increments of Z-length (e. g. , one carvefit for $0<Z\leq x$ and another for $Z>x$, etc.) were studied, but, again, no significant decrease in the standard error of estimate could be achieved. Since no significant decrease in the standard error of estimate could be found, and in an effort to keep the system software uncomplicated, the quadratic form of Table 3-4 was the adopted "standard" for the FTA.

It is now noted that Table 3-4 summarizes all of the flight data obtained during all of the zero-g parabolas with the exception of the first six and last two 1-second gauging intervals (where the propellant was obviously in a one-g configuration). Although the photographic data strongly suggested that some editing of the gauging data was in order, no firm, quantitative method for such editing was determined. For example, one method would have been to treat, as a class, the data from those parabolas in which the propellant behavior "looked" similar (say, perhaps, those parabolas where the propellant appeared turbulent as one class, and those more likened to a low-g slosh as another class, etc.). Unfortunately, however, this would have required the exercise of a large degree of engineering judgment, and it was decided not to perturb the data in any subjective manner. The one exception to this decision deals with the data obtained on the third and last flight, the (6-5) data. In two of the zero-g parabolas-viz, 18 and 20, the propellant unquestionably remained in a one-g configuration. With these two parabolas deleted, the result of Table 3-5 was obtained.

The values shown in Table 3-5 are based on the sum-of-the-Z-lengths with mass in grams and Z in centimenters. The (6-5) and

Table 3-5. Effect of Deleting Two Parabolas

	(Grams)	$\text{Mass} = A_0 + A_1 Z + A_2 Z^2$		
		A_0	A_1	A_2
(6-5) (All Parabolas)	277	251	68. 9	-0. 0081
(6-5) (18 and 20 Deleted)	252	232	74. 9	-0. 064
(6-3, 4, 5) (Data Combined)	377	195	97. 5	-0. 255
(6-3, 4, 5) (18 and 20 Deleted)	340	167	104	-0. 318

(6-3, 4, 5) represent all the parabolas, whereas the (18 and 20 deleted) indicate that those two parabolas were deleted from the (6-5) data. As shown, the effect of the deletion is to reduce the standard error of estimate. A plot of mass versus the sum-of-the-Z-lengths for all three flights is shown in Figure 3-44. The data points representing the data of the two deleted parabolas are also shown in this figure.

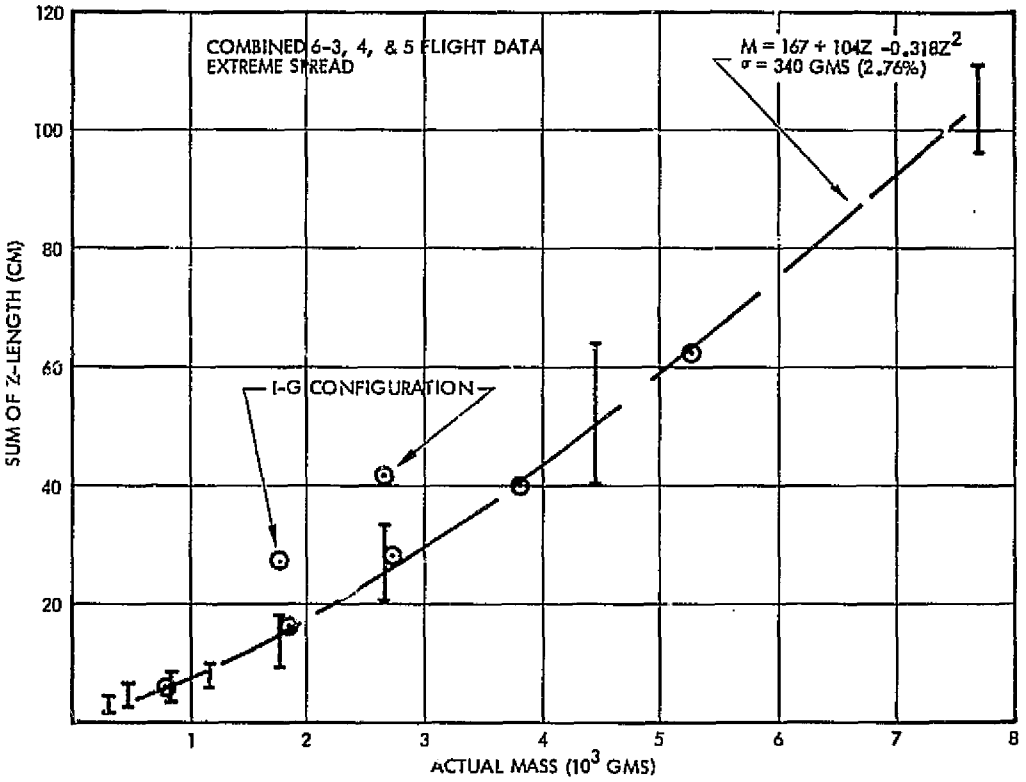

Figure 3-44. Mass Versus Sum-of-the-Z-Lengths, All Flight Data Combined

SECTION IV

CONCLUSIONS AND RECOMMENDATIONS

Three flights were flown on three separate days encompassing eight different tank loadings and eleven zero-g parabolas for each loading; gauging was also conducted at these loadings during level flight conditions (one-g).

At no time during any of the zero-g parabolas did the propellant ullage interface reach the stable, zero-g equilibrium configuration. Rather, the propellant was more appropriately characterized as turbulent or, at the least, in a high degree of low-g slosh. The photographic coverage also revealed that the propellant invariably remained in (or near) a one-g configuration for the first 4- to 6- seconds, and the last 1- to 2- seconds of each parabola.

Despite the erratic behavior of the propellant during the zero-g parabolas, the nucleonic gauging system was capable of gauging the propellant content for any particular day's flight (consisting of 24 to 32 zero-g parabolas) to a total system accuracy of 2.05 percent or better. When all three flights (encompassing all 88 zero-g trajectories) were considered in toto, the gauging system accuracy was 2.76 percent.

During the level flight conditions (one-g), the photographic coverage revealed a slight "shimmer" of the propellant surface. This "shimmer" was also detected by the nucleonic gauging system and was believed to be the result of aircraft vibration being transmitted to the propellant via the hard-attached FTA. The gauging system was capable of gauging the propellant content under the one-g conditions to an accuracy the order of 0.5 percent.

The accuracy of the nucleonic gauging system was found to be relatively insensitive to gauge integration time. The most significant factor affecting gauging accuracy appeared to be the flight number; i.e., for any given tank loading, the mass of propellant as determined by the gauging system depended primarily on which of the three days the flight was flown. This observation suggested that factors external to the gauging system — pilot proficiency, weather, etc. — were not without influence in the final determination of overall gauging system performance.

Only one failure in the gauging system was noted; this was a fail-safe in the protection circuitry, and the interim conclusion was that the cause was due to line transient(s) on the aircraft 28 vdc line bus.

During the course of the program, a total of eighteen people were issued film badges to monitor any radiation dose that might be received from the nucleonic gauging system; those people whose jobs involved physical contact with the gauging system were also issued ring badges. The minimum detectable dose for these badges is 10 millirems. During the entire program, only one ring badge was reported to have received this dose or more; this ring badge recorded a dose of 40 millirems during the same period that the worker's regular film badge recorded "minimal". On this basis, it was concluded that the nucleonic gauging system presents no undue hazard to operating personnel in either ground and/or flight testing.

Based on the stable and accurate performance achieved in gauging under one-g condition it is concluded that the nucleonic gauging system would achieve an accuracy the order of one percent for true zero-g environments; i.e., where the propellant-ullage interface is in the equilibrium zero-g configuration. It is also concluded that the nucleonic gauging system will function reliably in an adverse environment comparable to that experienced in this program (e.g., air freight shipping, trucking on paved roads, thermal variations, aircraft g-forces associated with the zero-g parabola initiation/recovery, etc.). Lastly, it is concluded that this accurate and reliable performance can be achieved with no undue radiation hazard to operating personnel.

It is recommended that the nucleonic gauging system be considered as a viable candidate for those gauging applications where high accuracy and reliable operation are of particular concern. The nucleonic gauging system--being mass sensitive--is a universal gauge and capable of gauging a variety of materials, including slurries, gels, cryogenics, etc., under a variety of conditions; i.e., stable propellant-ullage interface (one- or zero-g), highly agitated and/or slosh, tanking/de-tanking situations, etc.

REFERENCES

1. "Development of a Zero-G Gauging System," AFRPL-TR-74-53; September 1974.

2. User's Manual Zero-G Program; Requirements for Using Organizations, NASA Publication.